

# THE PROCEEDINGS OF THE PHYSICAL SOCIETY

VOL. 57, PART 2

1 March 1945

No. 320

## CONTENTS

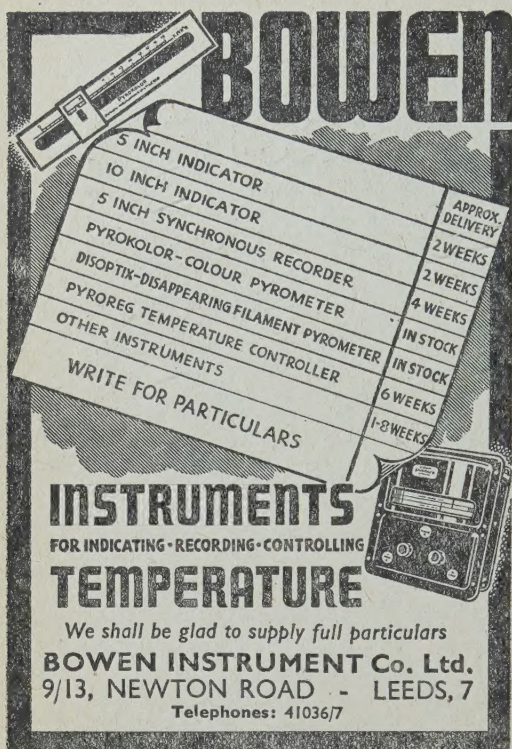
	PAGE
V. E. BALLARD. The formation of metal-sprayed deposits . . . . .	67
L. HOUGHTON. Combinations of spherical lenses to replace non-spherical refracting surfaces in optical systems . . . . .	84
D. H. SMITH. The non-reflecting termination of a transmission line . . . . .	90
C. CRAVEN. A study of the comparative method of determining gaseous refractivities . . . . .	97
A. TAYLOR and H. SINCLAIR. The influence of absorption on the shapes and positions of lines in Debye-Scherrer powder photographs . . . . .	108
A. TAYLOR and H. SINCLAIR. On the determination of lattice parameters by the Debye-Scherrer method . . . . .	126
JOHN JOB MANLEY. Recent improvements in a precision balance and the efficacy of rhodium plating for standard weights . . . . .	136
Reviews of books . . . . .	145
Corrigendum . . . . .	146
Recent reports and catalogues . . . . .	146

The fact that goods made of raw materials in short supply owing to war conditions are advertised in the *Proceedings of the Physical Society* should not be taken as an indication that they are necessarily available for export.

Price to non-Fellows 8s. 4d. net; post free 8s. 9d.  
Annual subscription 42s. post free, payable in advance

Published by  
**THE PHYSICAL SOCIETY**  
1 Lowther Gardens, Exhibition Road, London S.W.7

Printed by  
**TAYLOR AND FRANCIS, LTD.,**  
Red Lion Court, Fleet Street, London E.C.4



**BOWEN**

5 INCH INDICATOR	APPROX. DELIVERY
10 INCH INDICATOR	2 WEEKS
5 INCH SYNCHRONOUS RECORDER	2 WEEKS
PYROKOLOR-COLOUR PYROMETER	4 WEEKS
DISOPTIX-DISAPPEARING FILAMENT PYROMETER	IN STOCK
PYROREG TEMPERATURE CONTROLLER	IN STOCK
OTHER INSTRUMENTS	6 WEEKS
WRITE FOR PARTICULARS	1-8 WEEKS

**INSTRUMENTS**  
FOR INDICATING-RECORDING-CONTROLLING  
**TEMPERATURE**

We shall be glad to supply full particulars  
**BOWEN INSTRUMENT Co. Ltd.**  
9/13, NEWTON ROAD - LEEDS, 7  
Telephones: 41036/7

## We wish to Purchase Always

Complete sets and long and short runs of British and Foreign **SCIENTIFIC JOURNALS and PERIODICALS, and LEARNED SOCIETY PUBLICATIONS**

which libraries or private owners sometimes have for disposal. At present, however, we particularly require offers on Mathematics, Physics, Chemistry, Aeronautics (all branches), Plastics, Fuel and Rubber Technology, Engineering (Electrical, Chemical and Mechanical), Geology, and Metallurgy. Also standard reference works for library use. Please

send particulars (or phone) to :

**THE MUSEUM BOOK STORE, LTD.**

45, Museum Street, London, W.C.1  
Tel.: CHA. 8947 or HOL. 0400. (Est. 1900).

## for HEAVY DUTY ELECTRICAL AND INSTRUMENT SPRINGS

**G**REATER tensile, elastic and fatigue strengths than any other non-ferrous alloy, a higher conductivity than any of the bronzes and excellent resistance to corrosion and wear—these characteristics of Mallory 73 Beryllium Copper have made it first choice for instrument springs, diaphragms and bellows, current-carrying springs, snap action switch blades, contact blades and clips.

Supplied annealed or lightly cold worked, it has good forming properties and is readily fabricated into springs and parts of complicated shape. A simple heat treatment then develops its remarkable properties.

Available as sheet, strip and wire, in a range of tempers to suit users' requirements, and as rod, tube, precision rolled hair-spring strip, and silver-faced contact bi-metal strip.

**MALLORY**

**MALLORY METALLURGICAL PRODUCTS LTD.**

An Associate Company of JOHNSON, MATTHEY & CO. LTD.

78 Hatten Garden, London, E.C.1

Telephone: HOLborn 5027



Properties of  
**MALLORY 73 BERYLLIUM COPPER**  
after heat treatment

**Ultimate tensile stress**  
tons per sq. inch **75-100**

**Limit of proportionality**  
tons per sq. inch **47-50**

**Fatigue limit**  
tons per sq. inch **± 19-20**

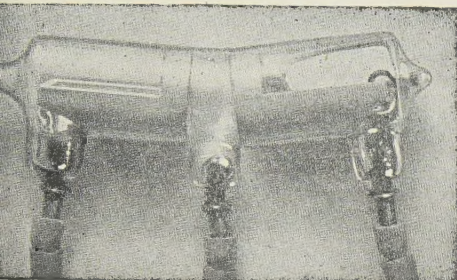
**Vickers pyramid hardness**  
**350-420**

**Electrical Conductivity**  
per cent I.A.C.S. **23-25**

Full details are given in our booklet,  
which will be sent on request.

# MERCURY SWITCHES

FOR  
RELAYS



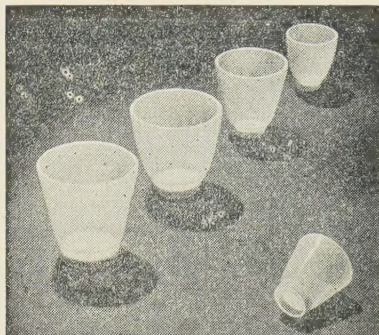
NEW LIST AVAILABLE

## I.A.C. LTD.

CHASE ROAD,  
LONDON, N.W.10

# POROUS VITREOSIL

(Pure Fused Silica)



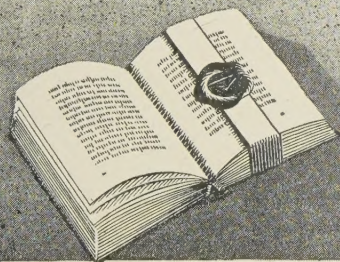
We are now able to supply VITREOSIL pure fused silica apparatus fitted with porous VITREOSIL discs. These are usable up to  $1100^{\circ}\text{C}$ . and are made in four grades of porosity.

Porous ALUMINA ware is also available.

**THE THERMAL SYNDICATE LTD.**

Head Office: Wallsend, Northumberland.  
London Depot: 12-14, Old Pye Street,  
Westminster, S.W.1.

# HALF the STORY



At the moment only half the story can be told. Not until the peace is won, can we tell you of the war developments which will be incorporated in the post-war design and manufacture of our Optical-Mechanical-Electrical Instruments and Aircraft Equipment.

AVIMO LTD., TAUNTON, SOM. (Eng.)

Approved under Air Navigation Rules for Civil Aviation

# AVIMO

PROGRESS by QUALITY



NEW LOW LEVELS in capacity and attenuation of CO-AX Cables mean new possibilities in electronic equipment design both for the war effort and for the post-war electronic age.

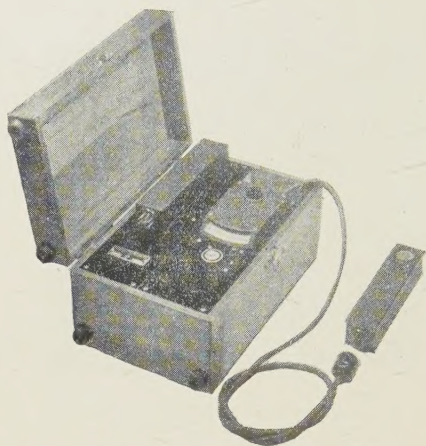
Write for characteristics

**BASICALLY BETTER  
AIR-SPACED**

# CO-AX LOW LOSS CABLES

TRANSRADIO LTD. 16 THE HIGHWAY, BEACONSFIELD, 14-BUCKS.

# PHOTOVOLT Electronic Photometer Mod. 512



Sensitivity 1/100000 foot-candle per division.

Phototube and DC amplifier, operated by built-in dry-cell batteries.

With interchangeable phototubes, available for sensitivity in the visible, in the infra-red, and in the ultra-violet as far as 2000 A.U.

For

**Spectrophotometry of solutions.**

**Densitometry of spectrographs and X-ray diffraction negatives.**

**Brightness of luminescent paints.**

**Ultra-violet radiation and absorption.**

**Fluorescence of solutions and solids.**

**Exposure determination in photomicrography by direct light measurement in focal plane.**

Write for literature to

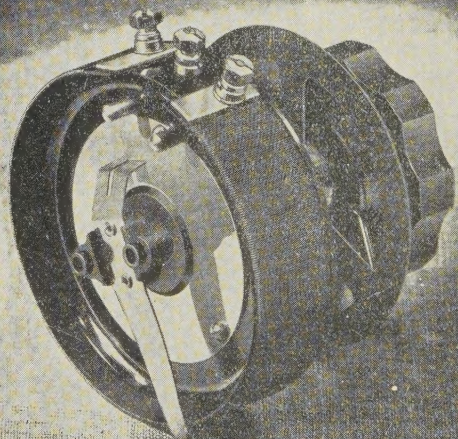
## PHOTOVOLT CORP.

95, Madison Ave.

New York 16, N.Y.

Also : Industrial and Clinical Colorimeters, Fluorescence Meters, Vitamin A Meters, Reflection Meters, Glossmeters, Smoke Meters, Opacimeters, Hemoglobinometers.

# BERCO



BERCO Wire-wound Potentiometer

## RESISTANCES

Although present circumstances render it difficult for us to give our pre-war service to all customers, we are still working in their interests.

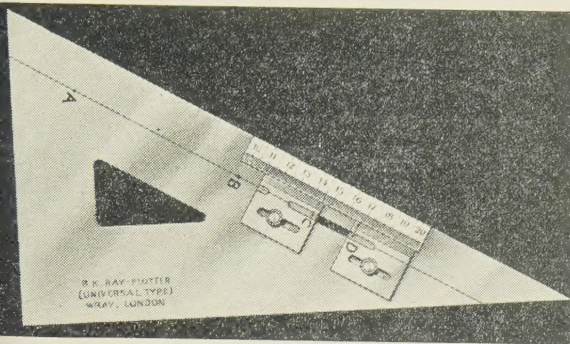
New materials and manufacturing processes, which we are now using to increase output, also contribute in large measure to improved performance and reliability of our products. Thus, when normal times return, all users of Berco Resistances will benefit by our work to-day.

THE BRITISH ELECTRIC RESISTANCE CO. LTD.  
QUEENSWAY, PONDERS END, MIDDLESEX

Telephone : HOWARD 1492.

Telegrams : "VITROHM, ENFIELD."

(R. 1)

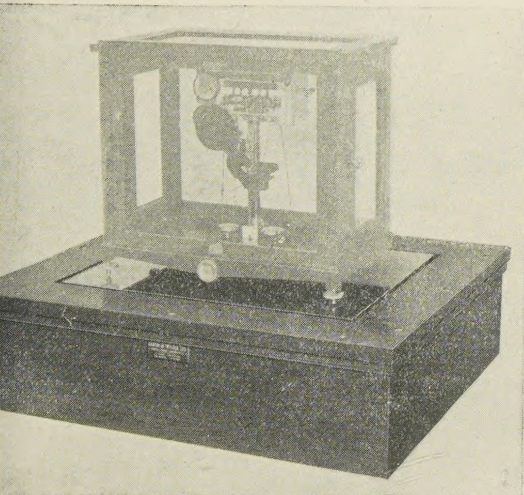


## AN OPTICAL RAY-PLOTTER

The B.K. Ray-Plotter enables rays to be plotted graphically through an optical system without auxiliary drawings. It can be used for rays from air to glass, from glass to air, or from glass to glass.

Write for particulars to

**WRAY LTD.**  
(OPTICAL WORKS)  
BROMLEY, KENT.



*Solves the most obstinate  
problem of balance vibration*

## The G & T ANTI-VIBRATION BALANCE TABLE

Balance vibration is a very troublesome problem. It is especially acute in many war factories where, to save time in the transit of samples, the laboratory is installed in the works. Cases are known where the vibration is so severe as to cause fractional weights of small denomination to jump out of the pan. The G. & T. Anti-Vibration Balance Table has been successful even under these conditions. It is applicable to any instrument in any situation where vibration is experienced—severe or mild, of high or low frequency, intermittent or continuous.

*Leaflet G.T. 1338/31 on application.*

**GRIFFIN and TATLOCK Ltd**

**LONDON**  
Kemble St., W.C.2.

**MANCHESTER**  
19, Cheetham Hill Rd., 4.

**GLASGOW**  
45, Renfrew St., C.2.

**EDINBURGH**  
7, Teviot Place, 1.

*Established as Scientific Instrument Makers in 1826*

**BIRMINGHAM: STANDLEY, BELCHER & MASON LTD., Church Street, 3.**

**AVO**  
REGD. TRADE MARK

THE Services and war-time industry are familiar with the high standard of dependability and accuracy of "AVO" Electrical Testing Instruments. They will be an equally dominant factor in the post-war rebuilding of our great industries and the advancement of amenities worthy of a world at well-earned peace.

*In the belligerent interim, orders can only be accepted which bear a Government Contract Number and Priority Rating.*

**THE AUTOMATIC COIL WINDER & ELECTRICAL EQUIPMENT CO.**  
WINDER HOUSE · DOUGLAS STREET · LONDON · S.W.1 · TELEPHONE: VICTORIA

# ELECTRONIC

## DEVICES for SCIENCE and INDUSTRY

**Osram**  
PHOTO CELLS

**G.E.C.**  
CATHODE RAY TUBE

**Osram**  
Valves

The G.E.C. are specialists in valves and other electronic devices which find many applications in industry and scientific research.

The following are a few of the classes of electronic tube which have already found their place in industry.

### VACUUM AMPLIFYING VALVES

For all cases in which the amplification of small voltages is required, with continuous control of amplification over a wide range of frequencies.

As self oscillators for generation of high frequency voltage and power.

### VACUUM RECTIFIERS

For Extra High Tension Voltages in cable and condenser testing, etc.

For power rectification at medium and high voltages.

For radio frequency detection. In peak voltmeters.

### HOT CATHODE MERCURY VAPOUR RECTIFIERS

For high current rectified outputs in radio transmitters and power circuits.

### GASFILLED RELAYS (THYRATRONS)

For trigger controls and various industrial research work used where an instantaneous release of power is required from a low voltage source.

### PHOTO CELLS

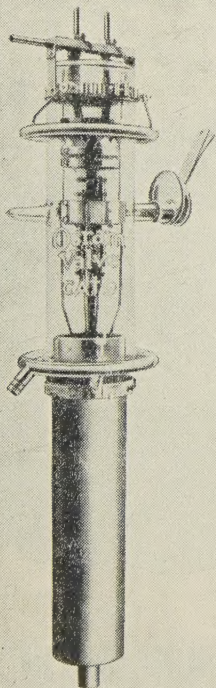
Vacuum or gasfilled — with various characteristics both in applied voltages and colour response.

### ELECTROMETER VALVES

Used in conjunction with glass electrode for pH determination.

### CATHODE RAY TUBES

For acoustic tests, sound and waveform analysis, pressure indication, chemical analysis, educational demonstrations, monitoring, laboratory instruments, electro-medical and biological investigation, navigation aids, etc.



# These dials will interest you :-

## DIALS & DRIVES

### TYPES D-115-A & D-206-A

Type D-115-A employs a 20 : 1 worm reduction gear providing a right-angle drive for two components.

Type D-206-A employs a 20 : 1 spur reduction gear providing a single in-line drive.

TYPE  
D-115-A

## Outstanding features:—

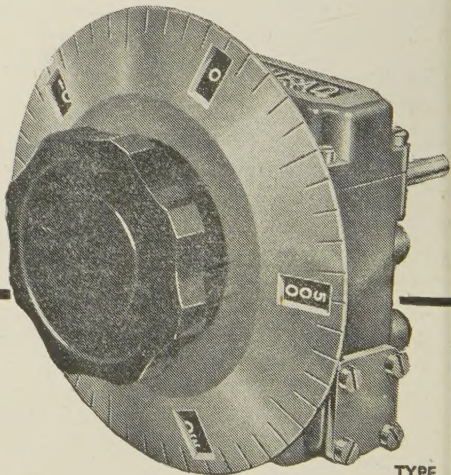
- High reading and setting accuracy by means of a dial embodying an added mechanism—effective scale length over 12 feet with 500 divisions.
- Gears spring-loaded to reduce backlash.
- Rugged die-cast construction and substantial bearings for long and continuous service.
- Shafts :  $\frac{1}{4}$  in. diameter and  $\frac{1}{2}$  in. projection.
- Finish : gunmetal with engraving filled white.
- Weight : 2½ lbs.

Dial manufactured under licence from the  
Sperry Gyroscope Co. Ltd., Pat. No. 419002.

Full description in Bulletins B-532-B and B-556-A.

# MUIRHEAD

MUIRHEAD & COMPANY LTD., ELMERS END,  
BECKENHAM, KENT • BECKENHAM 0041 - 0042.



TYPE  
D-206-A

FOR OVER 60 YEARS DESIGNERS & MAKERS OF PRECISION INSTRUMENTS



# FIRTH-BROWN

Polished and magnified 100 times, these examples show the progress of the Steelmaker's art. Most of the Steel user's troubles come from the unwelcome presence of "inclusions". Modern plant and modern methods remove these causes of service failure.

**THOS FIRTH & JOHN BROWN LTD** **SHEFFIELD**



POTENTIOMETERS	DYNAMOMETERS
ELECTROMETERS	WATTMETERS
GALVANOMETERS	THERMIONIC VOLTMETERS
BRIDGES	OSCILLOGRAPHS
RESISTANCES	A.C. BRIDGES & SOURCES
TESTING SETS	INDUCTANCES
UNIPIVOTS	CONDENSERS
SPECIAL INSTRUMENTS	

# A.C. AND D.C. MEASUREMENTS

THESE two folders give concise technical data of more than 120 electrical measuring instruments. They form handy reference sheets for laboratories, workshops and all organisations where electrical instruments are employed. May we send you one, or both?

**FOLDER 53-L.** describes D.C. instruments.

**FOLDER 54-L.** describes A.C. instruments.

**CAMBRIDGE INSTRUMENT COMPANY LTD.**

13, GROSVENOR PLACE, LONDON, S.W.1.  
WORKS: LONDON & CAMBRIDGE.

# THE PROCEEDINGS OF THE PHYSICAL SOCIETY

VOL. 57, PART 2

1 March 1945

No. 320

---

## THE FORMATION OF METAL-SPRAYED DEPOSITS

By W. E. BALLARD,  
Dudley

*MS. received 25 October 1944*

**ABSTRACT.** During the last two decades many papers on metal spraying have appeared, some of which are of very great technical importance, though very little of the published work has given any indication of the fundamentals of the process.

The difficulties of research on the process are examined, these difficulties being increased by the rapidity of the cycle of events in the process of wire spraying. Some difficulties have been overcome by the use of the high-speed ciné camera, which has indicated that the spray of metal is rapidly pulsating and that a retraction of the deposited agglomerates of particles takes place on the surface. A theory is put forward to show that surface tension plays a considerable rôle both in the pulsation of the spray and in the ultimate structure of the coating. Some indications are given that the amount of metal sprayed in unit time is controlled by well-known physical laws, and an empirical formula for speed of working is given and examined. Developing the theory of the action of surface tension at the moment of impact, explanations are given for certain phenomena observed in depositing the metal on smooth glass and roughened metallic surfaces, including the problem of adhesion. Some effects due to the spread of the spray, marginal deposits and the temperature of deposition are noted, and a tentative explanation for the varying percentage loss with different metals is advanced.

---

### § 1. INTRODUCTION

SINCE the invention of the metal-spraying processes by Schoop, in 1910, there has been published a great mass of technical literature; unfortunately a large percentage of this has described in detail special makes of tools and has been coloured by trade influence.

In the *Journal of the Institute of Metals* there may be found three papers describing metal spraying in various stages of development. The first, by Morcom (1924), was an account of what was then an entirely novel conception in the art of working metal. In 1924 the process was developing commercially in this country, and T. H. Turner and the present author described the wire process and the properties of the deposited metal. A period of considerable expansion in the industry then took place, and the third paper was contributed in 1937 by E. C. Rollason, in which the author surveyed a somewhat wider field and compared the results obtained by the three spraying processes in use in commerce. Since that date, the use of sprayed metal has become general in many branches of engineering and very great advances have been made, both in the apparatus used and in the application of the deposits. The present paper is not intended to describe these advances, interesting though they may be, but rather to endeavour to explore some of the fundamental physical considerations

involved in the art of metal spraying. The paper deals specifically with the wire process unless otherwise noted, but the comments do not refer to any one type of apparatus.

Comparatively few papers in the literature of the subject have described work of a fundamental character, and there are many contradictions and ambiguities. This is undoubtedly due to the many variables which affect the process, and the very great difficulties presented in exact evaluation. For example, it might appear to be easy to measure the exact adhesion of sprayed metal to the base by one of the methods developed for electro-deposits (see Hothersall, 1943); but in fact such methods are not applicable because it is necessary that the deposit be built up to sufficient thickness to resist the test load, and this increase of thickness will, unless the shape of the test piece be very carefully chosen, seriously affect the result. Methods relying on soldering the sprayed coating to the apparatus must also be suspect because even slight heating affects internal stress.

Recently Ingham and Wilson (1944) have described a method of testing adhesion which seeks to overcome these difficulties by depositing the metal on a shaft in which there is inserted a close-fitting plug. The method would seem to be very promising, but even so it is not entirely certain that the results give the measure of true adhesion. This does not mean that adhesion tests are valueless; it merely indicates difficulties in exploring the problems of spraying in what would appear to be a straightforward example.

Schoop (see Rollason, 1939) believed that the metal particles shot from the gun became solid during transit and became molten again at the moment of impact, due to the release of the kinetic energy. This view-point was contested by Arnold (1917) in one of the most instructive papers on the subject that has been written. Arnold's calculations are, however, open to question because he assumes that the temperature of each metal particle at the moment of impact is that of the surrounding envelope of gas. This is extremely unlikely. Furthermore, the temperature of 70° c. assumed by Arnold for the gaseous envelope is far too low, as will be seen later.

Turner and Ballard (1924) and Rollason (1937) have shown photographs of splashes of sprayed metal on glass, indicating that the metal is completely liquid in some cases, and Rollason, by means of back-reflection x-ray photographs, has shown evidence of some cold work in the deposits.

All workers agree that there is no alloying of the sprayed metal to the base metal, but many theories have been advanced to account for the adhesion of the deposit, none wholly satisfactory. The simplest idea appears to be that the deposit interlocks with the interstices of the shot-blasted base, giving a type of microscopical dove-tailing. This is undoubtedly true, but a molten metal allowed to solidify on a shot-blasted mould will also fill these interstices, though the adhesion will not be as high as that of a sprayed layer. There would seem, therefore, to be some other factor involved. In the paper of 1924, Turner and the author wrote: "It is possible that these illustrations may prove of interest to those engaged upon the problem of surface tension in metals". In this paper an attempt will be made to show that this suggestion contained a possible explanation of some of the phenomena of metal spraying.

Before considering this further, it should be appreciated that the difficulties of investigating these problems are intensified by the rapidity of the events of the process. The metal is melted, is divided into small particles, travels through the spraying distance and is deposited, all in an extremely small part of one second. It might be argued that a similar sequence of events, perhaps of a more complicated nature, takes place in electro-deposition, that is, the tearing off of metal from the anode, passing into chemical combination, migration, decomposition and deposition at the cathode, all of which may take place, under some conditions, in a short time. It should be remembered that although the particle size in spraying is very small, it is certainly very large when compared with the ion in electrolysis, and, therefore, the processes are not comparable. Except for Arnold's work, there are no definite data available on the speed of the sprayed particles.

It will be admitted that for a metal to be sprayed from a wire it must be melted. It is possible, by speeding up the wire-feed to the flame, to get lumps of plastic metal torn from the wire, but they are immediately apparent, being large and irregular in shape and not being a normal feature of the process. The first assumption is, therefore, not affected by this possibility.

Now the surface tension of metals is known to be very high (see Burden, 1940), and therefore as each drop of metal is pulled from the wire by the surrounding gases, it will assume a spherical shape, and it is reasonable to suppose that each drop will be accompanied by a very tiny drop, the well-known Plateau spherule. The author believes that much of the exceedingly fine dust generated during spraying is caused by the dissemination in the atmosphere of these spherules. They are so small that they cool quickly, and unless entrapped by a larger particle do not adhere to the surface to be sprayed but are carried away by the gases. Occasionally, however, one is so entrapped and can be seen in the micro-structure of the sprayed metal. Figure 1 shows these bodies in a sample of sprayed medium carbon steel. In the case of zinc, the existence of these spherules in the air around a pistol probably accounts for the beneficial physiological effects on the operators observed and reported elsewhere by the author (1943). The existence of the spherules does not modify the structure of the deposits to any extent, and their existence is merely noted as a matter of interest.

The spherical drop of metal, having left the wire, commences on its journey towards its final resting place in the deposit, and by the time this is reached, the drop

(i) may still be liquid;

(N.B. Or it may be solid, and so hot that the release of kinetic energy on impact remelts it, in which case it may be regarded as liquid for the purpose of this argument.)

(ii) it may be solidified, but hot enough to be plastic;

(iii) it may be solid, cool and not easily deformed.

Taking the last case first, because it is the least complicated, it will be noticed that the velocity of the particles is comparatively high, and it would be normal

to expect that the coefficient of restitution between the particle and the base would also be comparatively high. In other words, one would expect such a particle to bounce and be carried away by the gas stream, except in the case in which, by collision with another particle, it becomes entrapped by aggregation. Examination of the micro-structure of sprayed metal confirms this view, as entrapped bodies, roughly spherical in form, are not a general feature of the structure, but they occasionally occur at great nozzle distances, when it would be expected that more of the particles would have cooled and have lost their initial high velocity. Such an entrapment was shown by Rollason (1937), and another such body in sprayed aluminium is shown in figure 2.

Although these entrapments are unusual in wire-sprayed coatings, they are common in powder-sprayed coatings, because some powder always escapes the hot zone of the flame and remains solid, but becomes mixed with more plastic elements.

The behaviour of the spherical drops which are liquid at the time of impact is more interesting. If a light layer of sprayed metal is formed on glass it can be examined by transmitted light, and is found to consist of particles which have a definite splash formation. Figure 3 shows such a splash of sprayed copper. This formation can best be understood by reference to the work of Professor A. M. Worthington (1894), who studied the behaviour of drops of liquid falling on to a surface which they did not wet. The patterns of the splashes in metal-sprayed deposits are often similar in design to the formations observed towards the end of the cycle of incidents before the drop becomes static, and this indicates, therefore, that the freezing of the particles is not instantaneous. The possible results of these effects will be discussed later in the paper.

The remaining class of drops includes those which, although solid, are hot enough to remain plastic, and these probably represent a fairly large proportion of the marginal spray. On impact, their spherical form will be considerably flattened, particularly at the base, that is, the area of impact and the top will be flattened by the impact of the next particle arriving. The final shape therefore is that of a plate. These particles are not seriously deformed at the top on the outside of a deposit, as they have not received blows from above, and, therefore, they are the reason for the matt appearance of the outer surface of a deposit.

In practice, spraying is often carried out in layers, that is, a surface is coated with a light deposit and the pistol then traverses the same area again to give subsequent layers. The particles on the top of each layer will be less deformed, and, therefore, the micro-structure of a coating formed in this way will show broader bands of undeformed particles. Figures 4 and 5 show respectively a coating of copper built up continuously and a similar coating built up in two passes, and in the latter the broad band may be noted.

This type of particle is, of course, subject to some cold work, and the internal structure is equi-axed, whereas the structure of the interior of the splashed drops is columnar. Examples of these two types of structure were given in Rollason's paper.

Having now briefly described the types of units one expects in sprayed coatings, it is possible to examine some of the factors influencing their distribution and some of the results of their presence.



Figure 1. 0.4% carbon steel as sprayed, showing spherules.  $\times 200$

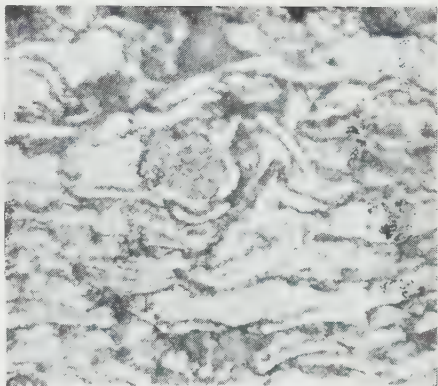


Figure 2. Aluminium as sprayed, showing entrapped particle.  $\times 200$ .

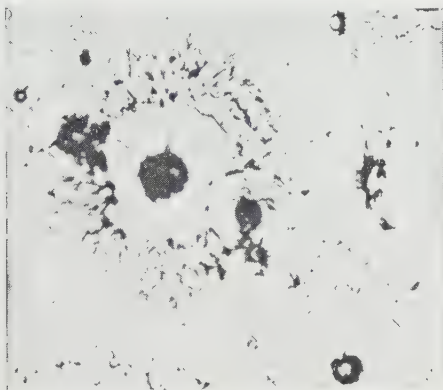


Figure 3. Copper particle sprayed on cold glass.  $\times 75$ .



Figure 4. Copper sprayed continuously.  $\times 200$ .

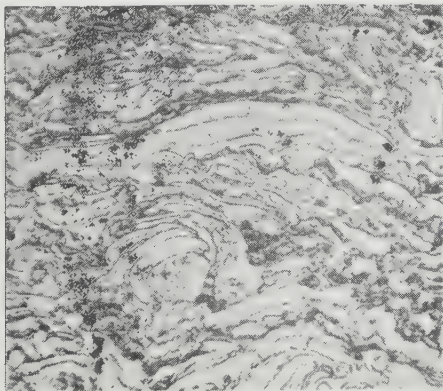


Figure 5. Copper sprayed in layers, showing one top layer.  $\times 200$ .



Figure 7. Ends of zinc and aluminium wire.  $\times 6$ .

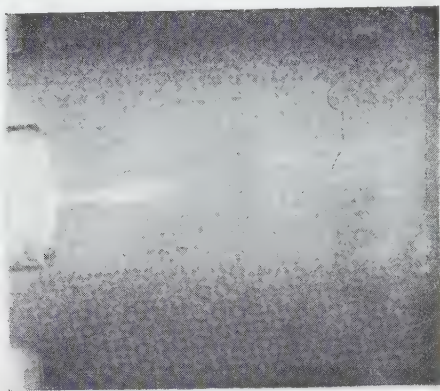


Figure 8. Still from film showing nozzle and spray. About actual size.

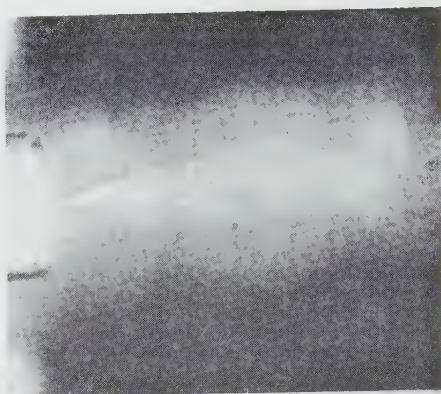


Figure 9. As figure 8, but about 1/300th of a second afterwards.

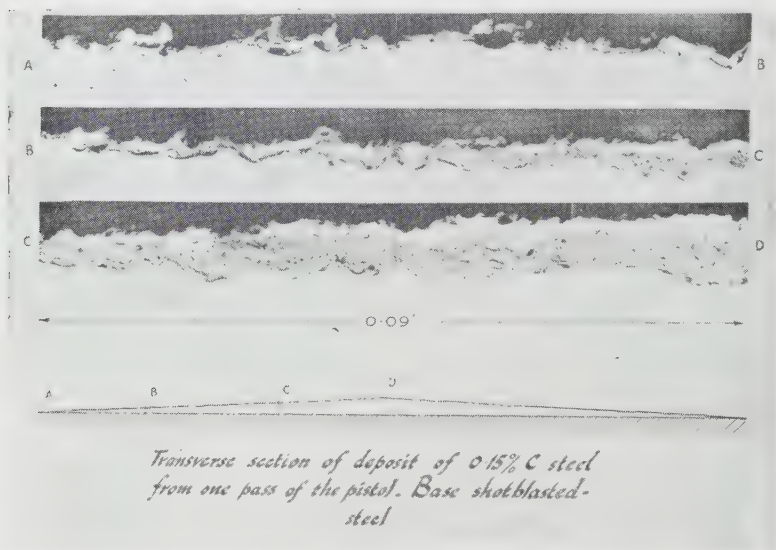


Figure 11. Composite micrographic section of steel deposit.

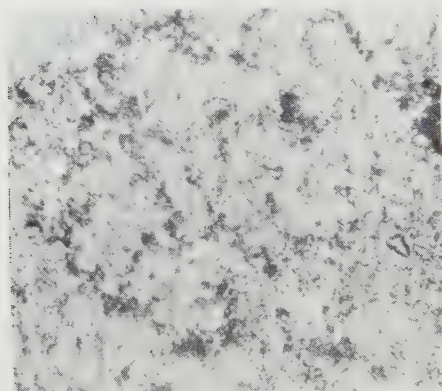


Figure 14. Under-surface of tin sprayed on glass.  $\times 30$ .

## § 2. TEMPERATURE OF GAS STREAM

Arnold assumed that the temperature of the gas stream at the working distance indicated the probable temperature of the metal particles within the stream. This was disproved by Thorman (1933), who, by means of a radiation pyrometer, sought to show that iron particles in the spray were at temperatures exceeding  $1000^{\circ}\text{C}$ . It may be suggested that this method is questionable because the majority of the particles which give incandescence to the iron spray may be themselves burning in the oxygen in the air blast. This is unlikely, as it cannot be disputed that at moderate working distances iron shows a splash effect. Furthermore, oxidation is not predominant, as the metal magnesium sprays with ease and shows little sign of burning.

It seems reasonable to suppose that the hotter the gas stream at the spraying distance the hotter will be the particles in general and the greater will be the

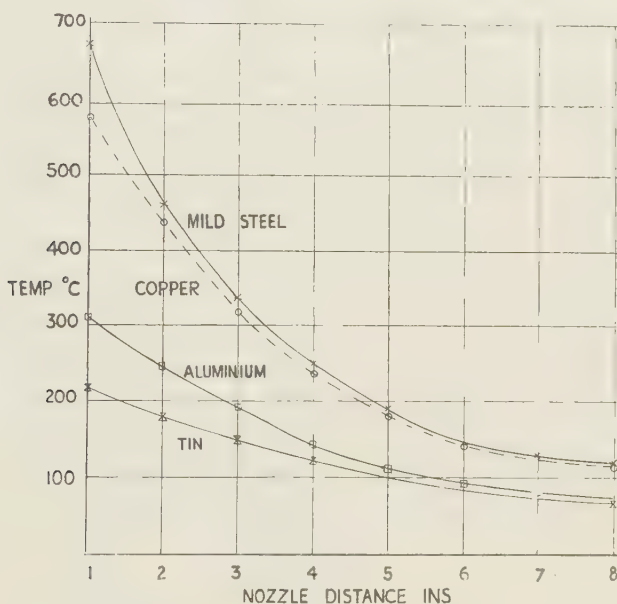


Figure 6. Curves showing temperature of gas stream at varying nozzle distances.

proportion of liquid drops. The temperature of the gases will of course depend largely on the type of pistol and the amount of combustible gas, oxygen and air that is used, besides bearing a relationship to the amount of metal sprayed and its melting point. Nevertheless, it seemed desirable to investigate the usual range of temperatures. This was done by exposing metal thermocouples of very fine-gauge nickel and nichrome wire, carefully standardized, immediately before the nozzle at measured distances. Careful blank tests were carried out to establish any effect of the metal deposit sticking to the wires. The amount of metal adhering was very small and it did not make any difference to the readings. The results are shown in figure 6, the pistol being of a standard pattern, the fuel compressed coal gas, and the wire 2 mm. diameter. It is apparent at once that the spraying process is not as cold as some have claimed. The form of the curve is interesting as it approximates quite closely to the logarithmic curve

expressing the law for bodies cooling in an air stream. It would be expected that greater divergence would be shown, because heat is absorbed by the expansion of the compressed air stream and by the air from the room, which is drawn into the pistol blast in very large quantities. It should be noted that in these experiments the thermocouple is placed in the axis of the wire, and therefore represents the maximum temperature of the gas stream at that particular nozzle distance, the outer streams of gas being much cooler. It is interesting also to note that the curve showing the pressure of the gas stream at varying nozzle distances is exactly similar in form to that showing temperature drop.

That the temperature of the gas stream is comparatively high is illustrated by the following experiment. A steel tube, 2' long  $\times$  0.6" o.d., was held in the chuck of a lathe, and a thermocouple was placed inside the tube. Brass was then sprayed on the tube with the pistol at varying nozzle distances. The time taken to reach a constant maximum temperature was noted, as was also the temperature in  $^{\circ}\text{C}$ .

Nozzle distance (in.)	Time to reach maximum (min.)	Maximum temperature ( $^{\circ}\text{C}$ .)
1	4.5	360
2	6	280
3	7	165
4	7.5	145
5	8	125
6	8.5	120
7	10	105
8	11.5	95

It is apparent from these figures that even if it is considered likely that the temperature of the particles and the gaseous stream are equal, Arnold's calculations showing that it is impossible to suppose that the particles reaching the surface could not be remelted by the release of kinetic energy are based on error, as he assumed a temperature on arrival of  $70^{\circ}\text{C}$ .

### § 3. THE FORMATION OF THE DROPS AT THE END OF THE WIRE

It was noticed long ago that if the flame of the pistol is extinguished suddenly by pinching the oxygen pipe, the wire will still be advanced by the pistol gearing, and the end of the wire which has been in the flame will show a conical form. This is only to be expected, and one would also assume that the cone will be longer the thicker the wire and the lower its conductivity. This assumption is found to be true by observation, the cone of 2-mm. lead wire having a smaller angle included at its apex than a 1.5-mm. copper wire. Further information can be gained by observation of these wire ends. Metals of higher melting point, e.g. nickel, often show spirally arranged grooves on the sides of the cone. Many metals show a thickening at the base of the cone, that is, the diameter of the base of the cone is slightly larger than the diameter of the original wire. This effect is particularly noticeable in the case of aluminium or aluminium alloys, see figure 7.

In order to examine more fully the spiral formation and the reason for this thickening, use was made of the high-speed cinematograph camera. The work was undertaken with the help of the research staff of Messrs. Kodak Limited. The camera exposes about 100 ft. of 16-mm. film in one second, and in one second between 2700 and 3000 pictures are taken. The 100-ft. length of film takes about five minutes to pass through the projector. The speed of the subject taken is therefore reduced about 300 times. Some stills from the film are shown in figures 8 and 9, which depict the spraying of a zinc wire, 2 mm. diameter, using propane as the combustible gas. It is unfortunate that while such a film is extremely revealing on projection, stills such as these reproduced from it are somewhat unsatisfactory, due in part to the texture of the sensitized layer. If the wire be examined after the pistol is stopped, zinc does not usually show the spiral effect, but the film shows that the spray is actually spiral in form, the helix being very open. The film shows also that the spray is not quite so steady as it appears to the ordinary observer, but pulsates rapidly, the periodicity being of the order of one three-hundredth of a second. The metal appears to melt on the side of the cone and to be sucked into the spiral of the flame zone. Then the suction becomes less, or surface tension increases, and the thin film of molten metals runs back and collects as a ridge on the base of the cone. Then suction again predominates and the cycle of events recommences. Whether the action of the thin film of metal on the cone side gives rise to the twisting action, or (as seems more likely) the expanding gases tend to take a swirling path, cannot be stated with certainty at the moment, but it is hoped to carry out further experiments by means of a different type of camera and illumination in the future. The pulsations may be due to irregularities in the wire feed, but this does not seem likely, as they are quite regular. The recession of the molten film towards the base due to surface tension would in itself produce the rapid regular pulsations observed. The particles themselves are too small to be examined by the ciné method, but work will be continued by means of spark photographs.

If it be accepted that the explanation of the phenomenon occurring at the end of the wire is as described, then it should be possible to make further deductions on this basis. The metal-spraying pistol will work equally well under water, and it is, therefore, a comparatively simple matter to determine moderately accurately the total heat generated in the process. All that is necessary is that the pistol be held for a certain time in an insulated vessel containing water, the temperature of which is known, and the rise in temperature of the water can be noted and the heat calculated, making allowances for the heat content of the pistol itself, and carefully checking the temperature of the air coming away from the surface of the water. By carefully arranging the apparatus, results have been obtained which are extremely close to the theoretical values obtained by taking note of the volume and the calorific value of the fuel gas. The amount of heat required to melt the metal passing through the pistol can also be calculated within reasonable limits, and a number of experiments under various conditions have indicated that the maximum amount of heat absorbed by the metal itself is seldom more than 5 % of the total heat generated in the flame. The major part of the heat is dissipated in raising the temperature of the air which is sucked in from the surrounding atmosphere by the injector effect of the burning gases

and of the propellant leaving the nozzle at high velocity. In these circumstances it is correct to assume that the metal entering the flame reacts as a cold body entering an atmosphere in which there is a huge excess of available heat. Therefore it follows that the temperature of the flame is high compared with that of the wire, and there will be a tendency for the film of metal on the outside of the wire to gather heat extremely quickly and become molten. As soon as it is molten it will be torn away by the suction effect. Where a metal has a very high conductivity, as is the case with copper and aluminium, the heat will pass very quickly from the surface film towards the centre of the wire, and the film of molten metal will tend to be thicker than the film of a metal with a lower conductivity. This is probably the explanation of the fact that the particle size of copper and aluminium tends to be larger than that of zinc or iron when sprayed under the best conditions.

Proceeding with the argument, it follows that if melting occurs in films as stated, the area of the hot film will have a predominating influence. Rejecting for the moment the length of the cone at the end of the wire, this area, which is always being renewed, will be dependent on the volume of wire used in a given interval of time, and this again, if the diameter of the wire is the same, will depend on the speed of wire passing. If the diameter of the wire be altered, then the area will also be subject to change, but if this is correct, then a change in wire diameter will bring about a proportional change in the volume of wire passing. There may, at first sight, appear to be an objection to this argument because the amount of heat taken up by various metals will be different in accordance with their specific heats and their latent heats of fusion. If, however, there is a large excess of heat available, then this factor would not appear to be so important as the area of metal presented to the flame, this area being, as already stated, largely dependent on wire diameter. The other factor which will affect the area considerably is the length of the cone if it varies within very wide limits, but as a rule the length of the cone is not very widely different with the same diameter of wire, although, as already stated, there is some variation.

If the length of wire sprayed in unit time be plotted against the melting point of the metal, the curve will, under certain conditions, be logarithmic, and it is found that with metals melting under  $700^{\circ}\text{C.}$  it will take the form which satisfies the equation

$$T = Ke^{-l},$$

where  $T$  = temperature ( $^{\circ}\text{C.}$ ),  $K$  = a constant,  $l$  = length of wire sprayed in unit time (ft. per min.).

This is closely parallel to the law for bodies cooling or being heated under these conditions. The value of  $K$  can be found by experiment for any one diameter of wire and spraying condition, but the reason for any particular value does not appear to be clear. Actually, the hot gases are in the state of turbulent flow, and the pick-up of heat will be dependent on transfer through the interfaces, i.e. hot gas to molten film and molten film to solid metal.

The value of  $K$  will vary to some extent with the particular fuel gas used and the shape of the nozzle. It is probably a composite of several factors, including dimensionless groups similar to the Reynolds number. The curves shown in figure 10 apply to a multi-fluted nozzle, using propane as the fuel gas. If the

same gas is used throughout and the nozzles are similar in construction,  $K$  is directly proportional to wire diameter. In the curves shown,  $K = 2100$  for wire of 1.5 mm. diameter. These facts seem to add confirmation to the theory of film formation on the wire tip.

It has been mentioned that this is only true for those metals or alloys melting at temperatures below  $700^{\circ}\text{C}$ . If the curves are extended above this range, they indicate false values in the case of the larger-diameter wire. The higher curve for 1.5-mm. wire appears to be merely an extension of the curve below  $700^{\circ}\text{C}$ ., i.e. the value of  $K$  remains unchanged. For 2-mm. wire the value of  $K$  is considerably reduced, and for 11-gauge B.S. the value of  $K$  closely approximates to that for 2-mm. wire below  $700^{\circ}\text{C}$ . This indicates that, considered from the point of view of thermal efficiency, the spraying of thick wires of the higher

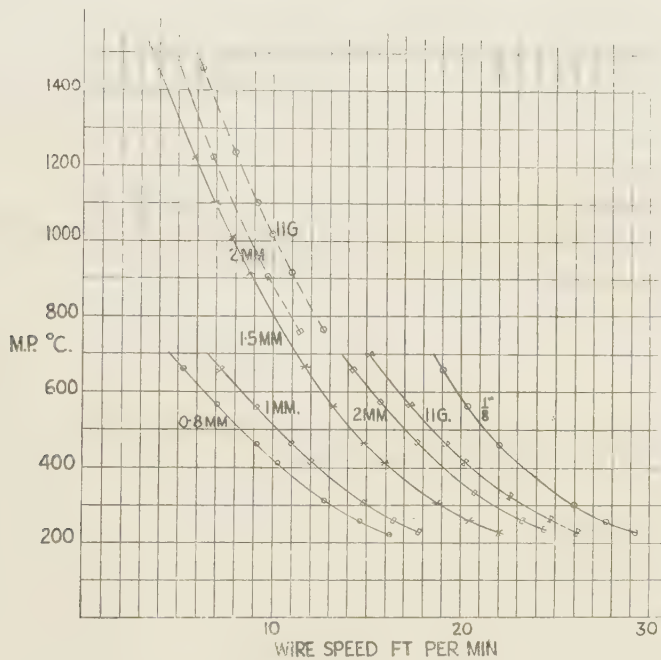


Figure 10. Curve showing relationship between melting point and wire speed.

melting-point range is not desirable. In practice this is recognized, e.g. in American practice, where the tendency is to use  $\frac{1}{8}$ " diameter wire for the lower range and 11 B.S. for the high range. The reason for this can be indicated. If one observes the end of the wire while spraying metals in the high range, it is seen that the wire tip is visibly hot, and as radiation increases rapidly with temperature one would expect a high heat-loss by radiation from the cone surface. This will reduce considerably the value of  $K$ . It is curious, however, that the curves as found by experiment take the same form as those in the lower range, at least for melting points up to  $1500^{\circ}\text{C}$ ., because as the amount of radiation increases rapidly with temperature it might be reasoned that the slope should be greater. Furthermore, the usual form of such curves requires the use of another constant in the negative power of the exponential, but in this case its

value is undetermined. Therefore these curves and formula can only be considered as empirical, but giving some indication of the mode of formation of the spray.

Another point with regard to the curves, showing relationships of the wire speed to temperature, is that it is interesting to note that the curves for very fine gauges of wire are misleading, as it is possible to spray at a very much faster rate than the curves indicate. The curves cross the temperature axis, which means that it should be impossible to spray small-diameter wires having a melting point above that shown by the intersection. This is certainly due to the fact that the reservoir of heat in the flame is so great that, with the thin wires, melting takes place by the formation of a small drop at the end of the wire rather than by the tearing of a film which has been described in the more commercial sizes of wire. Actually, this drop formation and the disintegration of the drop by the propellant gas is quite a satisfactory method of spraying, and, in fact, the coatings produced are much finer in texture because the metal has excess of heat, and is consequently broken down into fine sprayed particles much more easily by the gas stream. Hence in practice very fine coatings of steel can be obtained with 0.8 mm. or 1 mm. diameter wire.

#### § 4. THE PARTICLES IN FLIGHT

Little information is as yet available regarding the speed of transit. Arnold in 1917 carried out experiments to determine the speed of sprayed particles, and concluded that it approximated to 130 metres per second at normal spraying distances. There is no reason to dispute Arnold's work, but it is hoped to check it in the near future by means of high-speed photography. The actual speed, however, is not of great importance in considering the final coating. There is no reason to suppose that during transit the particles are other than spherical in shape, and it is extremely likely that they have a spinning motion in view of the spiral form of the mass of the spray.

#### § 5. THE FORM OF THE SPRAY

It would be expected that in common with the usual types of spray the metalliferous spray would be concentrated in the central zone and more diffuse in the outer portions. That this is so is apparent if one watches the spray of steel, this spray being itself luminous. What is not generally realized is that the central zone is comparatively narrow and the metal content highly concentrated. This can easily be shown by drawing the pistol along a suitably roughened surface at normal spraying distance and examining the result.

Figure 11 shows a composite microphotograph of a section of the deposit of steel from one pass of the pistol passing and depositing on to a shot-blasted surface of steel. It will be seen how loosely packed are the particles in the marginal deposit, and also how loosely it adheres to the surface until covered with the subsequent layers. It will be realized therefore that the porosity of sprayed coatings is largely dependent on the marginal particles. This explains the increase in porosity with increasing nozzle distances. It may be assumed that it might be preferable to spray very heavy layers and gradually cover the surface by slow movement, but this is not true because the marginal particles cause

porous layers to form on each side of the spraying area, and coarse porosity occurs from the base metal to the surface. This is often more dangerous than porous layers lying parallel to the base.

Reference to figure 12 shows the actual zones diagrammatically. The central zone responsible for the greater part of the deposit lies between AA in the case of steel. The spray is luminous between BB and some small deposit occurs in this area. Metals of lower melting point, e.g. zinc, give sprays containing much more metal (i.e. the metal consumption and deposition are greater), and these sprays tend to have a slightly wider throw, the particular pistol used spreading

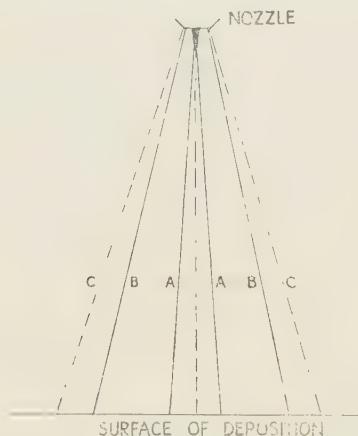


Figure 12. Diagram of form of spray.

between the limits CC. It is often suggested that pistols having a large spread should be made, i.e. "that a white-wash brush is needed instead of a camel-hair pencil". It will be seen that all the metal must come from a focal point, i.e. the apex of the wire cone, and increase in wire diameter does not necessarily mean larger spread. There are methods of increasing the area of deposit (e.g. fan-nozzles), but these necessitate many particles travelling great distances, and possibly becoming cooler. For that which follows it will be seen that this may not be advantageous.

#### § 6. THE DEPOSITION OF THE PARTICLES

In considering the events at the time of impact, it is desirable to consider deposition:—

1. On smooth surfaces, such as glass. (This, of course, is never carried out commercially.)
2. On suitably roughened surfaces, usually of metal.

##### (a) Deposition on glass

The surface of glass can be considered for the purpose of this discussion as being smooth, and it is also a surface which is not wetted by liquid metals, for example mercury. At the same time it is admitted that at exceedingly high temperatures, above the softening point of glass, some effect similar to wetting might be noticed. Such effects do not appear to be seen in metal spraying.

Also, glass is a poor conductor of heat (about  $0.0025$  calories  $\text{cm}^{-1} \text{sec}^{-1}$ , compared with  $0.167$  for iron and  $1.041$  for copper). That surface conductivity might have some effect must be realized, although the major dissipation of heat is caused by the gas stream. This was pointed out by Parkes in a written communication to Rollason's paper (1937). Also, by reference to the experiments already described, it will be seen that the steel tube sprayed with brass at  $1''$  distance reached a maximum of  $360^{\circ} \text{C}$ . The temperature of the gas stream was  $510^{\circ} \text{C}$ . at this distance. It follows, therefore, that in this case some dissipation does occur by way of the receiving surface, and also, that a hot particle arriving at a glass surface will cool slightly less quickly than a similar particle arriving on a steel surface.

Reference to the work of Turner and Rollason shows that the particles first deposited on glass surfaces form well defined splash figures, as shown in figure 3.

Now Worthington (1894) showed that drops of mercury falling on glass assume well defined forms, some of which are shown diagrammatically in figure 13. It is possible, also, by careful visual examination of spots of water on clean glass, to follow similar events. It is, of course, realized that here we are only concerned with those particles which arrive at the surface as molten drops or become molten at the moment of impact.

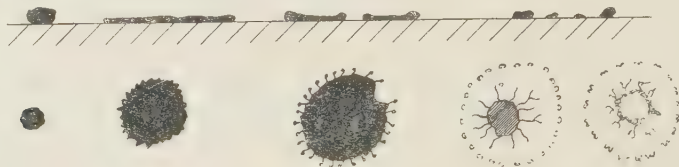


Figure 13. Diagram showing splash forms.

A molten drop, arriving at the surface which it does not wet, will first spread out as a flat plate, and will, if surface tension does not operate, continue to spread until the plate became of unimolecular thickness or the drop solidifies. The spreading is of course helped if the drop has arrived at high velocity, but even then, after a short interval, surface tension restrains this spreading tendency, the edge of the plate becomes thickened and there is a tendency for the thickened edge to break and form a ring of small spherical drops, leaving a spherical drop in the centre, smaller than the original. This action of retraction also causes a number of radial splashes. In the case of the sprayed drop, solidification may occur at any instant in the cycle of events. After examining the sprayed particles on glass, it will be seen that most of the forms of splashes described by Worthington are present. It is apparent, therefore, that in considering the formation of sprayed metal coatings, retraction of individual drops or aggregates of drops, due to surface tension, must be taken into account. Oxide films on the particles or aggregates also cause modifications to the splash effect, as they tend to interfere with the distribution of surface energy. A film of the arrival of drops of zinc and of steel on glass was prepared by the high-speed camera. The camera was focused on a glass plate and the plate was sprayed from the other side. On showing the film at normal speeds, the retraction of some of the

agglomerates of particles can be observed. It is unfortunate that it has been found impossible to take from the film representative stills showing this effect. In the case of some metals, most of the particles are frozen in the first stages of spreading and retraction and most of the particles appear roughly circular in shape, with serrated edges. This is shown by cadmium, lead, tin and zinc, and these metals have a comparatively low heat-content when fused. On the other hand, aluminium, iron, nickel and copper have high heat-content, and these metals show more variation in the pattern of the splashes.

One aspect of this is perhaps shown as follows : consider an ideal case, never obtained in practice, of all the particles being molten on impact. All particles of the metals with high heat-content will give pronounced splash effects and the patterns will be much broken up. Surface tension will have caused many small spheres, not connected if the layer be one particle in thickness. If the metal has low heat-content, the drops will be frozen when the surface tension is at its maximum value, considering the flattened drop as a whole. These metals will show, in general, higher adhesion, for reasons discussed below.

### *(b) Deposition on metals*

If a slightly roughened surface, such, for instance, as the normal surface of a coin, is sprayed, a very perfect negative is obtained, the smallest detail of the pattern being shown. On the other hand, if glass be sprayed, the surface of the metal film nearest the glass will not be smooth, but will contain a large number of regular pits. This fact has been noted by many workers, and Hoppelt gave as an explanation that the particles tended to glide on the smooth surface and lift before coming to rest. This explanation is difficult to follow and appears incorrect. The author believes that this phenomenon is due to the effect of surface tension. It is obvious that as the coin does not show this effect, the particle aggregates fill in every space in the first layer applied except, of course, the microscopical pores present in sprayed coatings. On the smooth surface of glass, possessing poor heat-conducting properties, there is nothing to impede the retraction due to surface tension. The first layer is covered before retraction has set in, then the first layer retracts, the second layer retracts a moment later, and so on, thus forming small pits.

It may be argued that it is unnecessary to bring in surface tension, because the same effect may be explained by ordinary contraction due to cooling. It will be seen from figure 14 that the area of the holes is too large to be covered by this explanation. The highest contraction allowed in making castings of most metals is about 2%. Taking area into account, this is insufficient to account for the phenomena described, although, of course, it is a contributing cause.

If the pistol be held at considerable distance from glass, the majority of the particles will be solid and plastic before reaching the glass. Splash effects will not be noted and the structure will appear to be built up of small, roughly circular units and the surface next to the glass will be nearly smooth. It should be noted, however, that adhesion is very small, and it takes a long time to form a coating, that is, such methods give a high percentage loss. It is impossible, however, to make a completely smooth coating in this way because some of the particles will be molten and act as described above.

## §7. LOSS IN SPRAYING

This is a very difficult subject for investigation, because losses in spraying are dependent on so many factors, the following all having a very great influence on the actual loss figures :—

1. The movement of the pistol nozzle in relation to the surface sprayed.
2. The nozzle distance.
3. The type of surface.
4. The actual contours of the surface.

Nevertheless, it is possible to prove in every case that the loss with aluminium and its light alloys is very much less than with the other metals. Also, although tin has a very low melting point, the tendency is for lead to show the highest loss. In extreme cases, the loss with aluminium is one-tenth that with lead and about one-sixth of the loss with such metals as zinc and tin.

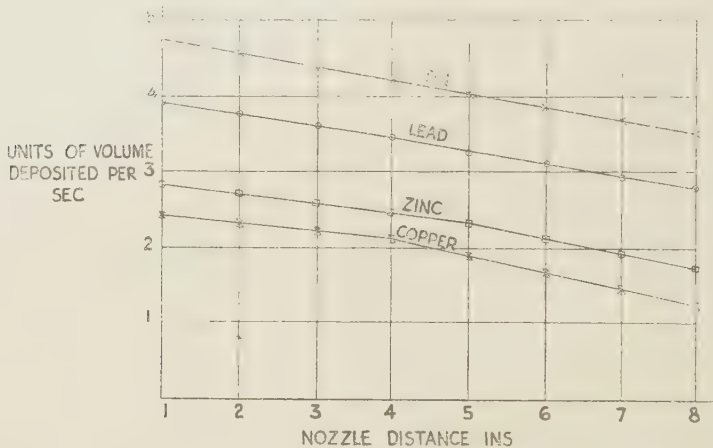


Figure 15. Curve showing volume of metal deposited at various nozzle distances.

If one assumes that the particle size is not widely different, and it is assumed that the speed of the particles also is of the same order, it follows that the kinetic energy in each particle will be a function of its mass, and, therefore, the kinetic energy will bear some relationship to the reciprocal of the density. The aluminium particle would therefore appear to be likely to have one-quarter of the energy of the lead particle and one-third that of most other metals. In these circumstances any solid particle reaching the surface would be likely to bounce off much more easily in the case of lead than in the case of aluminium. This, therefore, would seem to indicate that the argument is sound, although many other factors will contribute to the final figures obtained for loss. For instance the proportion of total heat in an aluminium particle just solid would be four times that of a similar sized particle of lead. The metals of high melting point, such as steel and nickel, give a lower loss figure than would be indicated by considerations of kinetic energy alone, but the amount of heat in a solid particle nearing its melting point would be five times that of the lead particle. It would appear, therefore, that while it would be extremely difficult to express in a

mathematical formula the probable losses for any metal, the main contributing factors are the kinetic energy and the heat content.

If the volume of the metal deposited in unit time, under similar spraying conditions, be plotted against nozzle distance as the only variant, it will be found that for the metals of low melting point a straight line is obtained (figure 15), indicating that loss increases proportionately to increased nozzle distance over the normal range of spraying distance. In the case of the metals of higher melting point, this is true to a certain critical distance, after which a straight line of greater slope is obtained. In other words, beyond this distance loss increases more rapidly with higher nozzle distance. It is submitted that beyond this critical distance the majority of the particles are solid—hence the change in slope.

#### § 8. DEPOSITS ON METAL AND SOME PRACTICAL OBSERVATIONS

We have considered the deposits made on smooth glass because the information gained leads to the assumption that surface tension has a considerable influence on their formation. Commercially, the deposits are usually applied to a roughened metal surface and the conditions are somewhat different. It is still true that there is no indication that the sprayed deposits actually wet the metal surface, but the conductivity of most metal surfaces will be considerably higher than the conductivity of a glass surface. Therefore, the particles will chill much faster than on glass, and the effects of surface tension will not be so apparent, as the metals will be solid before full retraction has taken place. If, therefore, surface tension is playing its part it would be expected that the adhesion of sprayed metal to an equally roughened surface of a metal of high conductivity would be somewhat less than that obtained on a metal surface of lower conductivity. This is, in fact, true, as it is more difficult to obtain high adhesion on cold copper or cold aluminium than it is on cold steel unless special arrangements are made with regard to surface roughness. Here again, however, the argument can be pressed too far because, if this is wholly true, the difficulty could be partly eradicated by heating the base metal, but this is not found to be particularly efficacious. It is obvious that the heating of the base may cause the formation of oxide films which may be torn apart by surface tension of the sprayed metal, and they in themselves will become loose and detachable from the surface.

The use of a suitably roughened surface such as that made by shot-blasting with a suitable grade of shot would seem to rely on the fact that the particles or agglomerates of particles, when they rest over the roughness of the surface, tend to retract in the way that has already been described, and this retraction will bind them on to each small mountain in the surface. As these mountains are more or less evenly spaced at very close intervals, retraction, instead of taking place over the whole sprayed surface, as in the case of smooth glass, is confined to shrinkage on to each raised portion, and, therefore, the effect of the shrinkage is to cause adherence to the surface as a whole rather than to tend to pull away in areas as is the case with glass. This effect, which is so important on shot-blasted surfaces, would not be found in the case of large contours such as a smooth screw-thread, because it will be seen that such large contours would be out of proportion to the size of the agglomerates of particles. In commercial practice,

however, the rough threading of shafts, for instance, does not leave a smooth surface within the thread, the surface itself being torn and so acting as a shot-blasted surface. Naturally, if the surface area is increased by such methods as screw threading, then the adhesion of the particles is increased per unit area of the original article, although it would not be increased in each very small area of the thread itself. As the thickness of the deposit increases, the shrinkage will go on in each layer, and obviously in the case of the grossly roughened surface, the shrinkage of the layers on top of each other will tend to bind it mechanically to the corrugation of the surface. In other words, on a normal shot-blasted surface the adhesion is largely due to surface-tension retraction effects, but on a screw surface this effect is increased by the retraction of the whole mass of metal on to the corrugations, so forming a mechanical lock.

One of the difficulties of the corrugated surface is that the solid particles passing down the margin of the sprayed cone do not so easily get carried away by the gases if they strike tangentially on the surface, and the result is that one may get porosities in the bottom of screw threads, for instance, due to the retention of the solid marginal particles. This is particularly obvious if the screw threads are too deep and too narrow.

If a pistol be held at an angle to the surface which is to be sprayed, there is a tendency to build up more quickly on the one side of the cone, and retraction, therefore, takes place preferentially towards the thickened section; this effect is likely to be cumulative. This is one of the causes of the rippling effect that is often shown when thick deposits are made under such conditions that the pistol cannot be applied at right angles to the surface to be sprayed.

It is known that the porosity of the coatings made by spraying increases with the nozzle distance (Fassbinder and Soular, 1936; Ballard and Harris, 1936; Sillifant, 1937), and this is understandable in the consideration of the theory set out. Obviously, as nozzle distance increases, so will the number of solid particles reaching the surface, and the marginal effects will be more pronounced. At small nozzle distances, when the greater part of the deposit is formed by molten particles subject to chilling and retraction, the porosity is very small, and it would appear that the inclusion of solid particles (mainly due to marginal spray) is the major factor in the formation of the pores in sprayed metal.

Futhermore, at small nozzle distances, contraction will be greater, due to normal contraction of cooling metal and to the retraction effects which have been noted. If the coating is comparatively weak, the contraction effects will be enough to cause cracks as it cools. This effect is not often very apparent, but in the case of deposition of mild steel, if the speed of wire is increased too much by increasing the oxygen pressure of the flame, the coating becomes very oxidized and very friable, and if the metal is deposited on a shaft, the force of contraction becomes greater than the strength of the coating and cracks appear. It is suggested in some trade literature that, to overcome this, nozzle distances must be increased to decrease contraction. It will be seen that this may not be a complete answer, as the coatings at greater nozzle distances quickly become more porous, and the structure will contain more solid particles. Under heavy loads this type or coating will tend to collapse and crack.

§ 9. CONCLUSION

This paper cannot claim to be exhaustive or to explain completely the phenomena connected with the art of metal spraying. Its purpose is to indicate some theoretical basis for observed facts, and to endeavour to describe some of the fundamentals involved. The author is deeply conscious of many problems yet unsolved. It is hoped that the ideas advanced may serve as a basis for further research.

ACKNOWLEDGMENTS

The author wishes to express his thanks to his laboratory staff, who have carried out the experimental work described, and to his colleagues on the Board of Metallisation, Ltd., for their encouragement of research.

REFERENCES

- ARNOLD, H., 1917. "Das Metallspritzverfahren : seine wissenschaftlichen, technischen und wirtschaftlichen Grundlagen." *Z. angew. Chem.* **30**, 209.
- BALLARD, W. E., 1943. *Brit. J. Phys. Med.* **6**, 21.
- BALLARD, W. E. and HARRIS, D. E. W., 1936. "Some observations on the metal spraying of copper". *Proceedings XII International Congress of Acetylene, Oxy-Acetylene and Allied Industries* (London), **5**, 1233.
- BURDEN, R. S., 1940. "Surface tension and the spreading of liquids", *Cambridge Physical Tracts*, p. 18.
- FASSBINDER, J. and SOULARY, P., 1936. "A contribution to the study of metal coating with the pistol". *Proceedings XII Internat. Congr. Acetylene, Oxy-Acetylene Welding and Allied Industries* (London), **5**, 1219.
- HOTHERSALL, A. W., 1943. "Repair of worn or over-machined parts by electro-deposition" (*Symposium of papers on Reclamation of Worn Parts*). *Inst. Mech. Engrs.* November.
- INGHAM, H. and WILSON, K., 1944. "Procedures for testing metallising bond", *Iron Age*, pp. 44-49.
- MORCOM, R. K., 1914. "Metal spraying". *J. Inst. Met.* **12**, 116 124.
- ROLLASON, E. C., 1937. "Metal spraying-processes and some characteristics of the deposits." *J. Inst. Met.* no. 1, **60**, 35 66.
- ROLLASON, E. C., 1939. *Metal Spraying* (Chas. Griffin and Co., Ltd.), p. 94.
- SILLIFANT, R. R., 1937. "Notes on some recent experiments in connection with the spraying of steel by the wire-fed metal-spraying pistol." *J. Iron Steel Inst.* **136**, 131.
- THORMANN, H., 1933. "Untersuchungen über das Metallspritzverfahren nach Schoop" (*Karlsruhe Badische technische Hochschule Fredericana*).
- TURNER, T. H. and BALLARD, W. E., 1924. "Metal spraying and sprayed metal." *J. Inst. Met.* no. 2, **32**, 291, 312.
- WORTHINGTON, A. M., 1894. *Proc. Roy. Instn.* **14**, 289.

# COMBINATIONS OF SPHERICAL LENSES TO REPLACE NON-SPHERICAL REFRACTING SURFACES IN OPTICAL SYSTEMS

By J. L. HOUGHTON,\*

Research Laboratories, Kodak. Ltd., Wealdstone, Harrow, Middlesex

*Paper read to the Optical Group 18 September 1942 ; MS. received 3 October 1944*

**ABSTRACT.** The substitution of lens systems of infinite focal length for non-spherical correcting plates is discussed, and formulae and examples are given for two- and three-component systems. It is pointed out that such systems may be used to introduce under- or over-correction of chromatic aberration and coma, in addition to spherical aberration, into a system. In the case of lens systems used in conjunction with spherical mirrors, the thicknesses and curvatures of the components are relatively small as compared with those found in more orthodox lenses of similar relative aperture, and the state of correction is good, though probably not so good as in the case where a non-spherical correcting plate is used.

## § 1. INTRODUCTION

**D**URING recent years several optical systems have been devised in which so-called *correcting plates* are used. The earliest and best-known example of such a system is the Schmidt camera, the basic principle of which has already been described many times. Although several ingenious methods have been developed for the manufacture of the plates, it is still a matter requiring skill and consuming much time because the figuring of the plates is extremely heavy. In view of these difficulties, the manufacture of these plates in glass on a mass-production scale is not possible at the present time, and the alternative of using plastic materials does not appear to be very promising because the accuracy of the moulding is not yet sufficiently good. Spherical refracting systems on the other hand are easy to make in quantity and easy to test, so that the replacement of non-spherical by spherical surfaces may be advantageous.

The earliest example of such a substitution is to be found in the Mangin mirror, a divergent meniscus lens with a silvered convex surface, used in projection apparatus. If the power and shape of the lens are suitably chosen, the system may be freed from spherical aberration. The non-spherical system which is the counterpart of the Mangin mirror is the paraboloid reflector familiar to all users of astronomical reflecting telescopes. Apart from its use in projection apparatus, the Mangin mirror is not of great interest as the angular field it is capable of covering is very small.

Turning now to systems covering a large field, such as the Schmidt camera, the proposal is to replace the usual correcting plate by a lens system consisting of two or more lenses, and this lens system must possess the properties of a correcting plate. It must therefore have a focal length which is large in comparison

\* Communication No. 988H from the Kodak Research Laboratories.

with the remainder of the optical system, it must be achromatic, and it must correct the spherical aberration of the remainder of the optical system. Other additional degrees of correction are possible in a lens system which are not obtainable in the conventional correcting plate. For example, the lens system may be over- or under-corrected chromatically.

## § 2. OUTLINE OF THE PRINCIPLES OF DESIGN

The approximate values of the powers and radii of curvatures of the components of the lens system are determined by the application of Seidel thin-lens equations. Most optical designers will prefer to use their own methods of design, but the following formulae from Chrétien (1938) have been found very convenient for the purpose.

Considering rays in the paraxial region, the incident height  $H_j$  of a ray on the  $j$ th lens will be proportional to the incident height  $H_1$  of the same ray on the first lens in the system, and we may write

$$H_j = h_j H_1,$$

where  $h_j$  is the factor of proportionality. Similarly, for a principal ray, the incident height  $K_j$  of the ray on the  $j$ th lens is proportional to  $\tan \theta_0$ , where  $\theta_0$  is the angle of inclination of the ray to the optic axis and

$$K_j = -k_j \tan \theta_0.$$

If a component happens to be at the diaphragm, the coefficient  $k$  will clearly be zero. The quantities  $h_j$  and  $k_j$  may be calculated once the powers and separations of the components in the optical system are known, and will be used later in the calculation of the aberrations.

The correcting lens system will be assumed to consist of two or more thin lenses in contact placed at the stop, and, if the system is achromatic, the following conditions are imposed:

$$\sum P = 0,$$

$$\sum \frac{P}{V} = 0,$$

where  $P$  represents the power of a component lens and  $V$  the dispersion figure for the glass of which it is made.

These equations are independent of the shapes of the components. The shape of the lens is expressed by

$$S = \frac{1}{2}(R_1 + R_2),$$

where  $R_1$  and  $R_2$  are the curvatures (reciprocal radii) of the two surfaces of the lens. If  $L_1$  and  $L_2$  are the object and image positions, real or virtual, on either side of a lens, a further variable  $T$  is defined as

$$T = \frac{1}{2} \left( \frac{1}{L_1} + \frac{1}{L_2} \right) = \frac{1}{2}(X_1 + X_2).$$

Quantities  $Q$  and  $E$  are then computed for each lens:

$$Q = AS^2 - 2BS + C$$

and 
$$E = GS - H,$$

where, if  $n$  is the refractive index of the material composing the lens,

$$A = \frac{n+2}{n}P, \quad B = \frac{2n+1}{n}PT, \quad C = \frac{3n+2}{2}PT^2 + \left[ \frac{n}{2(n-1)} \right]^2 P^3, \\ G = \frac{n+1}{n}P, \quad H = \frac{2n+1}{n}PT.$$

In the case of a mirror

$$P=2R, \quad Q=\frac{1}{4}P^3 + XP^2 + X^2P, \quad E = -\frac{1}{2}P^2 - XP.$$

The spherical aberration  $s$ , coma  $c$ , and astigmatism  $a$ , of the complete system are then given by

$$s = \Sigma h^4 Q, \\ c = \Sigma [h^3 k Q - h^2 E], \\ a = \Sigma [h^2 k^2 Q - 2hkE + P].$$

The insertion anywhere in the system of a correcting plate or lens system of infinite focal length will clearly not affect the  $h$ ,  $k$ ,  $Q$  and  $E$  values for the other components of the system. If, in particular, such a plate or lens system is placed at the stop, the only aberrations of the complete system to be modified will be spherical aberration and coma, because, for the correcting lens system

$$\Sigma P = 0 \quad \text{and} \quad k = 0.$$

The guiding principle, therefore, in the application of these equations to optical systems of the type under review is to design the main optical system without the correcting lenses, so that the desired state of astigmatic correction is obtained, and to ignore the spherical aberration and coma. The insertion at the stop of suitable correcting lenses will then permit the correction of the outstanding spherical aberration and coma.

Take, as an example, the Schmidt system and consider the spherical mirror alone. Assuming a mirror of unit focal length imaging an infinite object :

$$P=1, \quad h=1, \quad X=0, \quad Q=0.25.$$

The astigmatism equation then becomes

$$0.25k^2 + k + 1 = 0,$$

which yields the solution  $k = -2$ .

The stop must therefore be placed two focal lengths in front of the mirror, that is, at its centre of curvature. If this value of  $k$  is substituted in the coma equation, the coma will also be found to be zero. Hence the correcting lens system is placed at the centre of curvature of the mirror, and is designed to have

$$Q = -0.25 \quad \text{and} \quad E = 0.$$

The simplest type of correcting lens system is one consisting of two lenses, which must clearly be of equal but opposite powers. The condition for achromatism indicates that the two lenses must be made of glasses having the same dispersion. Several such pairs are to be found in the optical glass catalogues; for example, Chance Brothers list a Soft Crown 515570,  $N_D = 1.51508$ ,  $V = 57.0$ . and a Dense Barium Crown 621572,  $N_D = 1.62081$ ,  $V = 57.2$ . Let the lenses be of powers  $P_1$  and  $P_2$  and let the front lens be of Soft Crown,

The spherical aberration contributed by the first component will be found to be

$$Q_1 = 2.32006 P_1 S_1^2 - 3.32006 P_1^2 S_1 + 3.24304 P_1^3$$

and, for the second component of Dense Barium Crown,

$$Q_2 = 2.23395 P_2 S_2^2 + 3.23396 P_2^2 S_2 + 2.76256 P_2^3.$$

Similarly, the coma contribution will be

$$E_1 = 1.66003 P_1 S_1 - 1.33002 P_1^2,$$

$$E_2 = 1.61698 P_2 S_2 + 1.30849 P_2^2,$$

the  $h_3 k$  terms being zero since the lens system is at the stop.

Combining the spherical aberration and coma equations with the appropriate contributions of the mirror, which is of unit power,

$$S = 2.32006 P_1 S_1^2 - 3.32006 P_1^2 S_1 + 3.24304 P_1^3 - 2.23395 P_1 S_2^2 + 3.23396 P_1^2 S_2 - 2.76256 P_1^3 + 0.25 = 0.$$

$$C = 1.66003 P_1 S_1 - 1.33002 P_1^2 - 1.61698 P_1 S_2 + 1.30849 P_1^2 = 0.$$

There are three variables in these two equations, so that one can be fixed arbitrarily. A useful criterion to adopt is to make the front component symmetrical, that is  $S_1 = 0$ . Then from the coma equation

$$S_2 = -0.01331 P_1,$$

which is substituted in the spherical aberration equation to give a cubic equation for  $P_1$ . The final solution is

$$P_1 = -0.83012, \quad S_2 = 0.01105.$$

The curvatures are then easily determined by the relations

$$R_1 = S_1 \pm \frac{P_1}{2(n_1 - 1)} \quad R_2 = S_2 \pm \frac{P_2}{2(n_2 - 1)},$$

the positive sign being taken for the front surface of the lens and the negative sign for the rear surface.

The thin-lens specification is thus:

$$\begin{array}{ll} R_1 = -0.80582, & r_1 = -1.2410, \\ R_2 = 0.80582, & r_2 = 1.2410, \\ R_3 = 0.67963, & r_3 = 1.4714, \\ R_4 = -0.65753, & r_4 = -1.5208. \end{array}$$

The mirror, of course, will have a radius of  $-2.00$  and be distant  $2.00$  behind the above lens system. When the requisite thicknesses and diameters are introduced, trigonometric ray-tracing will reveal the outstanding errors in spherical aberration and coma. A slight adjustment of the radius of the mirror and the distance of the mirror from the correcting lens will allow the solution to be corrected perfectly.

The two-lens system may also be used in a modification of the Schmidt, first proposed by Y. Väisälä (1936). As is well known, the image field of the Schmidt is curved but anastigmatic, the radius of curvature being equal to the

focal length. By the introduction of some astigmatism the tangential field may be flattened in the manner recommended by Conrady (1929). It may be shown that the amount of astigmatism required for this purpose is one-third of the Petzval sum of the system. The Petzval sum of the correcting lens system is small compared with that of the mirror, and may be neglected. The Petzval sum of the mirror is equal to its power. Hence the equation for the stop position to give a flat tangential field is

$$\frac{1}{3} = \frac{k^2}{4} + k + 1,$$

the solution of which is  $k = -3.1547$  or  $-0.8453$ .

The first solution is not attractive, as a large mirror would be required to avoid vignetting, and the second requires a diagonal reflector or a central hole cut in the lens, because the correcting lens will then be between the mirror and image plane. If, however,  $k = -1$  is taken, that is, if the stop is at a distance equal to the focal length of the mirror, the astigmatism is 0.25, so that the tangential field is slightly "round". The coma is not zero for a stop in the focal plane; hence, if a correcting plate is used, it is necessary to figure the mirror to remove the coma. If a lens system is substituted for the usual correcting plate, the coma may be corrected in the lens system instead of by figuring the mirror. Details of the calculation of such a lens combination will not be given, as it follows closely the example already given.

The application of correcting lens systems is not of course limited to reflecting optical instruments, but may be introduced into refracting systems. As an example, consider a thin singlet lens. By choosing the shape of the lens and the position of the stop, such a system may be rendered flat-fielded and free from coma, but the spherical aberration cannot then be corrected. This correction may be carried out by inserting a correcting lens at the stop which is designed to be free from coma.

The above example is of academic interest only, when regarded from the point of view of lens designing; three components have been used to produce a system which would probably be inferior in performance to an anastigmat triplet of the Cooke type. The principle involved, however, is applicable to lens systems of various and more complicated types.

In the case of a Schmidt camera, a further lens system, suggesting itself as a substitute for the orthodox correcting plate, consists of three components, a pair of equiconvex and similar lenses with an equiconcave lens, the power of which is equal and opposite to the sum of the powers of the convex lenses, between them. A considerably wider choice of glass is possible with such a triplet formation than is the case with the doublet. Any pair of glasses may be used, including the same glass throughout, the only condition being that the glasses are of identical dispersions. The symmetrical system is free from coma regardless of the powers of the components, which can easily be verified from the formulae already given by the substitution of

$$S_1 = -S_3, \quad S_2 = 0 \quad \text{and} \quad T_1 = \frac{P_1}{2}, \quad T_2 = 0, \quad T_3 = -\frac{P_1}{2}.$$

Trial solutions will show that there is not much advantage to be gained by departing from the symmetrical shapes of the components and that a high refractive index

is advantageous in reducing zonal spherical aberration. If all the lenses are made of the same glass, the formulae become particularly simple.

Assuming  $S_1 = S_2 = S_3 = 0$ ;  $P_1 = P_3$ ;  $P_2 = -2P_1$ , the equation for  $P_1$  is

$$\left[ \frac{3n+2}{2n} - \frac{3}{2} \frac{n^2}{(n-1)^2} \right] P_1^3 + 0.25 = 0.$$

For  $N=1.8$ ,  $P_1=0.3561$  and  $P_2=-0.7122$ .

For a mirror of unit focal length the thin-lens specification for the lens system will be found to be

$$\begin{array}{ll} r_1 = 4.4932, & r_4 = 2.2466, \\ r_2 = -4.4932, & r_5 = 4.4932, \\ r_3 = -2.2466, & r_6 = -4.4932. \end{array}$$

Comparing these values for the radii with those obtained for the two-lens system, it will be seen that the curvatures are much smaller. This allows a larger numerical aperture to be used, and aperture ratios of about  $F/0.6$  are attainable with the triplet formation as compared with about  $F/1.4$  for the doublet, while still retaining adequate image sharpness.

The triplet systems are not necessarily limited to coma-free formations; for instance, by a suitable redistribution of the powers of the components with possibly differing shapes, coma may be introduced to correct that in some other part of the complete system. The design of such systems will, of course, be a little more complicated than is the case with the symmetrical systems, but it will again follow the formulae outlined earlier in this paper.

In the numerical examples given, the correcting lens systems are over-corrected for spherical aberration and are achromatic, but there is no reason why spherical under-correction may not be obtained if it is required. Chromatic over-correction may be desirable in certain cases; for example, an over-corrected system may be used in a Schmidt type of instrument where the field is flattened by an oil-immersion aplanatic lens similar to the front lens of an oil-immersion microscope objective. The system would consist of a concave lens of high-dispersion glass between two convex lenses of low-dispersion glass. The oil-immersion lens would then fulfil the double function of flattening the field and increasing the relative aperture.

Owing to the shallow curves and thin components, lens-mirror combinations of the types described in this paper are faster and more highly corrected than the more conventional lens systems, but they are probably slightly inferior in these respects to those systems using a correcting plate, since all systems using spherical surfaces are afflicted more or less with zonal aberrations. A few trigonometrically corrected examples will be found in B.P. 546,307, including the doublet and triplet Schmidt types and the flat-fielded type briefly described in this paper.

#### REFERENCES

- CHRÉTIEN, H., 1938. *Cours de Calcul des Combinaisons Optiques* (Revue d'Optique, théorique et instrumentale, Paris), pp. 228, 236, 254, 349, 477, 480, 616, 790.  
 CONRADY, A. E., 1929. *Applied Optics and Optical Design* (Oxford University Press), pp. 291-95.  
 VÄISÄLÄ, Y., 1936. *Astr. Nachr.* **259**, 198-203.

The following references, for which I wish to thank Dr. Kingslake, were brought to my notice after the above paper had been read to the Optical Group. They are offered as a small bibliographical supplement:—

Zeiss describe in B.P. 482,874 a mirror-lens system in which the reflecting element is a meniscus divergent lens silvered on the convex surface. In this case, the mirror-lens contributes strongly to the spherical correction of the complete system; in fact, it is practically a Mangin mirror. Gabor (B.P. 544,694) replaces the correcting plate of the conventional Schmidt camera by a meniscus divergent lens of which an annular ring only is used, and claims that effective apertures less than  $F/1.0$  can be obtained and fields of about  $23^\circ$  square can be covered. Martin, Flügge and Roll (U.S.P. 2,229,302) describe systems for use with curved image surfaces such as would be found in fluorescent screens of cathode-ray tubes in television apparatus. Cassegrain systems are described by Acht (U.S.P. 1,967,214 and U.S.P. 1,967,215) and by Tate (B.P. 426,539). A very important paper on the replacement of non-spherical surfaces by spherical surfaces has recently been published by D. Maksutov, "New Catadioptric Meniscus Systems", *J. Opt. Soc. Amer.* **34**, 270-284 (May 1944). Maksutov points out that a monocentric meniscus lens may be used instead of a corrector plate, and gives several examples of systems using such a lens, together with a detailed analysis of the aberrations. Empirical formulae for the design of systems of the Schmidt type are given.

## THE NON-REFLECTING TERMINATION OF A TRANSMISSION LINE

BY D. H. SMITH,  
Woolwich Polytechnic

*MS. received 13 October 1944*

**ABSTRACT.** In a recent paper, Willis Jackson and Huxley have presented some experimental results which appear not to agree with the theory of the non-reflecting termination of a transmission line when the latter is terminated by a thin film. The present paper shows that their results may be explained by the partial transparency of a very thin conducting film to electromagnetic waves, and that there is no real disagreement with the usual theory.

### §1. INTRODUCTION

THE simple theory of a transmission line shows that if it is terminated by an impedance which is equal to the characteristic impedance of the line, waves arriving at the termination will not be reflected and the line will behave as if it were infinitely long. If the losses may be neglected, as they may be in many practical applications of transmission lines at radio-frequencies, the characteristic impedance reduces to a pure resistance. It is sometimes necessary in laboratory work to provide the line with a non-reflecting load, and it becomes of interest to consider the physical nature of the conductor which is

needed. In the case of a line whose members are two similar parallel wires, it is apparently easy to place a resistance of the required value across the end of the line, in the form of a strip of suitable material, but when a coaxial line is used, this would appear to lead to an undesirable lack of symmetry. The conductor which naturally suggests itself is a disc or film of conducting material extending from the inner member to the outer member of the line, and it is easy to show that the resistance of such a film is

$$R = \frac{1}{2\pi gh} \ln \frac{r_2}{r_1} \text{ ohms,} \quad \dots\dots(1)$$

where  $g$  is the conductivity of the material,  $h$  is its thickness, and  $r_1$  and  $r_2$  are the radii of the inner and outer conductors respectively. The characteristic impedance of a loss-free coaxial line with air-spacing is

$$Z_{00} = 60 \ln \frac{r_2}{r_1} \text{ ohms,} \quad \dots\dots(2)$$

and  $R$  will therefore be equal to  $Z_{00}$  if

$$1/gh = 2\pi \times 60 = 377 \text{ ohms.} \quad \dots\dots(3)$$

The quantity  $1/gh$  is the resistance between opposite edges of a square piece of the film whose side is 1 cm., and in the current literature it is sometimes called, not too happily, the surface resistivity. The quantity 377 ohms is also the value in free space of  $377\sqrt{\mu/k}$ , where  $\mu$  is the permeability and  $k$  is the dielectric constant of the medium between the conductors; it has been called by Schelkunoff (1938) the *intrinsic impedance of free space*. It is usually assumed that, in these terms, there will be no reflection if a line is terminated with a thin film whose surface resistivity is equal to the intrinsic impedance of free space, but in a recent paper Willis Jackson and Huxley (1944) have described experiments which show that this is not the case. These authors found that when a coaxial line whose characteristic impedance was 76 ohms was terminated by a graphite film deposited on bakelized paper, of resistance 77 ohms between the inner and outer conductors, a pronounced system of standing waves was formed, and an analysis of the standing-wave pattern showed that the film behaved as a complex impedance  $23.1 - j20.1$  ohms, equivalent to a resistance of 40.5 ohms in parallel with a capacitive reactance of 46.5 ohms.

It was found, however, that the line could be correctly terminated by continuing it beyond the film to a distance of  $0.88 \lambda/4$ , where  $\lambda$  is the wave-length, and closing the extension by a short-circuiting disc. As the authors point out, there appears to be widespread misunderstanding of this problem. It has also been discussed by Howe (1944) in an editorial article in the *Wireless Engineer*.

## § 2. THE REFLECTION OF A PLANE ELECTROMAGNETIC WAVE BY A THIN CONDUCTING FILM

Neither in the original paper, nor in the discussions which have followed it, does attention appear to have been directed to the significant fact that a film so thin is markedly transparent to electromagnetic waves falling upon it, as was shown by Heaviside (1892).

There will be no loss of generality if we consider a transmission line made up of two plane-parallel slabs of perfectly conducting material,  $a$  cm. apart and  $b$  cm. wide, flanked by guard-plates separated from them by infinitesimal gaps (figure 1). The electric and magnetic lines of force are straight lines, and the geometrical relationships are peculiarly simple. The capacity per cm. of such a line is  $C = \kappa \cdot \frac{b}{a}$  farads, where  $\kappa = \frac{k}{36\pi \times 10^{11}}$ ,  $\kappa$  being the dielectric constant of the medium.

The inductance per cm. is  $L = \bar{\mu} \cdot \frac{a}{b}$  henries, where  $\bar{\mu} = 4\pi\mu \times 10^{-9}$ .

The characteristic impedance is, therefore,

$$Z_{00} = \sqrt{L/C} = \sqrt{\left(\frac{\bar{\mu}}{\kappa}\right)} \times \frac{b}{a} = 377 \frac{b}{a} \text{ ohms.} \quad \dots\dots(4)$$

Let the line be semi-infinite, and let a film of any "surface resistivity"  $R_0$  be placed across it at any point, with extensions across the guard-plates on each side.

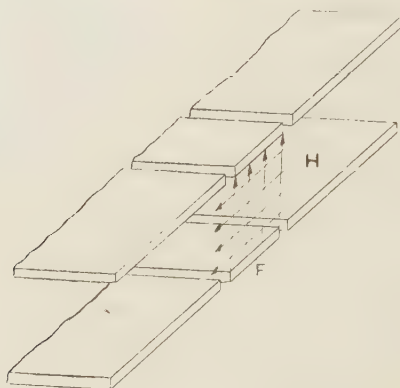


Figure 1.

The film must necessarily be very thin. Thus with graphite, which has been used in practice,  $g$  is of the order  $1250 \text{ ohm}^{-1} \text{ cm.}$ , and if  $R = 377 \text{ ohms}$ ,  $h$  will be of the order  $2 \times 10^{-6} \text{ cm.}$  With better conductors,  $h$  must be correspondingly smaller.

Consider now a plane electromagnetic wave, guided by the transmission line, which meets the film, and let  $H_1$  amperes per cm. and  $F_1$  volts per cm. be the strengths of the magnetic and electric fields in the wave.

In terms of these units, Maxwell's equations may be written

$$\int H \cos \theta \, ds = \iint \left( \kappa \frac{dF}{dt} + I \right) dS, \quad \dots\dots(5)$$

$$\int F \cos \theta \, ds = \iint \bar{\mu} \frac{dH}{dt} dS, \quad \dots\dots(6)$$

where in (5)  $H \cos \theta$  is the component of  $H$  tangential to the element  $ds$  of a closed curve and  $dS$  is an element of any area bounded by the curve.  $\kappa \frac{dF}{dt}$  is the displacement current density and  $I$  is the conduction-current density.

A similar terminology applies to (6).

In the plane waves considered, the general relationships

$$F = \bar{\mu} v H, \quad \dots\dots(7)$$

$$H = \kappa v F \quad \dots\dots(8)$$

exist between the fields, where  $v = \sqrt{1/\bar{\mu}\kappa}$  is the velocity.

At the first face of the film, the tangential component of the electric field must be continuous. Let  $(F_3, H_3)$  be the fields in the reflected wave, and let  $(F_2', H_2')$  be the fields in the wave transmitted into the film (figure 2).

Then from the equation of continuity,

$$F_1 - F_3 = F_2'. \quad \dots\dots(9)$$

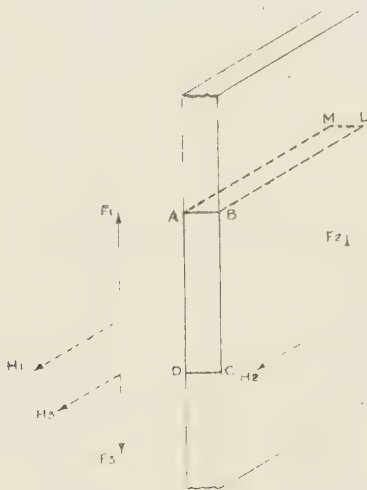


Figure 2.

Let  $(F_2, H_2)$  be the fields at the second face of the film. Applying equation (6) to the rectangle ABCD, we obtain

$$F_2 + F_3 - F_1 = \bar{\mu}_1 \int_0^h \frac{dH}{dt} dh = \bar{\mu}_1 \kappa_1 v_1 \int_0^h \frac{dF}{dt} dh = \frac{1}{v_1} \int_0^h \frac{dF}{dt} dh, \quad \dots\dots(10)$$

where  $\bar{\mu}_1$ ,  $\kappa_1$ , and  $v_1$  relate to the material of the film, and  $(F, H)$  are the fields at any point in the film.

If we consider sinusoidal waves, the right-hand side of (10) is of the order  $\omega Fh/v_1$ , and if the frequency is of the order  $10^8$  c./s., and  $h$  is of the order  $10^{-6}$  cm., the order of this quantity is  $2 \times 10^{-8}$  F.

Therefore  $F_2$  only differs from  $F_1 - F_3$  by an extremely small quantity, and, without serious error, we may say that  $F_2 = F_2'$ .

$$\therefore F_1 - F_3 = F_2. \quad \dots\dots(11)$$

Thus  $F$  is not attenuated. It is otherwise with  $H$ . Equation (5) may now be applied to the rectangle ABLM, and similar reasoning shows that the contribution

of the displacement current to the right-hand side is negligible. The conductive-current term is, however, important, and is given by

$$\iint I dS = F_2 \cdot gh \cdot \text{AM.}$$

Then  $(H_1 + H_3 - H_2) \text{AM} = F_2 gh \cdot \text{AM.}$

$$\therefore H_1 + H_3 - H_2 = F_2 gh. \quad \dots\dots(12)$$

From (11), (12), (7) and (8) we obtain

$$\frac{F_3}{F_1} = \frac{gh}{gh + 2\kappa v}, \quad \dots\dots(13)$$

$$\frac{F_2}{F_1} = \frac{2\kappa v}{gh + 2\kappa v}. \quad \dots\dots(14)$$

Now  $\kappa v = \frac{1}{\mu v} = \frac{1}{Z_{00}} \times \frac{b}{a}$  and  $gh = R_0$ , the surface resistivity of the film. In terms of  $Z_{00}$  and  $R$ , the total resistance of the film,

$$\frac{F_3}{F_1} = 1 / \left( 1 + \frac{2R}{Z_{00}} \right), \quad \dots\dots(15)$$

$$\frac{F_2}{F_1} = 1 / \left( 1 + \frac{Z_{00}}{2R} \right). \quad \dots\dots(16)$$

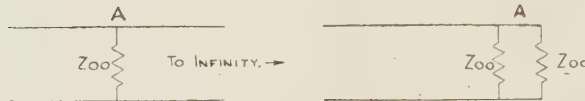


Figure 3.

If  $R$  is made equal to the characteristic impedance of the line, we shall have

$$\frac{F_3}{F_1} = \frac{1}{3}, \quad \frac{F_2}{F_1} = \frac{2}{3},$$

and the amplitude of the transmitted wave is thus two-thirds that of the incident wave. A somewhat more complicated analysis shows that for a coaxial line or a twin line, the corresponding voltages are in the ratios given by equations (15) and (16).

The above calculation applies only to the case where the line extends beyond the film to infinity, so that the transmitted wave can be guided on. In view of the mistrust shown by Willis Jackson and Huxley of the use of the impedance concept, it may be noted that the result obtained is precisely that given by a calculation in terms of impedances. For if a resistance  $Z_{00}$  ohms be connected at any point A across a semi-infinite line (figure 3), the impedance presented to a wave arriving at A is made up of  $Z_{00}$  in parallel with the input impedance  $Z_{00}$  of the rest of the line. It is therefore  $Z_i = \frac{Z_{00}}{2}$ , and the reflection coefficient is  $\frac{Z_i - Z_{00}}{Z_i + Z_{00}} = \frac{1}{3}$ .

In the experiments of Jackson and Huxley, the film was placed across the end of the coaxial line, and in such a case it is clear that a wave will be transmitted

through the film and radiated away. The terminating impedance will then be a parallel combination of the resistance of the film and the radiation impedance of the annular aperture, a quantity not easily predictable.

### § 3. THE NON-REFLECTING TERMINATION

It is of interest to examine, from the aspect of wave-propagation, the termination which Jackson and Huxley found to be effective in suppressing reflection. This was a short-circuited extension of the line, beyond the film.

Let  $x$  be the length of the extension. As before, let  $F_1$  be the amplitude in the wave advancing towards the film. Consider any film for which  $pF_1$  is the amplitude of the transmitted wave, and  $(1-p)F_1$  is the amplitude of the reflected wave where  $0 < p < 1$ . The transmitted wave is perfectly reflected by the short-circuiting disc, with reversal of the sense of the electric field, and this reflected wave is partly transmitted and partly reflected when it returns to the film. Successive reflections take place in this way at the boundaries of the extension piece, and if we take the phase of the first reflected component as standard phase, the

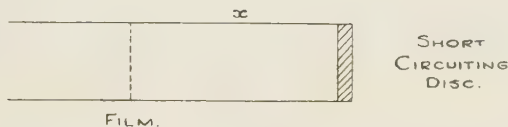


Figure 4.

electric field in the disturbance travelling back from the film towards the origin is the sum of the infinite series

$$F = F_1 \{ (1-p) \exp. j\omega t + p^2 \exp. j(\omega t - 2qx) + p^2(1-p) \exp. j(\omega t - 4qx) + p^2(1-p)^2 \exp. j(\omega t - 6qx) + p^2(1-p)^3 \exp. j(\omega t - 8qx) + \dots \},$$

where  $q = 2\pi/\lambda$ .

$$F = F_1 \exp. j\omega t \frac{(1-p) - (1-2p) \exp. (-2jqx)}{1 - (1-p) \exp. (-2jqx)}.$$

The square of the amplitude ( $F_0$ ) may be obtained by multiplying by the conjugate complex quantity. It is

$$F_0^2 = \frac{(1-p)^2 + (1-2p)^2 - (1-p)(1-2p)^2 \cos 2qx}{1 + (1-p)^2 - (1-p)^2 \cos 2qx}.$$

The condition for this to vanish is

$$\cos 2qx = - \frac{(1-p)^2 + (1-2p)^2}{(1-p)(1-2p)},$$

If  $p = \frac{2}{3}$ , which is the value obtaining when the resistance of the film is equal to the characteristic impedance of the line, as in Jackson and Huxley's experiments, this reduces to  $\cos 2qx = -1$ .

Therefore  $x = (2P+1) \frac{\lambda}{4}$ , where  $P = 0, 1, 2, \dots$ ,

Thus a suitable film, backed by a short-circuited extension of the line, one-quarter wave-length long, will correctly terminate the line, and the energy of the incident wave will be completely dissipated in the course of the successive passages through the film. The same result could be obtained by terminating the line with the film alone and using matching stubs, but the asymmetry introduced by stubs in the case of a coaxial line would be undesirable, and Jackson and Huxley's device is much to be preferred. The departure of the length of their extension ( $0.88 \lambda/4$ ) from the theoretical value of  $\lambda/4$  may be due to the sheet of bakelized paper on which the film was deposited, and to the method of mounting.

The result is again in agreement with that given by the concept of impedance. The input impedance of the short-circuited extension of length  $\lambda/4$  is infinite, and the impedance presented by the film and the extension to the oncoming wave is therefore  $Z_{00}$ . This agreement arises from the fact that the currents and the voltages, in terms of which the impedances are defined, are themselves variables derived by integration from the intensities of the magnetic and electric fields respectively; the latter are the fundamental entities. As correct relationships, satisfying Maxwell's equations, exist between the fields, so must they between the impedances. The use of impedance, however, obscures the physical realities. The subject is one which lends point to the aphorism of Hansen (quoted by Slater, 1942]: "The idea of impedance cannot be used as a substitute for thought".

Jackson and Huxley's terminating device is non-reflecting for one frequency only. The ideal non-reflecting termination for a coaxial line would be a length of distortionless line, with high attenuation, having the same physical dimensions and characteristic impedance as the line to be terminated, but it is doubtful whether this could be set up with known materials.

#### REFERENCES

- HEAVISIDE, 1892. *Electrical Papers*, vol. ii, p. 385.  
 HOWE, 1944. *Wireless Engr.* **21**, 409.  
 JACKSON and HUXLEY, 1944. *J. Instn. Elect. Engrs.* **91**, 105.  
 SCHELKUNOFF, 1938. *Bell Syst. Tech. J.* **17**, 24.  
 SLATER, 1942. *Microwave transmission*, p. 79.

# A STUDY OF THE COMPARATIVE METHOD OF DETERMINING GASEOUS REFRACTIVITIES\*

By E. C. CRAVEN

*MS. received 25 October 1944 ; in revised form 14 December 1944*

**ABSTRACT.** It is shown that the comparative method for the determination of refractive indices by white-light interferometry yields the ratio of the group refractivities and not the ratio of the phase refractivities.

The effective wave-length of the ordinary gas-filled lamp was found to be close to that of sodium light. For ordinary gases, however, any wave-length in the same region may be taken without serious error.

Observation of the shift of the central achromatic fringe due to differences of dispersion in the two paths enables the difference of dispersion to be measured. This enables the group index to be corrected and the phase index calculated at any point in the visual range of the spectrum.

The method has been applied to several common gases and to mixtures of the vapours of volatile organic solvents with air, and appears to give results comparing not unfavourably in accuracy with those obtained by the absolute method in monochromatic light.

## § 1. INTRODUCTION

THE interferometric determination of the refractive index of a gas or vapour may be carried out either by an absolute method or by a comparative method. In the former, monochromatic light is used and the band-shifts for various changes of pressures are observed. By extrapolation, the band-shift for the pressure change from zero to one atmosphere is calculated, and hence the refractive index. The appropriate corrections are applied to give the result at N.T.P.

In the comparative method, instead of counting the fringe difference, optical balance is restored in effect by introducing a suitable thickness of a comparison substance, usually air or glass. The variation of path in the comparison gas is most easily effected by varying its pressure in a tube of constant length. This method of varying the gas pressure has the advantage of giving a substantially automatic correction for normal changes of room temperature and pressure. When a glass compensator is used, both temperature and pressure of the gas have to be taken into account.

Now the measurement of the apparent relative retardation of two gases merely involves the determination of the ratio of the two gas pressures at optical balance, a determination which can obviously be made with considerable precision. The comparative method is more rapid and convenient than the absolute method. For the determination of the concentration of a solvent vapour in air, for example, there is no method which has anything like the combined speed and precision of the interferometric one.

\* Abstracted from a thesis approved by the University of London for the Ph.D. degree,

There is, however, no way of identifying the central fringe of the interference system in monochromatic light, so that white light has to be employed to give an achromatic central fringe, and thus to enable restoration of optical balance to be observed. It appeared desirable to examine the possibilities of the comparative method, and to find what differences are introduced by the necessary substitution of white light for monochromatic light.

As a comparison gas there can be no doubt that dry  $\text{CO}_2$ -free air is the most convenient to employ, as has already been suggested by Werner (1925) even for mixtures containing no air. Where mixtures of air and vapour are concerned, the use of air commends itself even more strongly.

The degree of accuracy aimed at in the present work was of the order of about 1 part in 1000 in measurements of  $(n-1)$ , which should be attained by pressure measurements on the air compensation tube within a few tenths of a millimetre of mercury.

The chief source of uncertainty in the comparative method arises from the necessary use of white light for the identification of the central fringe. A theory is developed below dealing with the corrections introduced by the shift of the achromatic fringe due to dispersion. It was proposed to verify this theory by measurements on pure gases, the optical constants of which had been reasonably well established by previous workers, taking into account any corrections arising from departure from the ideal gas laws, and finally to apply the method to mixtures of solvent vapours with air. The published values for solvent vapours are in general rather old.\*

The problem of the determination of refractive index by white-light interferometry has been dealt with to some extent by Adams (1915) and by Clack (1925), both of whom were concerned with aqueous solutions, and used tilting-plate compensators. The present treatment applies primarily to the (gas) pressure-variation method of compensation, but can readily be extended to cover the tilting plate or any other method.

Apart from an observational refinement due to Clack, the present treatment is in principle exactly the same as the theory of the method of the determination of the index of refraction and dispersion of a glass plate as given by Mann (1902).

## § 2. THE DENSITY CHANGE FOR BALANCE

The density change required to obtain optical balance in non-homogeneous light may be calculated as follows :—

Suppose two tubes of unit length, containing two gases of refractive indices  $n_1$  and  $n_2$  and densities  $\rho_1$  and  $\rho_2$ . Optical balance is obtained by increasing the pressure of the second gas until its density is  $f\rho_2$ , where  $f$  is a density ratio. Applying the Gladstone-Dale law, the change rate of phase or order with wave-length will be zero at the centre of the system, when

$$f = (n_1 - \lambda \frac{dn_1}{d\lambda} - 1) / (n_2 - \lambda \frac{dn_2}{d\lambda} - 1).$$

It can readily be shown by assuming some dispersion formula, such as

$$n - 1 = A + B\lambda^{-2},$$

\* e.g. the 1941 edition of Kaye and Laby's *Tables* quotes values mostly determined about 1878,

or by graphical methods, that the ratio

$$(n - \lambda dn/d\lambda - 1)/(n - 1) = 1 - (\lambda dn/d\lambda)/(n - 1)$$

is very closely equal to  $1 + 3\omega$ , where  $\omega$  is the dispersive power expressed as

$$\omega = (n_F - n_C)/(n_D - 1).$$

### § 3. VERIFICATION OF GROUP-INDEX FORMULA

The ratio  $f$  may be obtained in practice from the ratio of the initial and final pressures by making the appropriate correction, determined if necessary by the method of limiting densities.

The replacement of  $n$  in monochromatic light by  $n - \lambda dn/d\lambda$  in non-homogeneous light was pointed out long ago by Rayleigh, Cornu and others. As emphasized, especially by Schuster for the analogous case of a plate of some dispersive solid, the same result is obtained by considering that what is involved is the *group velocity* of the trains of waves resulting from white-light impulses. For the velocity  $V = c/n$  of monochromatic light in the medium must be substituted the smaller group velocity  $U = V - \lambda dV/d\lambda$ . The path retardation in each tube of gas at the original density is given by the numerator and denominator in the expression for  $f$  above.

By analogy with the ordinary phase refractive index  $n = c/V$ , the quantity  $c/U = n - \lambda dn/d\lambda$  may be termed a "group index". A summary of applications of this quantity is given later, and the symbol  $\bar{n}$  is tentatively proposed for it.

Although the above theory is old, the author is not aware of any measurements which have been made to confirm it with the exception of the classical determination of Michelson, in 1883, of the velocity of white light in water and  $\text{CS}_2$  by the rotating-mirror method, and further direct determinations of velocity in liquids more recently by others (Gutton, 1911; Houstoun, 1944).

The following measurements may, therefore, be of special interest. In a Rayleigh refractometer with 50-cm. tubes (Craven, 1939) the change in air pressure necessary to balance equal films (about 0.02 cm.) of various liquids in turn was determined. The cell was made of ordinary plate glass and was mounted

Fluid	$p$	$n_D$	$\bar{n}$	$\frac{\bar{n}-1}{n-1}$	$1+3\omega$
Air	0	1.000	1.000	—	—
Water	353	1.333	(1.351)	(1.054)	(1.054)
Methyl alcohol	348.5	1.329	1.346	1.052	1.050
Ethyl alcohol	381	1.362	1.379	1.047	1.050
Acetone	383	1.359	1.380	1.059	1.059
Benzene	557	1.501	1.554	1.105	1.100
Anilin	662	1.586	1.658	1.123	1.127
Carbon disulphide	731	1.628	1.727	1.158	1.162

$p$  = the air pressure in mm. of Hg required to restore balance.

$n_D$  = refractive index for sodium light.

$\bar{n}$  = apparent index for white light, i.e. the group index.

The observed ratio of  $\bar{n} - 1$  to  $n - 1$  is in reasonable agreement with the value of  $(1 + 3\omega)$ , calculated from published values of  $n_F$ ,  $n_D$  and  $n_C$ , and given in the last column.

in front of the gas tubes. and the fiduciary air system\* was formed. as usual. above the tubes.

The temperature was 20° c. throughout, and the results are calculated by comparison with water as the standard substance.

No doubt with a cell of optically worked parts and attention to a further small correction mentioned in a later section, even closer results would be obtained.

The number  $\bar{n}$  represents the reciprocal of the velocity of white light in the medium as compared with the velocity of light in free space. Michelson's direct determinations in 1883 were made with a tube 3 metres long, whereas in the present work the film thickness was barely 0.2 mm. The result obtained by Michelson for CS<sub>2</sub> was 1.758, and the temperature appears to have been 0° c.

Further experiments were made in which 1cm. of water was optically balanced by a suitable thickness of glass, and others in which microscope cover-glass was balanced by air pressure. The results were all closely in agreement with the group-index principle. Measurements were also made on flakes of mica and the disappearance of the fringes with  $\lambda/2$  plate and a  $3\lambda/2$  plate was noted.

#### § 4. SOME GENERAL THEORETICAL POINTS

The present work appears to confirm that, to a first approximation, interferometry in white light yields the group index and not the ordinary phase index. The question has been asked by Williams (1932) at what breadth of source we pass from phase index to group index. The answer appears to be that any real source will give group-index results by alignment of the achromatic centres. The position of the achromatic centre, however, quickly becomes obscure with reduction of spectral width of the source.

Some general applications of the group-index idea may be of interest. The well-known Rayleigh formula for group velocity is based on two contiguous wave-lengths,  $\lambda$  and  $\lambda + d\lambda$ . With a source of greater width,  $\lambda$  becomes the "dominant" or effective wave-length and the group index  $n - \lambda dn/d\lambda$  becomes an average value, and it is therefore tentatively proposed to denote it by  $\bar{n}$ .

According to the group-index idea, a thin pulse of non-homogeneous light passing through any real medium is spread into a train of waves and the condition for achromatism in any system is that on every such train there shall be superposed an equal and opposite train. By such considerations many of the ordinary formulae of optics may be derived and expressed in terms of the group index  $\bar{n}$  and the ordinary phase index  $n$  :

Retardation of slab	$t(\bar{n} - 1)$
Interferometric balance	$t_1(\bar{n}_1 - 1) = t_2(\bar{n}_2 - 1)$
Resolving power of echelon	$Nt(\bar{n} - 1)\lambda$
Resolving power of prism	$t(\bar{n} - n)\lambda$
Condition for thin achromatic prism	$t_1(\bar{n}_1 - n_1) = t_2(\bar{n}_2 - n_2)$
Condition for thin achromatic doublet	same as prism.

In each case  $t$  is the effective thickness, i.e. difference of thickest and thinnest parts in use, and  $N$  is the number of elements in the echelon.

\* The use of the fiduciary system is often ascribed to Haber and Lowe, but is in fact explicitly described by Lord Rayleigh (*Sci. Papers*, 4, 221).

It may be asked why the group index appears so little in ordinary optical measurements. It is suggested tentatively that this is because in general such measurements are concerned with angular deviation. As a dimensionless quantity, an angle has no relation to the mode of propagation of light in the medium, neither does it give any direct information as to the velocity of propagation. The group mechanism relates only to effects in the line of sight, and these are seldom examined.

## § 5. DISPLACEMENT OF THE ACHROMATIC FRINGE

In the expression for the change in density ratio required to obtain optical balance in white light, viz.,

$$f = (\bar{n}_1 - 1)/(\bar{n}_2 - 1),$$

if a simple Cauchy dispersion formula  $(n - 1) = A + B\lambda^{-2}$ , be accepted for each gas, then the corresponding group refractivity will be

$$\bar{n} - 1 = A + 3B\lambda^{-2}.$$

Applying this, for example, to the case of the relative refractivities hydrogen/air it will be found that

$$\text{Relative refractivity in sodium light} = 1394/2926 = 0.4763.$$

$$\text{Relative refractivity in white light} = 1453/3016 = 0.4817.$$

The above difference in relative refractivity is equivalent to  $0.0054 \times 462 = 2.5$  fringes of Na light in a 100-cm. tube at  $20^\circ$  C. In monochromatic light there would be an equal number of fringes in each of the paths through the tubes at optical balance, whereas in white light, owing to the dispersion of the medium, there are unequal numbers. This is manifested by a wandering of the central achromatic band from the position it had under the original symmetrical conditions.

## § 6. THE DISCONTINUITY RESULTING FROM THE SHIFT OF THE ACHROMATIC FRINGE

In the above calculation it is assumed that in restoring optical balance, the optical centres of the fiduciary and gas-tube fringe systems are brought to coincidence, whereas in actual fact what is done is to align the achromatic band of the reference system with the most nearly achromatic band of the gas system. It has already been shown by Clack (*loc. cit.*) that the effect of this natural technique is that at balance the numbers of periods in the two paths are either equal or differ by an integral number. If, therefore, starting with the two gas tubes full of the same gas A, a second gas B of higher refraction and dispersion is gradually substituted in one tube, the resulting curve is as indicated diagrammatically by the full lines in the figure.

The line OXF' gives the balance in monochromatic light corresponding to the equation

$$f' = (n_B - 1)/(n_A - 1).$$

In white light there is a discontinuity at X, the achromatic centre having shifted half a fringe, so that there are two equally achromatic fringes in the gas system. This condition is frequently observed in practice. At Y the displacement is

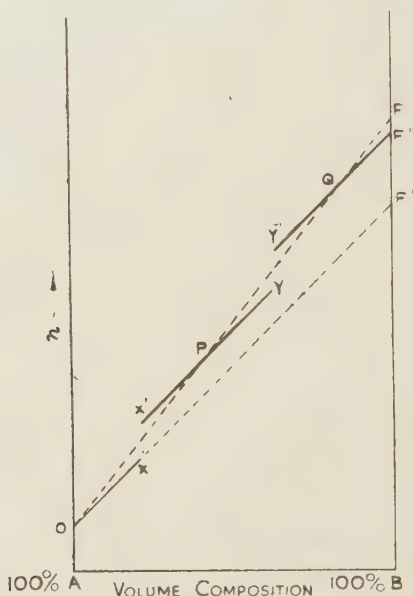
$1\frac{1}{2}$  fringes and the same effect is observed, and so on. The point O corresponds to the refractive index  $n_A$  of the gas A and the point F' to  $n_B$ .

At points P and Q the dispersion shift is an integral number of wave-bands, and the interference system of the gas tubes is symmetrical and can be brought into exact coincidence with the fiduciary system. The spine O, P, Q....F indicates the balance in non-homogeneous light which would be obtained if the achromatic centres of the fiduciary and gas systems were brought into coincidence and corresponds to the equation

$$f = (\bar{n}_B - 1)/(\bar{n}_A - 1).$$

The practical balance in which the nearest achromatic band of the gas-tube system is brought into coincidence with the central band of the fiduciary system is given by the family of parallel segments

$$OX, \quad X'Y, \quad \dots Y'F''.$$



A total dispersion shift of 2.4 bands has been shown in the above diagram.

In addition, therefore, to the two values of the density ratio  $f$  and  $f'$  already considered, there may be added a third value,  $f''$ , which is the one actually observed. In practice it is sometimes difficult to distinguish between  $f$  and  $f'$ , and in the experiments with liquids already described no attempt was made because of the experimental difficulty.

It may be noted that any observation in white light will agree with monochromatic light if it fall on the first segment OX of the broken line; on other segments there will be a dispersion error of an integral number of wave-bands.

The difference in slope of OF and OF' depends on the difference in dispersivity of the two gases. It happens that the dispersive power of air is low, so that in using it as a comparison fluid, the effect of the dispersion difference is almost always in the sense to make the apparent index of refraction of the second gas or vapour higher than the true value.

Measurements made on mixtures of benzene vapour with air gave a family of curves exactly like those in the figure. It was later found that the same observations had already been made by Kinder (1938), who refers to an important paper by Hansen (1930) in which a formula is given for the location of the *Sprungstellen*.

As already indicated, however, this discontinuity effect is implicit in the earlier treatment by Clack.

#### § 7. THE EFFECTIVE WAVE-LENGTH OF THE SOURCE

It is usually assumed that white-light observations correspond to a wave-length of about  $0.56\mu$  at the maximum sensitivity of a normal eye. With a tungsten lamp, however, the emission varies rapidly at this wave-length. A rough calculation from specimen curves indicates a visual maximum some  $0.02\mu$  higher on this account.

With the writer's right eye (of distinctly different colour sensitivity from the left eye) no difference in band spacing could be seen or measured as between sodium fringes or white-light fringes.

Measurement of the change of air pressure necessary to give a shift of a few fringes showed an effective wave-length of  $0.59\mu$  for an ordinary clear half-watt lamp, and  $0.585\mu$  for a daylight lamp. It must be admitted, however, that neither of these tests is very satisfactory. So long as a white-light fringe is sufficiently clear to be separated, a sodium fringe will necessarily coincide more or less with the brightest part of it, and in the other case where measurements of fringe shift are attempted, the fringes compared are of reversed colouring. The results in any case refer only to the observer's eye.

With two substances of moderate dispersive power, an error of  $0.02\mu$  in the effective wave-length will have little effect on the ratio of the refractivities. It is a point, however, which needs further experiment.

The introduction of strongly coloured filters—tricolour filters for example—has practically no effect on the position of optical balance. The only effect is to trim off the coloured edges from the fringes. It is probable that this would remain true if the spectral width of the source were decreased down to something approaching monochromatic light. On this assumption it is clear that any method based on identifying the central band, even if the final balance were made in monochromatic light, would still yield results governed by group-velocity considerations.

#### § 8. THE DISPERSION DETERMINATION

Since the optical balance in white light is a sort of integration result, it would be unwise to expect that refractive indices for values of  $\lambda$  far removed from the effective wave-length of the source could be determined with equal precision. It is possible, however, by careful observation, to determine the extent of the shift of the achromatic band of the gas system and so to find the difference between the dispersion of the gas under examination and that of the reference substance. Since it is the difference which is measured, the total dispersion can be assessed with fair accuracy.

In the observations on gases which follow it has been assumed that the dispersion is sufficiently well expressed by a simple two-term Cauchy expression,  $(n-1)=(A+B\lambda^{-2})$ , and this is probably true for all colourless gases in the middle of the visual region; indeed. the expression fits many liquids and solids surprisingly well.

From the considerations already mentioned, the values of  $A$  and  $B$  may be determined. It is of interest to note that  $n_F$  and  $n_C$  may also be obtained with fair accuracy by correcting the value of  $f'$  found by the quantity corresponding to the integral dispersion band-shift at the given wave-length.

The extent of the dispersion shift is sometimes very considerable. For example with 100-cm. tubes, in changing from air to ammonia, there is a wandering of the achromatic centre of 19 wave-bands and with air to ethylene about 40 wave-bands. The suggestion appearing in text-books that the central band should be identified in white light and the fractional part determined in monochromatic light is entirely misleading.

### § 9. THE REFRACTION OF AIR

A mean of the determinations by various authors up to about 1930 gave the following values for the refraction of air at N.T.P.:—

$\lambda$	0.486 (F)	0.589 (D)	0.656 (C)
$(n-1)10^7$	2947	2926	2916

These values were used in all the present author's work on gases. After this part of the work was finished, it was found that Barrell and Sears, of the N.P.L., had published the results of an elaborate investigation (1939) leading to a value of  $(n_D-1)10^7$  at N.T.P. of 2924 and a slightly greater dispersion than is given above. It was not thought necessary to recalculate all the present work on account of these small changes.

### § 10. MEASUREMENTS ON GASES

The interferometer used for the bulk of the work was the laboratory-constructed instrument of the Rayleigh pattern with 50-cm. tubes mentioned above. The light source was an ordinary "coiled-coil" half-watt lamp.

The increase or decrease of pressure in the air tube required to restore optical balance was measured on suitable mercury manometers of 8 mm. bore.

The pure gases were made by approved chemical methods and dried, when possible, by a long tube of potassium hydroxide. Measurements were also made on commercial gases from cylinders, and were found to differ only slightly from those on the pure gases.

The dispersion shift in replacing air by the gas under examination was determined by allowing the gas to mix in slowly, and measuring the change in pressure for each half-fringe shift of the achromatic centre, i.e. from a clearly defined single central achromatic band, to the condition where there are two equally coloured bands,

The following table summarizes the mean results obtained for  $(n-1)10^7$  at N.T.P.:—

Gas	$\lambda 0.486$	$\lambda 0.589$	$\lambda 0.656$	Dispersion shift
$H_2$	1408	1394	1388	1.3
	1411	1395	1387	
$O_2$	2738	2713	2702	2.0
	2743	2714	2701	
$N_2$	3004	2982	2973	none
	3006	2984	2973	
$NH_3$	3902	3846	3823	9.5
	3918	3846	3826	
$CO_2$	4524	4490	4469	1.0
	4528	4492	4473	

The top line of figures gives the observed values for each gas, and the second line shows recent results determined in monochromatic light by other observers.

There appears to be a general tendency for the present method to give a somewhat low result at the blue end of the spectrum. It is likely that this is due to the paucity of blue light in artificial illumination ; the refractive index is rising most sharply where visual acuity is rapidly diminishing, and, therefore, the average is somewhat low.

A specimen of the observations and calculations is given for  $H_2$ . In the case of  $NH_3$ , a special correction was necessary from  $20^\circ$  to  $0^\circ$  owing to its abnormal coefficient of expansion.

*Specimen observation and calculation for  $H_2$*

	cm. Hg
Barometer	77.09 temp. $20^\circ$ C.
Air pressure at balance	37.07
Avogadro correction	0.02 (negligible)
	<u>37.05</u>

Allowing 1 band dispersion shift = 0.33 cm. pressure,

$$f' = 36.72/77.09 = 0.4763.$$

$$\therefore (n_D - 1)10^7 = 2926 \times 0.4763 = \underline{1394}.$$

For the dispersion :

Total shift of achromatic centre = 1.3 bands = 0.43 cm. Hg. Hence

$$f = 37.15/77.09 = 0.4819$$

$$-(\lambda dn/d\lambda)_D = 2B\lambda^{-2} = 3017 \times 0.4819 - 1394 = 60.$$

$$\therefore B = 30.0/2.88 = 10.4.$$

From which

$$n_F = 1394 + 10.4 \times 1.35 = 1408,$$

$$n_C = 1394 - 10.4 \times 0.56 = 1388.$$

An alternative approximate procedure which entirely ignores the light quality is to use the appropriate pressure corrections for the F and C lines instead of 0.33 cm. as for D above.

This gives

$$n_F = \frac{37.05 - 0.27}{77.09} \times 2947 = 1406,$$

$$n_C = \frac{37.05 - 0.37}{77.09} \times 2916 = 1387.$$

As the pressure measurements are purely relative, it may be noted that there is no need to apply any corrections to the barometer or manometer readings, providing, of course, that these instruments are not far apart.

Using the values of  $n_D$  obtained in the present work, and published values for other quantities, the molecular refraction was calculated for the gaseous and liquid state for these gases.

For gases, the formula  $M_D = 14940(n_D - 1)/(1 + \alpha)$  was used, where  $(1 + \alpha)$  = Avogadro factor or apparent degree of association.

#### Values of $M_D$

Gas	Gaseous	Liquid
H <sub>2</sub>	2.08	2.09
O <sub>2</sub>	4.05	4.05
N <sub>2</sub>	4.45	4.37
NH <sub>3</sub>	5.65	5.56
CO <sub>2</sub>	6.66	6.57

Considering the difficulties of observation on liquefied gases, the agreement must be regarded as remarkably close.

#### § 11. MEASUREMENTS ON AIR-VAPOUR MIXTURES

Mixtures of air with the vapour of organic liquids were made by breaking sealed bulbs of the liquid in a 20-litre bottle which was rotated until the liquid had entirely vaporized. By suitable temperature and pressure measurements, the initial and final volumes were determined, and hence the volume of the vapour found by difference. The mixture was drawn through the tube of the refractometer, which had already been charged with an air-vapour mixture of approximately the same composition in order to minimize sorption effects.

It was found (contrary to usual belief) that the solvent vapours at quite low concentrations (1 to 5 % vol.) are appreciably associated, the following values being obtained :—

Methyl alcohol	1.03
Formic acid	1.65
Ethyl alcohol	1.03
Acetic acid	1.84
Acetone	1.01
Methyl ethyl ketone	1.03
Benzene	1.04
Paraldehyde	1.01
<i>n</i> -Heptane	1.04

Vapour refractions are commonly reported at N.T.P. This practice has little to commend it since it involves a most uncertain extrapolation to impossible conditions. It appears more useful to give the specific or molecular refraction and the apparent association factor.

With all the above solvents, the molecular refractions, with the single exception of formic acid, were within 1 % of the liquid values (Lorenz-Lorentz). In the case of formic acid somewhat lower and inconsistent results were obtained, but this appeared to be due to actual chemical attack on the brass refractometer tube.

Attempts were also made to take measurements on mixtures of vapours with hydrogen, but owing to various experimental difficulties this had to be abandoned.

## § 12. TILTING-PLATE COMPENSATORS

The group-velocity or group-index principle may easily be applied to calculate a calibration curve for this type of compensator. Such compensators, however, appear to show quite perceptible changes in calibration in use and are not suitable for work of more than moderate precision.

In some applications, however, they are useful as null indicators, or for measuring small deviations. For example, if it be desired to make a 10 % vol. mixture of a given gas with air, two gas tubes can be used, one 100 cm. long for the mixture and one 10 cm. long for the given gas, and optical balance should result.

This device of a short tube is incidentally, also useful for balancing gases of high refraction by a reasonable pressure of air in the longer comparison tube.

## REFERENCES

- ADAMS, L., 1915. *J. Amer. Chem. Soc.* **37**, 1181.  
 BARRELL, H. and SEARS, J. E., 1939. *Trans. Roy. Soc. A*, **238**, 1.  
 CLACK, B., 1925. *Proc. Phys. Soc.* **37**, 116.  
 CRAVEN, E. C., 1939. *Ind. Chemist*, **15**, 354.  
 GUTTON, C., 1911. *C.R. Acad. Sci., Paris*, **152**, 1089.  
 HANSEN, G., 1930. *Z. InstrumKde*, **50**, 460.  
 HOUSTOUN, R. A., 1944. *Proc. Roy. Soc. Edinb. A*, **62**, 58.  
 KINDER, W., 1938. *Z. Nachr.* **1**, 223.  
 MANN, C., 1902. *Manual of Advanced Optics*.  
 WERNER, G., 1925. *Z. angew. Chem* **38**, 905.  
 WILLIAMS, W. E., 1932. *Proc. Phys. Soc.* **44**, 453.

# THE INFLUENCE OF ABSORPTION ON THE SHAPES AND POSITIONS OF LINES IN DEBYE-SCHERRER POWDER PHOTOGRAPHS

BY A. TAYLOR AND H. SINCLAIR

*Communicated by Sir Lawrence Bragg, F.R.S. ; MS. received 23 October 1944*

**ABSTRACT.** Simple graphical methods of determining the basic line-contours for powder diagrams taken in cylindrical Debye-Scherrer cameras are described. From these contours the absorption factor may be obtained for any given Bragg angle and dilution of the specimen. The contours also enable the position of the line peaks to be calculated for different sets of experimental conditions. This, in turn, opens up the possibilities of new types of extrapolation curves for the accurate determination of lattice parameters.

## § 1. INTRODUCTION

### *The absorption factor*

THE usual experimental arrangement for taking Debye-Scherrer powder photographs is one which employs a cylindrical specimen made of an aggregate of crystal fragments which is placed at the centre of a cylindrical camera. The slit system of the camera is fixed and limits the height of specimen irradiated. In the absence of any absorption of the x-ray beam within the powder aggregate, the intensity of an x-ray reflexion is proportional to the volume of powder irradiated and, therefore, to the area of cross-section of the specimen. In practice there is an appreciable amount of absorption, and the intensity of the reflexion is cut down to a fraction  $A$  of the original amount.  $A$  is termed the absorption factor. It may be thought of as consisting of two parts, the one being concerned with absorption within the bulk of the powder aggregate (macro-absorption), and the other being a function of absorption and extinction within the reflecting polycrystalline particle (micro-absorption).

We may write the absorption factor in the form

$$A = \tau\alpha, \quad \dots\dots(1)$$

where  $\tau$  is the micro-absorption factor and  $\alpha$  the macro-absorption factor (Schäfer, 1933; Brentano, 1935; Brindley and Spiers, 1938; Taylor, 1944). With very small particles ( $\sim 10^{-5}$  cm.),  $\tau$  is nearly 100 %, and the main term in the absorption factor is  $\alpha$ . The value of  $\alpha$  also has a considerable influence on the distribution of energy in the diffraction line. We shall, accordingly, define the shape of the line as determined solely by  $\alpha$ , the basic line-contour, and we shall modify it according to the experimental conditions to obtain the line shapes observed in practice.

The value of the macro-absorption factor  $\alpha$  depends on  $\mu$ , the mean linear absorption coefficient of the powder specimen, and also on  $r$ , the radius of the specimen, and on the Bragg angle  $\theta$ . It is most convenient to compute  $\alpha$  in

terms of the product  $\mu r$  for a number of discrete values of  $\theta$  and to obtain the intermediate values by interpolation. These computations have been carried out analytically by G. Greenwood (1927), A. Rusterholz (1931) for special cases, and graphically by A. Claassen (1930). F. C. Blake (1933) used Claassen's graphical construction with a higher degree of accuracy. The graphical method of Claassen was also given analytical expression by A. J. Bradley (1935), who claims greater accuracy when  $\mu r > 2$ . L. W. McKeehan (1922) used a very involved analytical method of determining the line shapes for a number of special cases, but did not evaluate the absorption factors from them.

Briefly, and omitting the geometrical constructions involved, the Claassen method is as follows:—In figure 1 the circle represents a cross-section of the cylindrical powder specimen irradiated by a parallel beam of x rays. The total length of path of a ray entering along  $p$  and leaving the specimen along  $q$  after

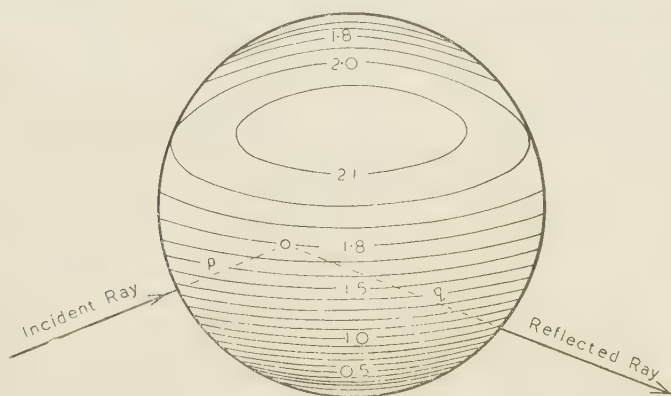


Figure 1. The Claassen loci. Division of specimen cross-section into loci of  $z = p + q$  taken at intervals  $0.1r$  in  $z$ : (After F. C. Blake, *Rev. Mod. Phys.* **5**, 169, 1933.)

reflexion from a small element of area  $d\sigma$  is  $z = p + q$ . The macro-absorption factor is given by the expression

$$\begin{aligned} \alpha &= \frac{1}{\pi r^2} \iint e^{-\mu z} d\sigma \\ &= \frac{1}{\pi} \iint e^{-\mu r x} ds, \end{aligned} \quad \dots\dots (2)$$

where  $x = z/r$  and  $ds = d\sigma/r^2$ . We may treat this final expression as if it referred to a circle of unit radius with an effective linear absorption coefficient  $\mu r$ . We then evaluate the integral for specific values of  $\mu r$  and  $\theta$ .

In order to evaluate the integral (2), the cross-section of the specimen is divided into loci for which  $z$  (or  $x$ ) is a constant. In figure 1, adapted from Blake's paper, the loci are drawn at intervals of  $x = z/r = 0.1$ . The integration, in the graphical solution, is then carried out by determining the areas between the loci with the aid of a planimeter, multiplying the area of each strip by  $e^{-\mu r x}$  and summing the results. The analytical approach achieves the same results by finding the equations to the loci and writing down the values of  $s$  and  $(ds/dx)$  as a series in  $x$ . Bradley gives his results as tables of absolute values of  $100\alpha$

for different  $\mu r$  and  $\theta$  values, while Blake plots the ratios of  $\alpha(\theta)/\alpha(90^\circ)$  against  $\theta$ . This latter form of expression has the disadvantage of yielding only relative values of  $\alpha$ .

Now although the analytical and graphical methods described above yield the absorption factor, they do not, in themselves, furnish a simple means of drawing the line shapes. These line shapes are of fundamental importance, for it is essential to know just how far absorption influences the positions of the line peaks in making lattice-parameter determinations, and in the measurement of particle sizes and lattice distortion we must know all the factors which may or may not affect the angular spread of the lines.

We can derive the line shapes directly by means of a very simple strip method, assuming the radiation to be strictly parallel, and from them determine the absorption factors with a high degree of accuracy. In practice, conditions of parallel radiation are not encountered, since the rays diverge from every point in the focal spot. The divergence, as far as the specimen is concerned, is very small, for the angle subtended by the specimen at any point in the focus is only of the order of 40 minutes of arc. The absorption factor is not appreciably influenced by this divergence. However, as we shall see, the line shapes and the peak positions are influenced to a considerable extent by the divergence, for the radius of the camera is comparable with the specimen-focus distance.

To determine the line shapes for divergent radiation, we have to modify the strip method and employ a *line-contour matrix*. This yields the line shape for a point focus, which is then suitably modified to take into account the finite size of the focal spot and the distribution of intensity across it.

## § 2. BASIC LINE-CONTOURS FOR PARALLEL RADIATION

### (a) *Line contour and absorption factor by the direct-strip method*

In figure 2, the circle represents a cross-section through the specimen. The parallel beam of radiation travelling in the direction XA completely bathes the specimen, and is diffracted through  $2\theta$  in a direction parallel to the central ray AB. The example shown in the figure is drawn for  $\theta = 22\frac{1}{2}^\circ$  and  $\mu r = 2.0$ . It is clear that all the energy in the shaded region of the line-contour must have travelled from the shaded strip EF of the specimen. The total energy given

by such a strip must clearly be proportional to  $\int e^{-\mu(p+q)} d\sigma$  or to  $\int_E^F e^{-\mu r x} ds$  when referred to a unit circle. In practice, it is convenient to make the strips infinitely narrow when the integral taken along a chord such as EF yields the corresponding height of the strip in the line-contour. These integrations are carried out by graphing the function  $e^{-\mu r x}$  on a large scale and determining the areas by counting squares.

The accuracy with which the integrations yield the heights of the line elements depends, ultimately, on the accuracy with which the lengths  $p$  and  $q$  can be measured. This accuracy becomes all the more important as the value of  $\mu r$  increases, for then  $e^{-\mu r x}$  falls rapidly and only the outer skin of the specimen is effective. As long as  $\mu r < 5$ , a circle 40 cm. in diameter suffices to represent the unit circle on which  $p$  and  $q$  are measured.

Chords EF were drawn across the unit circle at intervals of 2 cm. In the region of the peak, where additional accuracy was required, the chords were spaced at intervals of  $\frac{1}{4}$  cm. Starting at the ends F, where the specimen makes its major contribution to the line intensity and the need for accuracy is greatest, the chords were divided into 1-cm. intervals and the corresponding series of lengths  $p+q$  measured off. Smaller subdivisions were taken as required. Tables of  $e^{-\mu r}$  were then constructed for each chord EF and for different values of  $\mu r$  and  $\theta$ , maintaining five-figure accuracy throughout. Thus when the functions were plotted to a large scale for carrying out the integrations, it was possible to obtain an accuracy of at least  $\pm \frac{1}{4}\%$  for the ordinates of the line contours.

The area of the basic line-contour is, of course, proportional to the intensity of the diffracted beam, while its outline gives the intensity distribution. When the value of  $\mu$  is zero, the contour becomes a semi-ellipse of axial ratio 2, with an

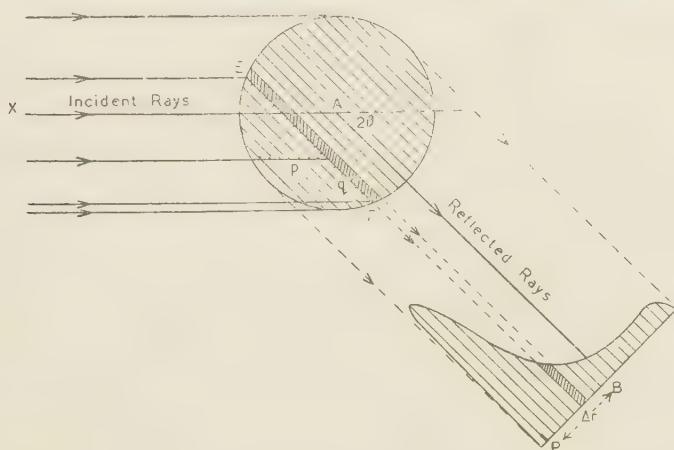


Figure 2. Direct strip method of obtaining line-contour for parallel radiation.  
Drawn for  $\theta = 22\frac{1}{2}^\circ$ ,  $\mu r = 2.0$ .

area equal to that of the unit circle,  $\pi$ . The absorption factor  $\alpha$  for a given value of  $\mu r$  is thus the area under the basic line-contour divided by the factor  $\pi$ .

The method involves a considerable amount of arithmetic and graphical work if high accuracy is aimed at. For the special cases of  $\theta = 0^\circ$  and  $90^\circ$  it is possible to cut down the work appreciably without sacrificing any of the accuracy, since the integrations along the chords can be carried out directly.

At  $0^\circ$ , the incident and reflected rays lie in the same straight line, and the total path  $p+q$  is equal to the chord length. Thus the total contribution by a given chord of length  $c$  of the unit circle is simply equal to  $ce^{-\mu r c}$ . We can thus draw the contour of the diffraction line at  $0^\circ$  with a minimum of error by replacing all measurements of chord length and graphical integrations by direct calculation.

At  $\theta = 90^\circ$ , the reflected rays travel back along the incident paths, and now  $p=q$ . The maximum distance traversed by a given ray is now twice the length of the chord whose integrated effect is  $\int_0^c e^{-\mu r \cdot 2x} dx$  or  $\frac{1}{2\mu r} (1 - e^{-2\mu r c})$ . Thus

the ordinates of the line-contour at  $\theta = 90^\circ$  may also be computed without the need of intermediate graphical integrations.

A comparison of our final results for the macro-absorption factors at  $0, 22\frac{1}{2}, 45, 67\frac{1}{2}$  and  $90^\circ$  with those obtained by Bradley is made in table 1. On the whole the measure of agreement is exceptionally good.

Table 1. Absorption factors  $100\alpha$  when  $\mu r < 5$

$\sin^2\theta$ $\theta^\circ$	0.0000 $0^\circ$		0.1464 $22\frac{1}{2}^\circ$		0.5000 $45^\circ$		0.8536 $67\frac{1}{2}^\circ$		1.0000 $90^\circ$	
$\mu r$	Strip method	Bradley	Strip method	Bradley	Strip method	Bradley	Strip method	Bradley	Strip method	Bradley
0.00	100.00	100.00	100.00	100.00	100.00	100.00	100.00	100.00	100.00	100.00
0.25	65.9	65.4	66.2	66.0	65.5	65.5	67.5	67.5	68.0	68.0
0.50	43.0	43.5	44.0	44.2	45.0	44.8	46.8	47.8	48.9	49.0
0.75	28.9	29.0	29.8	29.8	32.8	32.5	35.3	35.4	37.5	37.5
1.00	19.4	19.77	21.0	20.95	23.9	24.2	27.5	27.85	29.5	29.5
2.00	4.71	4.71	6.34	6.35	9.93	10.05	13.8	13.84	15.7	15.67
3.00	1.40	1.436	2.89	2.885	5.75	5.82	8.9	8.89	10.54	10.54
4.00	0.50	0.568	1.71	1.706	3.95	4.02	6.53	6.53	7.94	7.94
5.00	0.26	0.276	1.19	1.189	2.96	3.05	5.14	5.14	6.35	6.35

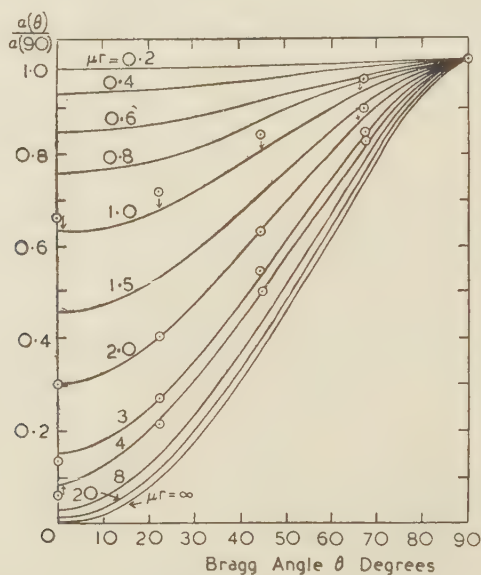


Figure 3. Ratio of absorption factors  $a(\theta)/a(90^\circ)$ . (F. C. Blake.)  
Circles show present set of results.

We have also expressed our results in the form  $\alpha(\theta)/\alpha(90^\circ)$ , and plotted them on Blake's curves, shown in figure 3. The agreement is almost perfect except for  $\mu r = 1.0$ , when the points come appreciably higher.

The measure of agreement shown between calculations based on the strip method and the values of  $\alpha$  given by Blake and Bradley is a verification of the

high accuracy with which the basic line-contours have been drawn. A set of these contours is illustrated in figure 4. For convenience of representation they have all been drawn the same height. The basal widths are on the same scale, being equal to  $2r$ , the diameter of the specimen. When they appear to be much narrower, as, for example, when  $\theta = 45^\circ$  and  $\mu r = 4.0$ , it is because the intensity falls steeply and the vertical scale is too small to reveal the weak tails on the lines. The numbers uppermost on the curves are the corresponding values of  $100\alpha$ . These are proportional to the areas beneath the contours and give some idea of the magnification employed in plotting the contours of lines with high values of  $\mu r$ .

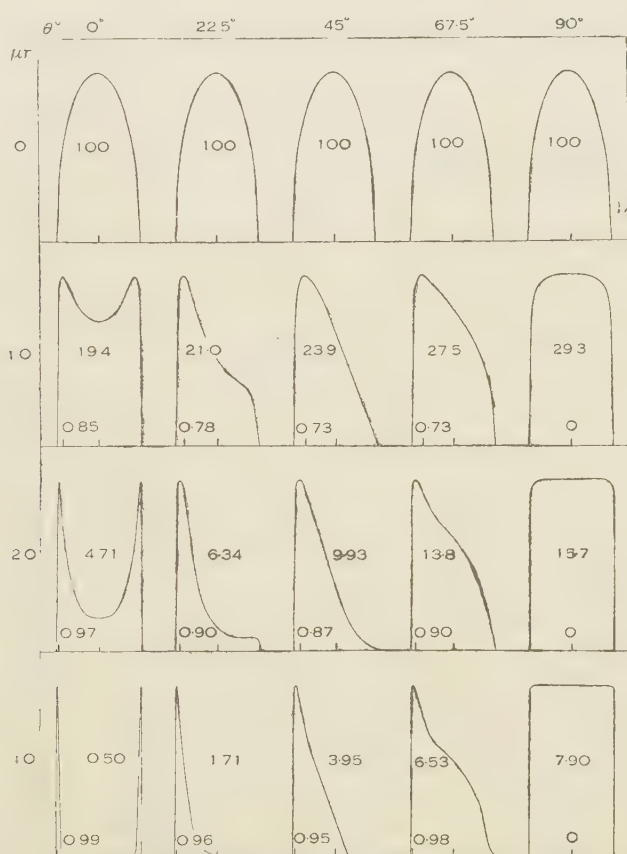


Figure 4. Basic line shapes of Debye-Scherrer lines with parallel radiation obtained with the direct-strip method.

#### (b) Position of line peaks with parallel radiation

The peaks of the lines are displaced from the central ray in the direction of greater  $\theta$  by a distance  $\Delta r$  along the film. For parallel radiation and a given value of  $\theta$ ,  $\Delta r$  will be proportional to the radius of the specimen, provided  $\mu r$  is maintained constant. Thus it is convenient to express the peak displacement as a fraction of the radius  $\Delta r/r$ , and, since parallel radiation is employed, this fraction must be the same for all values of the camera radius  $R$ . Values of  $\Delta r/r$  are given at the base of the lines in figure 4.

For a line having a flat top, we have adopted the convention of referring  $\Delta r/r$  to the centre of the flat portion, as, for example, at  $\theta = 90^\circ$ . When the line displays a definite peak, the measurement is taken at the point of maximum intensity.  $\theta = 0^\circ$  represents a special case. Here the peak is at the centre for

Table 2. Values of  $\Delta r/r$  for parallel radiation

$\mu r$	$\theta = 0^\circ$	$22\frac{1}{2}^\circ$	$45^\circ$	$67\frac{1}{2}^\circ$	$85^\circ$	$90^\circ$
0.00	0.00	0.00	0.00	0.00	0.00	0.00
0.25	0.00	0.28	0.30	0.24	0.07 <sub>5</sub>	0.00
0.50	0.00	0.58	0.47	0.48	0.22	0.00
0.75	0.72 <sub>5</sub>	0.72 <sub>5</sub>	0.64	0.64	0.50	0.00
1.00	0.85	0.78	0.72 <sub>5</sub>	0.73	0.67 <sub>5</sub>	0.00
2.00	0.97	0.90	0.87	0.90	0.90	0.00
3.00	0.98	0.94	0.92	0.96	0.97	0.00
4.00	0.98 <sub>8</sub>	0.96	0.95	0.97 <sub>5</sub>	1.00	0.00
5.00	0.99 <sub>8</sub>	0.97 <sub>5</sub>	0.97 <sub>5</sub>	0.98 <sub>5</sub>	1.00	0.00
$\infty$	1.00	1.00	1.00	1.00	1.00	0.00

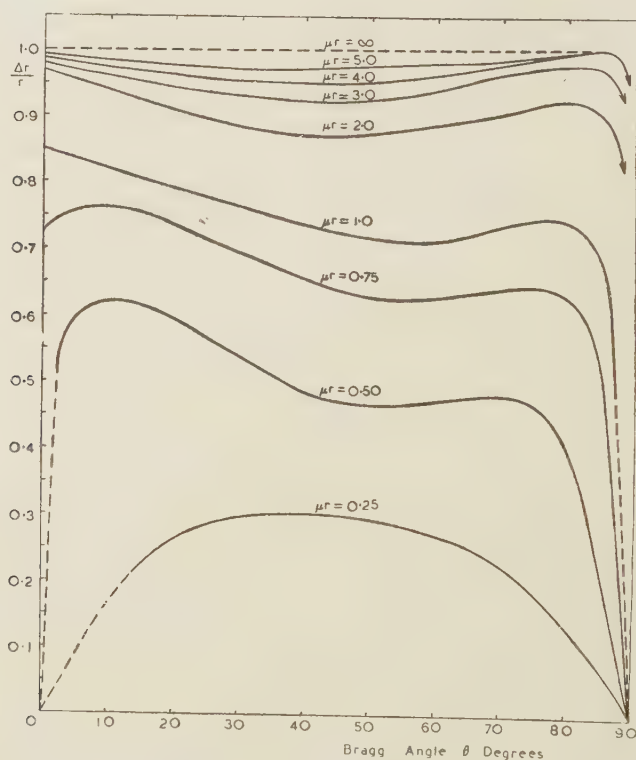


Figure 5. Values of  $\Delta r/r$  as a function of  $\mu r$  and Bragg angle  $\theta$ . Calculated for parallel radiation.

$\mu r = 0$ . As  $\mu r$  increases, the contour flattens out and then becomes slightly depressed at  $\mu r \simeq 0.5$ . The line suddenly switches over from having one peak to having two, which lie close to the outer edges of the line. Near the value of

$\mu r = 0.5$ , when the change-over is on the point of taking place, the position of the peak is indeterminate.

Values of  $\Delta r/r$  are given in table 2. Between  $67\frac{1}{2}^\circ$  and  $90^\circ$  the values fall rapidly to zero. This angular region is of particular importance in lattice-parameter determinations, for the resolving power of the powder diagram increases as  $\tan \theta$ . The maximum value of  $\theta$  recorded in cylindrical cameras rarely exceeds  $86^\circ$ . The line-contours for  $\theta = 85^\circ$  were therefore calculated, and values of  $\Delta r/r$  obtained from them to bridge the gap between  $67\frac{1}{2}^\circ$  and  $90^\circ$ . These values are also recorded in the table.

Figure 5 illustrates the remarkable variations of  $\Delta r/r$  much more clearly than the table. At angles below  $22\frac{1}{2}^\circ$  the positions of the peaks for  $\mu r < 0.75$  are difficult to determine even with very accurately drawn contours. Between  $80^\circ$  and  $90^\circ$  the curves suddenly fall to zero and make interpolation in this region very difficult.

### § 3. BASIC LINE-CONTOURS FOR RADIATION DIVERGING FROM A POINT SOURCE

When we consider the line-contours for divergent radiation, we find that, except for the special cases of  $\theta = 0^\circ$  and  $90^\circ$ , they cannot be derived from the contours for parallel radiation by any simple geometrical construction. The contours of the lines now become dependent on the camera radius  $R$ , and the specimen-focus distance  $AX$  in addition to  $\theta$  and  $\mu r$ . We shall find that as long as the focus may be regarded as a point source, the dimensions of the line-contour will change in proportion to  $r$  provided  $\mu r$  is maintained at the same value and the other variables are unchanged. When the focus becomes finite, the proportions of the line-contour then change according to the ratio: size of focal spot/radius of specimen.

In our analysis we have considered two sizes of camera, namely, cylindrical cameras of radius  $R = 95.0$  mm. and  $45.00$  mm. For these cameras, specimen-focus distances of  $150$  mm. and  $100$  mm. respectively have been taken as values most nearly realized in practice.

In figure 6,  $X$  represents the point source, radiation from which completely bathes the specimen. We may divide the specimen into strips  $EF$ , which subtend equal angles at the point  $X$ . Since, for a specimen of  $1$  mm. radius at a distance  $AX = 150$  mm., the total angle subtended by the specimen is only  $2/150$  radian, or  $0.76^\circ$  approximately, these narrow strips may be considered as rectangles tilted slightly with respect to each other.

The rays diffracted from the strip  $EF$  through an angle  $2\theta$  will strike the film over the range  $GH$  with an intensity distribution shown schematically by the shaded area. This distribution is easily obtained from the tabulated values of  $e^{-\mu(p+q)}$  obtained for parallel radiation. We then have to determine the relative positions on the film of the contributions from strips such as  $EF$ . This is done by calculating the exact location of points  $G$  with respect to  $B$ , the point where the central ray, unaffected by divergence, strikes the film. The overlapping contributions from  $EF$  and from the central strip are shown (not to scale) in the figure.

To compute the ordinates which yield the line-contour, we proceed as follows. We divide the basic circle into twenty parallel strips and plot graphs of the functions  $e^{-\mu(p+q)}$  for each of the strips. (These were already available from the previous work for parallel radiation.) Starting with the graph for the outermost strip near the peak, we read off values of  $e^{-\mu(p+q)}$  at set intervals and write these down in a row. We then calculate the position of G, the origin of the next strip, and commence reading values from the appropriate curve of  $e^{-\mu(p+q)}$  at positions which coincide with the intervals in the preceding strip. These numbers form the next row of figures. Proceeding in this manner for all the chords EF, we build up the *line-contour matrix*. Such a matrix for  $R=45.0$  mm.,  $AX=100.0$  mm. and  $\mu r=2.0$  for  $\theta=45^\circ$  is shown in figure 7.

The figures along each horizontal row of the matrix correspond to the energy contributions given by each strip EF, and the envelope of the matrix corresponds to the relative positions of the terminal points GH of the strip contributions. The ordinates of the basic line-contour are then obtained by graphing the numbers

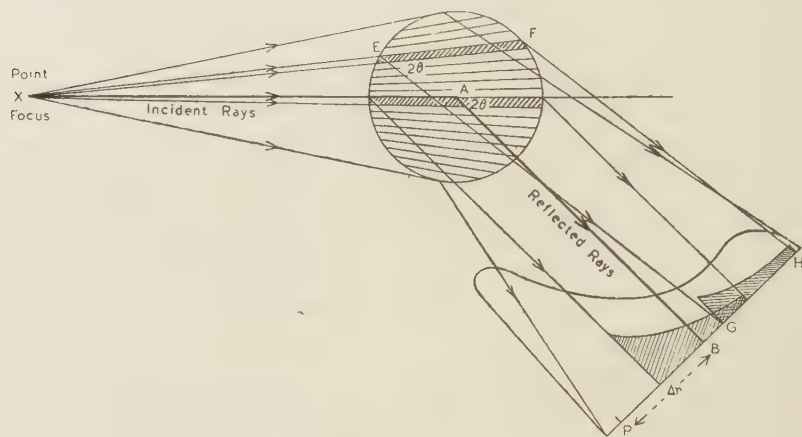


Figure 6. Construction of basic line-contour for divergent radiation.

in the vertical columns and finding the areas beneath the curves. This yields a much greater degree of accuracy than is to be obtained by simply adding the numbers together. In the region of the peak, the vertical columns are taken at  $\frac{1}{2}$  and  $\frac{1}{4}$  intervals in order to determine the peak positions with greater accuracy. For the sake of clarity, these extra columns have been omitted from the diagram.

In figure 8 we give a comparison of line-contours for parallel radiation and for a point focus when  $R=95.0$  mm.,  $AX=150$  mm., and  $\mu r=2.0$ . For convenience of reproduction they are all drawn to the same maximum height. At angles below  $\theta=45^\circ$  the lines from the point focus are broadened, while above  $45^\circ$  there is a marked focusing effect and the lines are sharpened. At  $0^\circ$  the horizontal dimensions are increased by a factor  $\left(1 + \frac{R}{AX}\right)$  while at  $90^\circ$  they are reduced in the ratio  $\left(1 - \frac{R}{AX}\right)$ . Despite these dimensional changes, the final areas under the contours, and, therefore, the absorption factors, must remain unchanged,

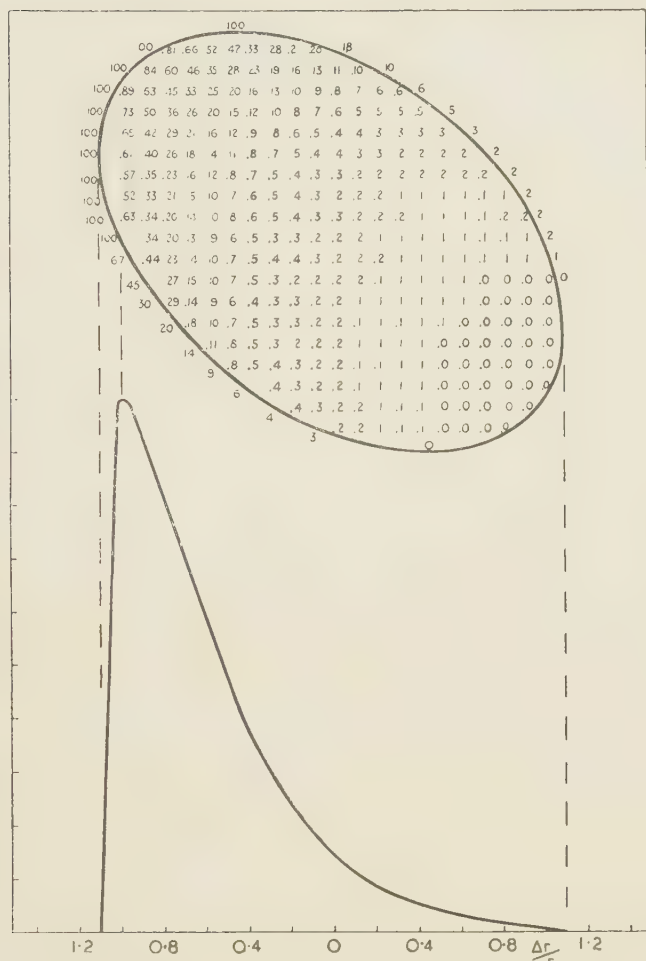


Figure 7. Generation of line-contour by means of a contour-matrix.

Drawn for  $\theta=45^\circ$ ,  $\mu r=2.0$ ,  $R=45.0$  mm.,  $AX=100.0$  mm. and for point focus.

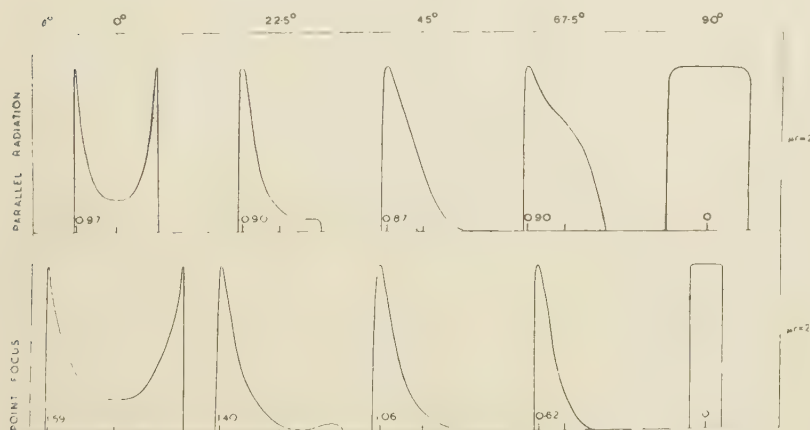


Figure 8. Comparison of basic line-contours for parallel radiation and for point focus.

Drawn for  $AX=150.0$  mm.,  $R=95.0$  mm.,  $\mu r=2.0$ .

for the summations for divergent radiation must be the same as for parallel radiation. All we have done is to change the order in which the summations are carried out. This result agrees with the analytical expression of Rusterholz (1931) when the divergence is small.

If we increase the radius  $r$  of the specimen, we increase the lengths of the rows in the matrix in proportion. We also increase the angle subtended by the

Table 3. Values of  $\Delta r/r$  for divergent radiation

Small camera of radius  $R=45.0$  mm.  
Focus-specimen distance  $AX=100.0$  mm.

$\mu r \backslash \sin^2 \theta$ $\theta$	0 0°	0.1464 22½°	0.5000 45°	0.8536 67½°	1.0000 90°
0.00	0.00	0.00	0.00	0.00	0.00
0.25	0.00	0.36	0.30	0.15 <sub>5</sub>	0.00
0.50	0.00	0.69 <sub>5</sub>	0.55	0.28	0.00
0.75	1.05 <sub>0</sub>	0.95 <sub>5</sub>	0.72	0.38	0.00
1.00	1.23 <sub>2</sub>	1.09	0.83 <sub>5</sub>	0.46	0.00
2.00	1.40 <sub>9</sub>	1.25	1.00	0.63	0.00
3.00	1.42	1.30	1.02 <sub>7</sub>	0.71	0.00
4.00	1.43 <sub>5</sub>	1.33	1.05	0.73	0.00
5.00	1.44	1.33 <sub>8</sub>	1.06	0.73 <sub>5</sub>	0.00
$\infty$	1.45 <sub>0</sub>	1.34 <sub>5</sub>	1.09 <sub>8</sub>	0.75 <sub>0</sub>	0.00

Table 4. Values of  $\Delta r/r$  for divergent radiation

Large camera of radius  $R=95.0$  mm.  
Focus-specimen distance  $AX=150.0$  mm.

$\mu r \backslash \sin^2 \theta$ $\theta$	0 0°	0.1464 22½°	0.5000 45°	0.8536 67½°	1.0000 90°
0.00	0.00	0.00	0.00	0.00	0.00
0.25	0.00	0.54	0.44	0.23	0.00
0.50	0.00	0.96	0.76	0.41	0.00
0.75	1.18 <sub>5</sub>	1.81 <sub>1</sub>	0.90	0.49 <sub>5</sub>	0.00
1.00	1.39	1.28	0.97	0.55	0.00
2.00	1.58 <sub>5</sub>	1.40	1.06	0.62	0.00
3.00	1.60	1.45	1.07 <sub>5</sub>	0.65 <sub>5</sub>	0.00
4.00	1.61 <sub>5</sub>	1.46	1.12	0.66 <sub>5</sub>	0.00
5.00	1.62 <sub>2</sub>	1.47	1.13	0.68	0.00
$\infty$	1.63 <sub>5</sub>	1.51	1.18 <sub>8</sub>	0.71 <sub>1</sub>	0.00

specimen in the same ratio, and so the matrix rows move a proportional amount relative to each other. In other words, it is as if the matrix were drawn out on a sheet of elastic which can be stretched horizontally in proportion to the radius of the specimen. If, therefore, we keep  $\mu r$  constant while at the same time increasing  $r$ , by diluting the specimen, the numbers in the matrix remain exactly the same, and the line-contour retains the same relative proportions. Thus

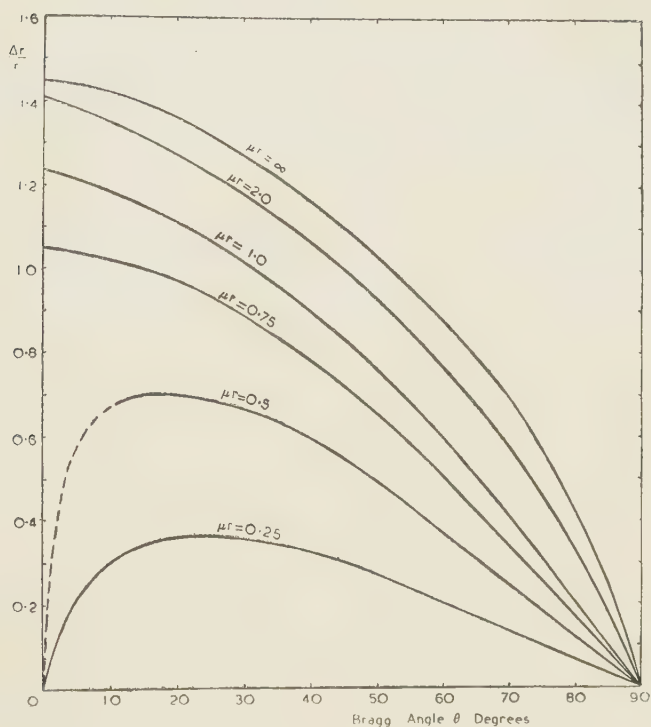


Figure 9. Peak displacement of curves  $\Delta r/r$  for point focus.  
For  $R=45.0$  mm.,  $AX=100.0$  mm.

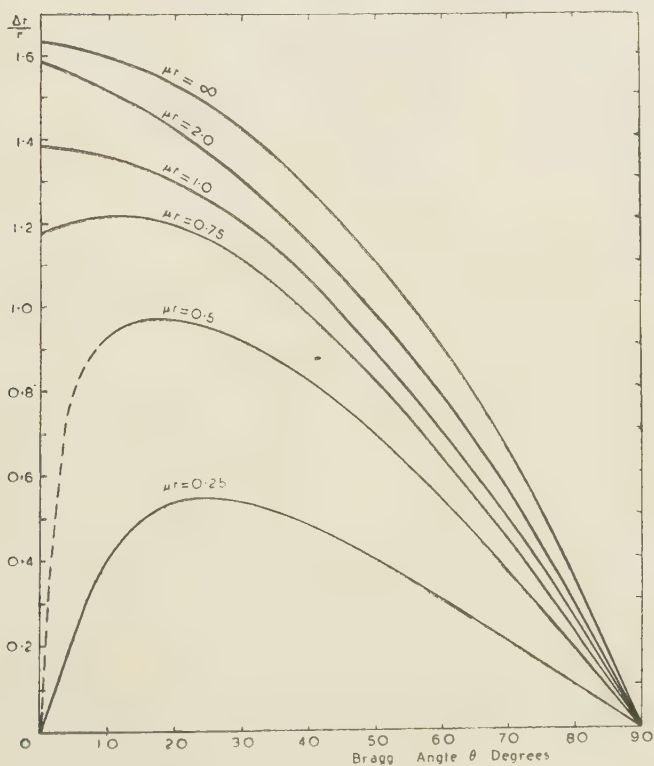


Figure 10. Peak displacement curves  $\Delta r/r$  for point focus.  
For  $R=95.0$  mm.,  $AX=150.0$  mm.

the displacement of the peak  $\Delta r$  from the central ray PB in figure 6 is directly proportional to the radius of the specimen. Thus the ratio  $\Delta r/r$  is constant for a given set of conditions for all values of the radius  $r$ , provided  $\mu r$  is kept the same. This breaks down in the case of a finite focus.

Values of  $\Delta r/r$  for divergent radiation for two standard camera sizes are given in tables 3 and 4.

The variations in  $\Delta r/r$  with  $\mu r$  for different values of  $\theta$  are best followed from figures 9 and 10. The run of these curves is totally different from those shown in figure 5 for parallel radiation, being almost linear in the range from  $\theta = 45^\circ$  to  $\theta = 90^\circ$ . For  $\mu r < 0.75$  and  $\theta < 22\frac{1}{2}^\circ$  the curves drop suddenly to the origin. The precise positions of the peaks in this region are difficult to determine with accuracy, and the  $\Delta r/r$  curves are drawn dotted to suggest their probable courses. When  $\mu r$  becomes greater than 1.0, the curves of  $\Delta r/r$  crowd together very rapidly on the limiting curve for  $\mu r = \infty$ . Values of  $\Delta r/r$  for  $\mu r = \infty$  are easily determined, for they coincide with the high-angle outer edge of the line-contour matrices.

#### § 4. MODIFIED LINE-CONTOURS

In the above derivations of the basic line-contours we have chosen a set of highly idealized conditions. In practice, neither a truly point source nor an exactly parallel beam of x rays is encountered. Moreover, the monochromatic beam we tacitly assumed to exist occupies in reality a definite, though very narrow, wave-band. We have also assumed the reflecting crystals to be perfect and to reflect the incident radiation over a negligibly small range of  $\theta$ . When the crystals are very small ( $\sim 10^{-5}$  cm.) or distorted, there is an additional angular spread which may be many degrees, corresponding to several millimetres spread on the powder diagram. Finally, when the line is microphotometered, we have to consider the effect of the finite slit in the instrument and the characteristic curve of the film emulsion. All we can do here is to indicate which factors are operative, and we shall limit ourselves to the effects produced by the focal spot and the photometer slit upon the basic line shapes.

##### (a) *Effect of focal spot*

In the majority of crystallographic tubes, the focal spot is in the form of a horizontal bar with approximate dimensions  $8.0 \times 1.0$  mm. The beam is taken off at an angle of  $5^\circ$  to  $10^\circ$ , thus foreshortening the focus to an effective area  $\simeq 1$  mm. square. Treating each point in the focus as a source of divergent rays, each point will give rise to a basic line-contour slightly displaced from its neighbour on the x-ray film. The final line shape is the integrated effect of all these contours.

We shall consider the case of  $R = 95.0$  mm. and  $AX = 150$  mm. A focus with projected area 1 mm. square corresponds to a movement of a basic line along the film of  $95 \times 1/150 = 0.633$  mm. For simplicity of calculation we shall assume the focus to be slightly smaller than this 1 mm. and make the movement across the film 0.60 mm.

We shall first take the case of a focus with a uniform distribution of energy. The basic line will move through a distance of  $\pm 0.3$  mm. on each side of its mean position as shown in figure 11 (*d*), drawn for  $\mu r = 2.0$ ,  $r = 0.25$  mm.,  $\theta = 22\frac{1}{2}^\circ$

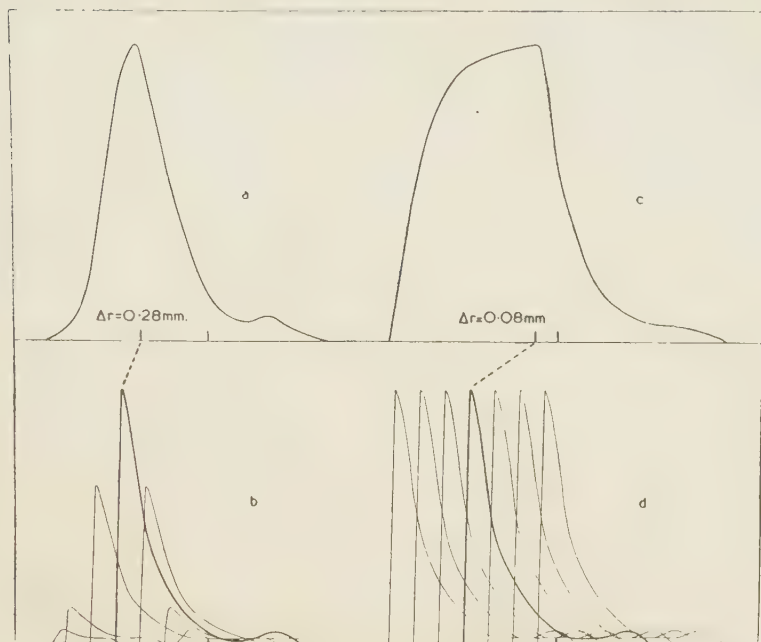


Figure 11. Generation of line-contours for uniform and exponential foci.

For  $R=95.0$  mm.,  $AX=150$  mm.,  $r=0.25$  mm.,  $\mu r=2.0$ ,  $\theta=22\frac{1}{2}^\circ$ .

(a) Line from exponential focus to form  $e^{-k^2x^2}$ .

(c) Line from uniform focus 1 mm. across.

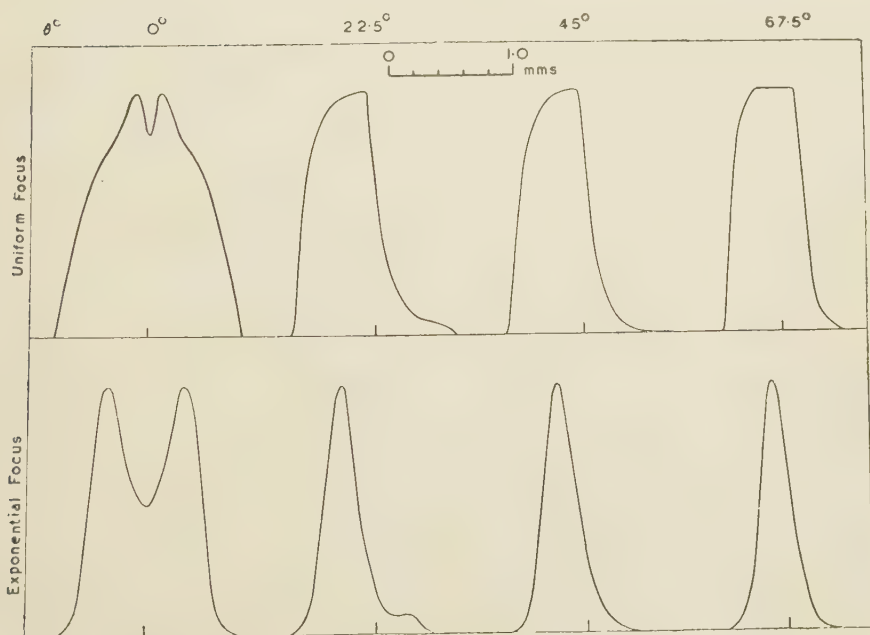


Figure 12. Effect of finite focus on line-contours.

For  $R=95.0$  mm.,  $AX=150$  mm.,  $r=0.25$  mm.,  $\mu r=2.0$ .

The net effect of the movement is the line-contour shown above it in figure 11 (c). The ordinates of the final contour were obtained by forming a matrix having 25 horizontal rows, each row being displaced through an amount equal to  $0.60/24$  mm. with respect to its neighbour. The final line shape is now quite different in appearance from the basic line-contour, and the displacement of the peak from the central ray is also very much smaller. Had the focus been broader still, the top of the line would have developed a flat central portion.

In figure 11 (a) we illustrate the effect of an energy distribution of the form  $e^{-k^2x^2}$  across the focal spot. Some of the components of the line at  $\theta = 22\frac{1}{2}^\circ$  for  $\mu r = 2.0$  and  $r = 0.25$  mm. are shown in figure 11 (b) to illustrate the build-up,

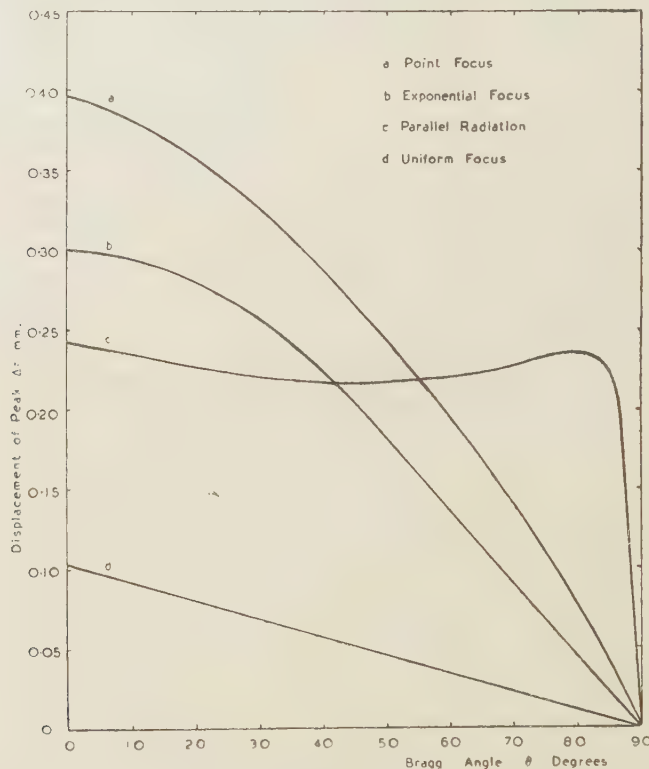


Figure 13. Values of peak displacement  $\Delta r$  mm. for different types of focus. For  $R=95.0$  mm.,  $AX=150.0$  mm.,  $r=0.25$  mm. and  $\mu r=2.0$ .

which was carried out, as in the previous example, by forming a 25-row line-contour matrix. This line shape corresponds quite closely to the shape found in practice.

A comparison of the line shapes when  $AX=150$  mm.,  $R=95$  mm.,  $\mu r=2.0$  and  $r=0.25$  obtained for uniform and exponential foci is made in figure 12. The effect of crystal imperfection and the finite width of the wave-band employed will be to broaden out the lines still further. These corrections have not been applied, as they vary from case to case.

In table 5 is shown how the experimental conditions influence the peak positions. We see that a uniform focus produces least movement of the peak from

the central ray, but the line shape is bad for satisfactory resolution of the spectra. Parallel radiation gives the sharpest peaks, but the lines are very asymmetrical. The line shapes for the exponential focus are by far the most symmetrical, and their well-defined peaks suffer rather less displacement than those for the point focus. The line shapes also correspond most closely to those found in practice.

Table 5. Values of  $\Delta r$  (mm.) for different types of focus

For  $R=95.0$  mm.,  $AX=150$  mm.,  $r=0.25$  mm.,  $\mu r=2.0$ .

Radiation	$\theta=0^\circ$	$22\frac{1}{2}^\circ$	$45^\circ$	$67\frac{1}{2}^\circ$	$90^\circ$
Parallel	0.243	0.225	0.218	0.225	0.000
Point source	0.396	0.350	0.265	0.155	0.000
Uniform source	0.105	0.080	0.050	0.030	0.000
Exponential source	0.300	0.275	0.205	0.100	0.000

Plots of  $\Delta r$  against Bragg angle  $\theta$  are shown in figure 13. Curve (d) for the uniform focus is interesting, for it reveals an almost perfectly linear relation between  $\Delta r$  and  $\theta$  for the conditions set forth in the calculation. Curves (a) and (b) for point and exponential foci are almost linear from  $45^\circ$  to  $90^\circ$ .

#### (b) Effect of finite microphotometer slit

When measuring the intensities of the spectrum lines, or their half-peak widths, a microphotometer is generally employed. The density of photographic blackening  $B$  is a measure of the x-ray intensity incident on that portion of the film where the measurement is made. For the relatively high densities obtained in x-ray diffraction work an absorption microphotometer is used. In such an instrument, the image of an incandescent source is focused on the film and the transmitted rays of light are then focused on to a narrow slit stationed in front of a photo-electric cell which registers the amount of transmitted light. The effective slit-width usually corresponds to 0.10 mm. of film, and the film is moved in steps of 0.10 mm., taking readings in each position. These readings, translated into units of photographic density  $B$ , give a curve representative of the energy distribution in the spectrum lines. For Debye-Scherrer work the Dobson type of microphotometer is perhaps the most satisfactory, as it yields values of  $B$  directly (Taylor, 1945).

If the slit is made too wide, resolving power is lost, whereas if it is made too narrow, the grain in the emulsion tends to be exaggerated. These practical considerations restrict the dimensions of the photometer slit within well-defined limits, and we must see what effect it has on the line shapes.

If the intensity of the light beam focused on the point  $x$  of density  $B_x$  is  $i_0$ , the amount  $i$  transmitted through the film is given by the expression  $i=i_0e^{-B_x}$ . If the finite slit lies with its centre at  $x$ , the instrument reading will only be an average value  $\bar{B}$  if there is a density gradient across it. It can easily be shown that  $\bar{B}=\log_e \left( 1/\int e^{-B_x} dx \right)$ , where the integration (performed graphically) is taken over the slit width.

In figure 14 we have chosen the line-contours for  $\theta = 45^\circ$  and  $\theta = 22\frac{1}{2}^\circ$  to illustrate the effect of a slit 0.10 mm. wide. We find that the lines are slightly broadened at the base while the steeply rising portions are appreciably reduced in intensity. This has the effect of reducing the peak height and reducing the line width without affecting the peak position in curve A for  $22\frac{1}{2}^\circ$ , while in B, where the density falls sharply on one side of the maximum, there is a marked rounding-off of the peak, and the peak position is displaced away from the steep portion of the curve.

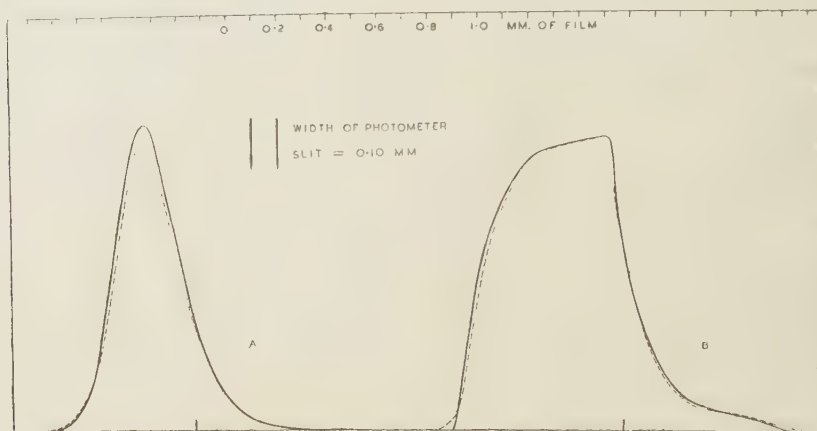


Figure 14. Effect of photometer slit on line shape.

A.  $\theta = 45^\circ$ ,  $\mu r = 2.0$ , exponential focus.

B.  $\theta = 22\frac{1}{2}^\circ$ ,  $\mu r = 2.0$ , uniform focus.

$R = 95.0$  mm.,  $AX = 150.0$  mm.,  $r = 0.25$  mm.

Provided that the photometer slit is not too wide in relation to the width of the line, its effect on line shape will be relatively small. Assuming the crystals themselves do not produce an excessive amount of broadening, due to lattice distortion or small grain size, the distribution of the energy in the focal spot will produce the most important modifications in the basic line-contours. This energy distribution is most easily obtained by taking a "pin-hole" photograph of the focal spot.

##### § 5. THE INFLUENCE OF LINE SHAPE UPON THE DETERMINATION OF LATTICE PARAMETERS

We have seen that absorption tends to move the peaks in a direction of increasing  $\theta$  by amounts depending on the experimental conditions. This, in turn, considerably influences the value of the lattice parameters computed from the corresponding  $\theta$  values of the peaks. To eliminate the errors due to absorption and the displacement of the specimen from the geometrical centre of the camera, various extrapolation methods have been devised which make full use of the high-angle reflexions for which the resolving power of the powder photograph is greatest.

Briefly, values of the lattice parameter  $a$  obtained from the observed value of  $\theta$  are plotted against corresponding values of  $\theta$ ,  $\cos^2 \theta$ ,  $\cot \theta$  or  $(\pi/2 - \theta) \cot \theta$ .

The value obtained by extrapolation against the selected function of  $\theta = 90^\circ$  is substantially free from error. A small correction, approximately one part in 50,000, is added to the parameter to correct for refractivity.

Most generally used is the plot of parameter against  $\cos^2 \theta$  with extrapolation to  $\cos^2 \theta = 0$ . Considerations of the curves for  $\Delta r/r$  show that plot to be eminently suitable for lattice-parameter determinations when there are sufficient reflexions above  $45^\circ$ . Further consideration shows that if the parameters are plotted against  $\frac{1}{2} \left( \frac{\cos^2 \theta}{\theta} + \frac{\cos^2 \theta}{\sin \theta} \right)$ , a perfectly straight line plot is obtained from  $\theta = 0^\circ$  to  $\theta = 90^\circ$ , provided the focus takes the form  $e^{-k^2 x^2}$  and the specimen is accurately centred in the camera.\* In this case one high-order reflexion in the region of  $\theta = 70$  to  $80^\circ$  and a very low-order reflexion,  $\theta \simeq 10^\circ$ , are sufficient to obtain the very highest accuracy in parameter. This important result, and other extrapolation possibilities, are discussed in a later communication.

#### § 6. CONCLUSIONS

It has been shown possible to draw the contours of Debye-Scherrer lines for conditions of parallel and divergent radiation, and to obtain from them the macro-absorption factors  $\alpha$  with a high degree of accuracy. The distribution of energy in the focal spot was shown to exert a considerable influence on the ultimate line shape, while the effect of the photometer slit was relatively small, though by no means negligible. The accurate determination of peak displacements leads to new forms of lattice-parameter extrapolation curves.

#### ACKNOWLEDGMENT

The authors wish to thank the English Electric Co., Ltd., for permission to publish this paper.

\* The authors are much indebted to Dr. D. P. Riley, of the Cavendish Laboratory, Cambridge, who first used this expression, and for which a theoretical basis can now be given.

#### REFERENCES

- BLAKE, F. C., 1933. *Rev. Mod. Phys.* **5**, 169.  
 BRADLEY, A. J., 1935. *Proc. Phys. Soc.* **47**, 879.  
 BRADLEY, A. J. and JAY, A. H., 1932. *Proc. Phys. Soc.* **44**, 563.  
 BRENTANO, J., 1935. *Proc. Phys. Soc.* **47**, 932.  
 BRINDLEY, G. W., *Phil. Mag.* (In the press.)  
 BRINDLEY, G. W. and SPIERS, F. W., 1938. *Proc. Phys. Soc.* **50**, 17.  
 CLAASSEN, A., 1930. *Phil. Mag.* **9**, 57.  
 GREENWOOD, G., 1927. *Phil. Mag.* **3**, 963.  
 MCKEEHAN, L. W., 1922. *J. Franklin Inst.* **193**, 231.  
 RUSTERHOLZ, A., 1931. *Helv. phys. Acta*, **4**, 68.  
 SCHÄFER, K., 1933. *Z. Phys.* **86**, 738.  
 TAYLOR, A., 1944. *Phil. Mag.* **35**, 215.  
 TAYLOR, A., 1945. *Introduction to X-ray Metallography*, p. 92. (Chapman and Hall.)

# ON THE DETERMINATION OF LATTICE PARAMETERS BY THE DEBYE-SCHERRER METHOD

BY A. TAYLOR AND H. SINCLAIR

*Communicated by Sir Lawrence Bragg, F.R.S. ; MS. received 23 October 1944*

**ABSTRACT.** The types of systematic error arising in the determination of lattice parameters by the use of Debye-Scherrer powder diagrams are discussed. The various extrapolation methods are reviewed, and it is shown how a consideration of the absorption factor and geometry of the focal spot lead to the most satisfactory forms of extrapolation curve. It is shown how the absence of specimen eccentricity enables perfectly linear extrapolation curves to be drawn, thus allowing fullest use to be made of low-angle reflexions, whereby the very highest accuracy in parameter determination may be achieved.

## § 1. THE DETERMINATION OF LATTICE PARAMETERS

CIRCULAR Debye-Scherrer powder cameras are most conveniently used in the identification of compounds and alloy phases. When the structures have relatively high symmetry, powder photographs may also be employed for the elucidation of their atomic arrangements. At some stage of the work, particularly in the case of alloys when the course of a phase boundary is being followed, it becomes necessary to make precision measurements on the dimensions of the unit cell. If the Debye-Scherrer camera has been satisfactorily designed, it is possible to record diffraction spectra at Bragg angles in the region of 85 to 86°. It is then possible to achieve an accuracy in lattice-parameter measurement comparable with that yielded by flat-film back-reflexion cameras recording only a limited portion of the diffraction pattern.

All parameter determinations by x-ray methods involve the derivation of the Bragg angle  $\theta$  for a given set of reflecting planes from measurements on the peak positions of the diffraction spectra. These peak positions are very sensitive to the experimental conditions, which introduce various systematic errors into the parameter determinations. In our discussion, we shall consider only cubic crystals, and thus confine ourselves to one lattice parameter, although the methods under consideration can, in many cases, be applied to more complicated unit cells.

For a cubic crystal, the lattice parameter  $a$  is related to the wave-length within the crystal of the radiation  $\lambda$ , the Bragg angle  $\theta$ , and the indices of reflexion  $hkl$ , by the equation

$$a = \frac{\lambda}{2} \frac{\sqrt{h^2 + k^2 + l^2}}{\sin \theta}. \quad \dots\dots(1)$$

The fractional error in  $a$ , caused by errors in measuring  $\theta$ , is obtained by differentiating equation (1), and is

$$\frac{da}{a} = -\cot \theta d\theta. \quad \dots\dots(2)$$

Thus in the region where  $\theta$  approaches  $90^\circ$ ,  $\cot \theta$  tends to zero, and any error in measuring  $\theta$  produces only a small variation in the lattice parameter. In aiming at the highest accuracy in parameter determination, it is thus essential to design a camera which will record as high a Bragg angle as possible, and to choose a radiation which will give spectra at a high Bragg angle.

If  $R$  is the camera radius and  $S$  the distance between corresponding reflexions on each side of the incident ray,

$$S = 4R\theta, \quad \text{so that} \quad dS = 4Rd\theta.$$

Hence

$$\frac{da}{a} = -\frac{\cot \theta}{4R} dS. \quad \dots\dots(3)$$

The errors  $dS$  which arise from the experimental conditions may be classified under the following headings :—

- (a) Finite length of specimen irradiated by the beam.
- (b) Film shrinkage.
- (c) Refractive index of the crystal for x rays.
- (d) Eccentricity of the specimen.
- (e) Absorption of the beam within the specimen.

A. J. Bradley and A. H. Jay (1932) have shown that the error in lattice parameter caused by (a) is negligibly small. They eliminate the effects of (uniform) film shrinkage by fitting the camera with knife-edges which subtend a standard angle  $\theta_k$  in the region of  $\theta = 90^\circ$ .  $\theta_k$  is obtained by measuring the camera directly or by taking a photograph of a standard material such as rock-salt or quartz for which the angles of reflexion are known to a very high accuracy (Bradley and Jay, 1933; Wilson and Lipson, 1941). The angle  $\theta$  of any pair of lines on the film is related to  $S$ , the distance between the lines, by the relation  $\theta/\theta_k = S/S_k$ , where  $S_k$  is the distance apart of the fiducial marks on the film produced by the knife-edge shadows.

The correction for refractive index is very small, being of the order of one part in 50,000. This is added to the final value of the lattice parameter (Weigle, 1934; Jette and Foote, 1935).

The errors in lattice parameter introduced by the eccentricity of the specimen and by absorption are most easily eliminated by extrapolation methods making use of high-angle reflexions where the resolving power of the powder photograph is greatest and errors in  $\theta$  least. The simplest of these methods was described by G. Kettman (1929), who plotted values of lattice parameter  $a$  calculated for each line on the film against corresponding values of Bragg angle  $\theta$ . A smooth curve was drawn through the points, and by extrapolating to  $\theta = 90^\circ$ , a value of  $a$  was obtained largely freed from experimental error. A similar process is described by Bradley and Jay, who plot values of  $a$  against the corresponding values of  $\cos^2 \theta$  and extrapolate to  $\cos^2 \theta = 0$ . Extrapolations may also be carried out against  $\cot \theta$  or  $(\pi/2 - \theta) \cot \theta$ , as pointed out by Buerger (1942).

All these methods of graphical extrapolation yield slightly different values of  $a$ . The source of the differences lies in not really knowing the exact equation of the function plotted and trying to eliminate the effects of absorption and

eccentricity with one and the same extrapolation curve. Although the errors vanish when  $\theta = 90^\circ$ , and, therefore, when  $\cos^2 \theta$ ,  $\cot \theta$  and  $(\pi/2 - \theta) \cot \theta = 0$ , the highest angle at which a line can be measured is set by the geometry of the camera and the wave-length of the radiation, and this angle is in the region of  $80$  to  $85^\circ$ . Because the extrapolation curves have different shapes, and the distances over which the extrapolations are carried out differ greatly, they cut the  $a$ -parameter axis in different places. To decide which form of the extrapolation curve we should take we must see how the line-contours and the eccentricity of the specimen influence the peak positions.

## § 2. ERRORS PRODUCED BY ECCENTRICITY AND ABSORPTION

### (a) Errors produced by eccentricity

In (a) of figure 1 the specimen B is displaced from the centre of the camera A through the distance  $p$  at an angle  $\phi$  with respect to the incident beam. Bradley and Jay (1932) have shown that the displacement may be considered as a vector split into the two components  $p \sin \phi$  and  $p \cos \phi$ , as shown in (b) and (c) of figure 1.

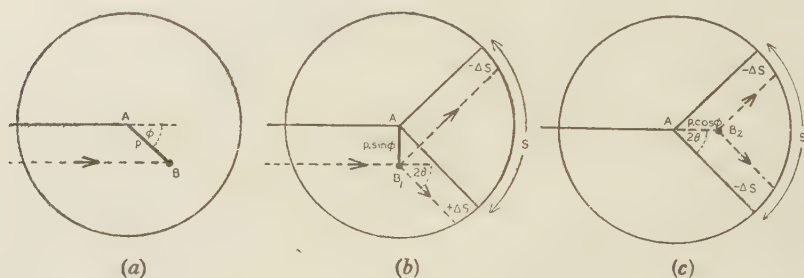


Figure 1. Effect of specimen eccentricity on line position.  
(After A. J. Bradley and A. H. Jay, *Proc. Phys. Soc.* **44**, 563, 1932.)

The former displacement produces a change in  $S$  of  $-\Delta S + \Delta S = 0$ , while the latter produces a net change of  $-\Delta S - \Delta S = -\Delta S_{ecc} = 2p \cos \phi \sin 2\theta$  in the value of  $S$ . Thus, in considering the errors introduced by the eccentricity of the specimen, we find that only displacements along the line of the undeviated incident beam have any effect.

### (b) Errors produced by absorption

In a previous communication (1945) we showed how absorption displaced the peaks of the lines in the direction of greater  $\theta$  by an amount which depended on the experimental conditions. If  $\Delta r$  is the shift of a diffraction line due to absorption alone, the error in  $S$  must be  $\Delta S_a = 2\Delta r$ , considering the two symmetrical portions of the film lying on each side of the incident ray. Hence the total line displacement due to absorption and eccentricity is

$$\begin{aligned} \Delta S &= \Delta S_a + \Delta S_{ecc} \\ &= 2\Delta r - 2p \cos \phi \sin 2\theta. \end{aligned} \quad \dots\dots(4)$$

The corresponding error in lattice parameter is, therefore,

$$\begin{aligned}\frac{da}{a} &= -\frac{dS}{4R} \cot \theta \\ &= -\frac{1}{4R} (2\Delta r - 2p \cos \phi \sin 2\theta) \cot \theta \\ &= -\frac{\Delta r}{2R} \cot \theta + \frac{p \cos \phi}{R} \cos^2 \theta. \quad \dots\dots(5)\end{aligned}$$

Thus when  $\theta$  tends to  $90^\circ$ ,  $\cot \theta$ ,  $\cos^2 \theta$ , and also  $\Delta r$ , all tend to zero, and, therefore, at  $\theta = 90^\circ$ ,  $da/a = 0$ . To determine the most satisfactory form of extrapolation curve, we must obtain an expression for the variation of  $\Delta r$  with  $\theta$ .

### § 3. FORMS OF EXTRAPOLATION CURVE

#### a) The Bradley and Jay $\cos^2 \theta$ extrapolation

In figure 2 we show curves of  $\Delta r$  for different types of tube focus covering the angle from  $\theta = 0$  to  $90^\circ$ . They have been drawn for a Debye-Scherrer camera of radius  $R = 95.0$  mm. and a distance AX of 150 mm. between the specimen

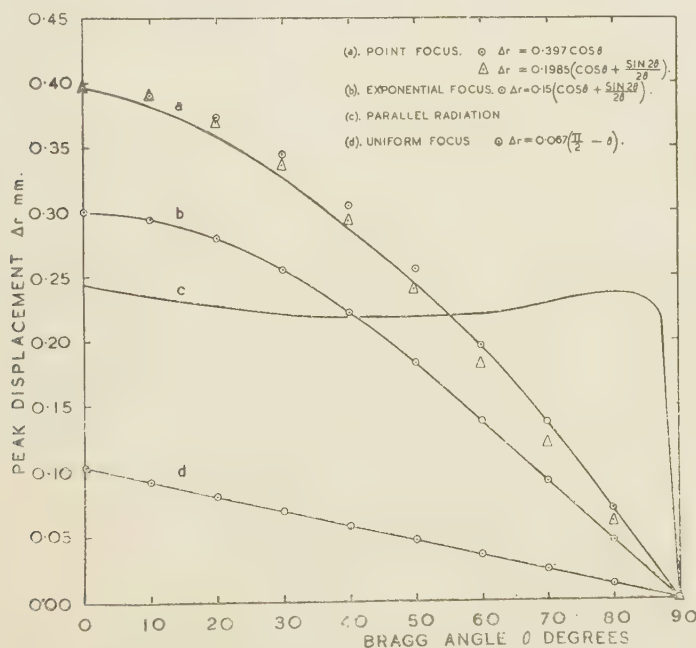


Figure 2. Values of  $\Delta r$  for different types of focus.

Full curves are those obtained from the line contours calculated for camera radius  $R = 95.0$  mm., specimen-focus distance  $AX = 150.0$  mm., specimen radius  $r = 0.25$  mm.,  $\mu r = 2.0$ . Points are values obtained by empirical formulae.

and focus. The radius of the specimen,  $r$ , was taken to be  $0.25$  mm., a figure quite close to the one occurring in practice. The value  $\mu r = 2.0$  was taken, the line-contours for this case being the ones most accurately determined. It should be borne in mind that  $\Delta r$  does not vary a great deal between the values  $\mu r = 1.0$

and  $\mu r = \infty$ . although, of course, the macro-absorption factor  $\alpha$  varies quite considerably.

If we compute the values of  $\frac{\Delta r}{2R} \cot \theta$  for the cases of divergent radiation from uniform, exponential and point foci, we find they plot as near-linear functions of  $\cos^2 \theta$  over the limited range from 60 to 90°. The R.H.S. of equation (5) is thus a near-linear function of  $\cos^2 \theta$ . By plotting  $a$  against  $\cos^2 \theta$ , it is possible to obtain almost straight extrapolation curves which simultaneously eliminate eccentricity and absorption errors. Provided we have sufficient spectra in the high-angle region, the  $\cos^2 \theta$  extrapolation would seem to be the best one to use.

The possible case of parallel radiation is worthy of mention as it may arise if a perfect crystal is used as a means of producing monochromatic radiation.

The term  $\frac{\Delta r}{2R} \cot \theta$  is then no longer a linear function of  $\cos^2 \theta$ , because of the abrupt manner in which  $\Delta r$  falls to zero between 85 and 90°. In such an instance the Bradley and Jay extrapolation against  $\cos^2 \theta$  will no longer apply, and it then becomes necessary to correct all individual values of  $S$  by the amount  $\Delta r$  before computing the values of  $\theta$ . The residual error in  $a$  would then be entirely due to the eccentricity factor alone and would simply be  $\frac{da}{a} = -\frac{p \cos \phi}{R} \cos^2 \theta$ , which plots as a straight line against  $\cos^2 \theta$ .

For comparison purposes it is easiest to plot curves of  $da/a$  rather than  $a$  against  $\cos^2 \theta$ . These are shown in figure 3 for conditions of parallel radiation and divergent radiation. The values for the eccentricity in each example are  $p \cos \phi = 0$  and  $\pm 0.5$  mm.

For parallel radiation, the curves show a sudden upward inflexion below  $\cos^2 \theta = 0.025$ , which corresponds to the sudden change in  $\Delta r$  in the range  $85^\circ < \theta < 90^\circ$ . For divergent radiation, the extrapolation curves are very slightly convex upwards and are almost straight for the case of a uniform focus. This is no longer true if the plots are made against  $\theta$  or  $\cot \theta$  unless  $p \cos \phi = 0$ .

In their original derivation of the  $\cos^2 \theta$  extrapolation rule, Bradley and Jay take an extreme case by assuming  $\mu r = \infty$  and a point focus. The positions of the peaks are assumed to be near the high-angle outer edge of the lines at a fractional distance

$$\frac{\Delta r}{r} = \frac{\sin 2\theta}{2\theta} \left( 1 + \frac{R}{AX} \right) \quad \dots\dots(6)$$

from the central ray. No formal proof is given for this relation, its sole justification apparently lying in the fact that when added to the eccentricity correction one arrives at the expression

$$\frac{da}{a} = \left( \frac{p \cos \phi}{R} - \frac{r}{2\theta R} - \frac{r}{2\theta AX} \right) \cos^2 \theta, \quad \dots\dots(7)$$

which plots almost linearly against  $\cos^2 \theta$ .

Equation (6) gives results for  $\Delta r/r$  rather different from our own, which are obtained directly from the line-contours. In the following table we make a comparison of  $\Delta r/r$  calculated from equation (6) and the line-contour method for a point focus when  $R = 95$  mm.,  $AX = 150$  mm. and  $\mu r = \infty$ ,

Comparison of  $\Delta r/r$  with  $\mu r = \infty$  and point focus

$\theta$ ( $^\circ$ )	0	$22\frac{1}{2}$	45	50	60	70	80	90
Bradley and Jay	1.635	1.432	1.042	0.930	0.670	0.430	0.225	0.000
Contour method	1.635	1.510	1.185	1.115	0.910	0.665	0.370	0.000

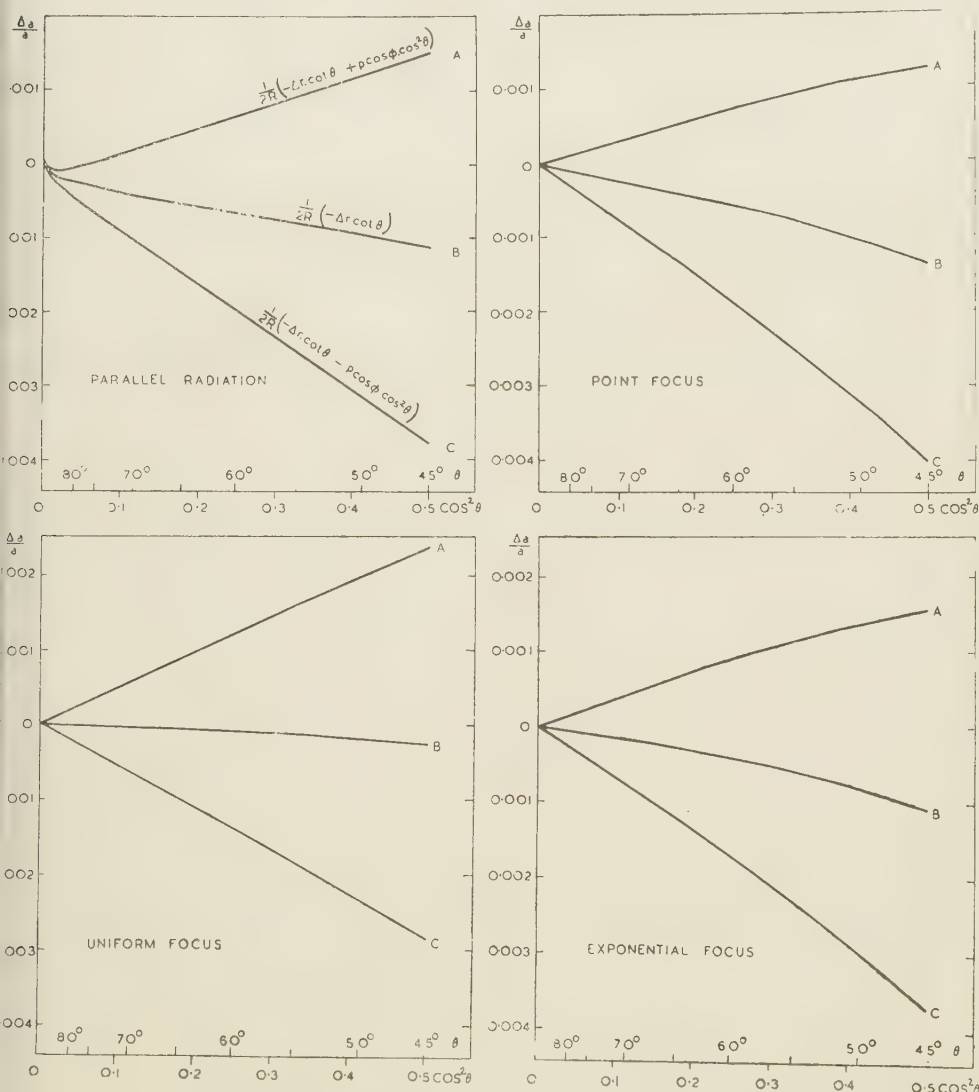


Figure 3. Plots of  $da/a$  against  $\cos^2 \theta$ .

$$(A) \quad \frac{da}{a} = \frac{1}{2R} (-\Delta r \cot \theta + p \cos \phi \cos^2 \theta).$$

$$(B) \quad \frac{da}{a} = \frac{1}{2R} (-\Delta r \cot \theta),$$

$$(C) \quad \frac{da}{a} = \frac{1}{2R} (-\Delta r \cot \theta - p \cos \phi \cos^2 \theta),$$

with  $AX=150.0$  mm.,  $R=95.0$  mm.,  $r=0.25$  mm.,  $\mu r=2.0$ ,  $p \cos \phi=0$  and  $\pm 0.5$  mm.

Although Bradley and Jay's results differ appreciably from our own, they follow substantially the same course, and it is for this reason that their approximation works. Their theory does not include the effects of a finite focal spot, which, as we have seen, has a major influence on the final positions of the peaks. Our investigation has shown that in the real case of a finite focus, the extrapolations against  $\cos^2 \theta$  actually plot straighter than those given by the original theory for all values of  $\mu r > 1.0$ .

(b) *Other extrapolation possibilities—uniform focus, no eccentricity*

We have seen how over the limited range extending from  $\theta = 60$  to  $90^\circ$ , the term  $\Delta r/2R \cot \theta$  of equation (5) was a near-linear function of  $\cos^2 \theta$ . This leads us to examine the curves of  $\Delta r$  against  $\theta$  to see if we can express them as simple trigonometrical functions.

Consider first of all curve (d) in fig. 2, which refers to a uniform focus. This is a straight line, and its equation is of the form

$$\Delta r = k (\pi/2 - \theta). \quad \dots\dots(8)$$

Thus in the absence of eccentricity, equation (5) reduces to the very simple form

$$\frac{da}{a} = -\frac{k}{2R} (\pi/2 - \theta) \cot \theta. \quad \dots\dots(9)$$

If, then, the focal spot were uniform, as would most likely be the case in a gas tube, and if the camera were so accurately constructed that the specimen holder were at its geometrical centre, then the correct extrapolation procedure to use would be to plot  $a$  against the function  $(\pi/2 - \theta) \cot \theta$ . This would be a *perfectly straight-line plot* from  $0$  to  $90^\circ$ , and two reflexions, one in the region of  $80^\circ$  and one in the low orders, say  $10$  to  $20^\circ$ , would be quite sufficient to yield a high enough accuracy in the parameter determination. This opens up entirely new possibilities in the accurate determination of the lattice parameters of non-cubic crystals when very few suitable reflexions are available.

*Exponential focus*

The exponential focus with an intensity distribution of the form  $e^{-k^2 x^2}$  is probably the most prevalent type. The nature of the  $\Delta r$  curve given by such a focus is illustrated by (b) in figure 2. This curve can be matched *exactly* by the expression

$$\Delta r = k \left( \cos \theta + \frac{\sin 2\theta}{2\theta} \right), \quad \dots\dots(10)$$

where  $k = 0.15$  for the experimental conditions considered.

In the absence of eccentricity we have

$$\begin{aligned} \frac{da}{a} &= -\frac{\Delta r}{2R} \cot \theta \\ &= -\frac{k}{2R} \left( \frac{\cos^2 \theta}{\sin \theta} + \frac{\cos^2 \theta}{\theta} \right). \quad \dots\dots(11) \end{aligned}$$

In this particular case of exponential focus and no eccentricity, we obtain a perfectly linear extrapolation curve between  $\theta = 0^\circ$  and  $\theta = 90^\circ$  if we plot  $a$  against corresponding values of  $\frac{1}{2} \left( \frac{\cos^2 \theta}{\sin \theta} + \frac{\cos^2 \theta}{\theta} \right)$ . This plot should be even more valuable than the previous example given in equation (9), since an exponential focus is much more likely to be encountered in practice.

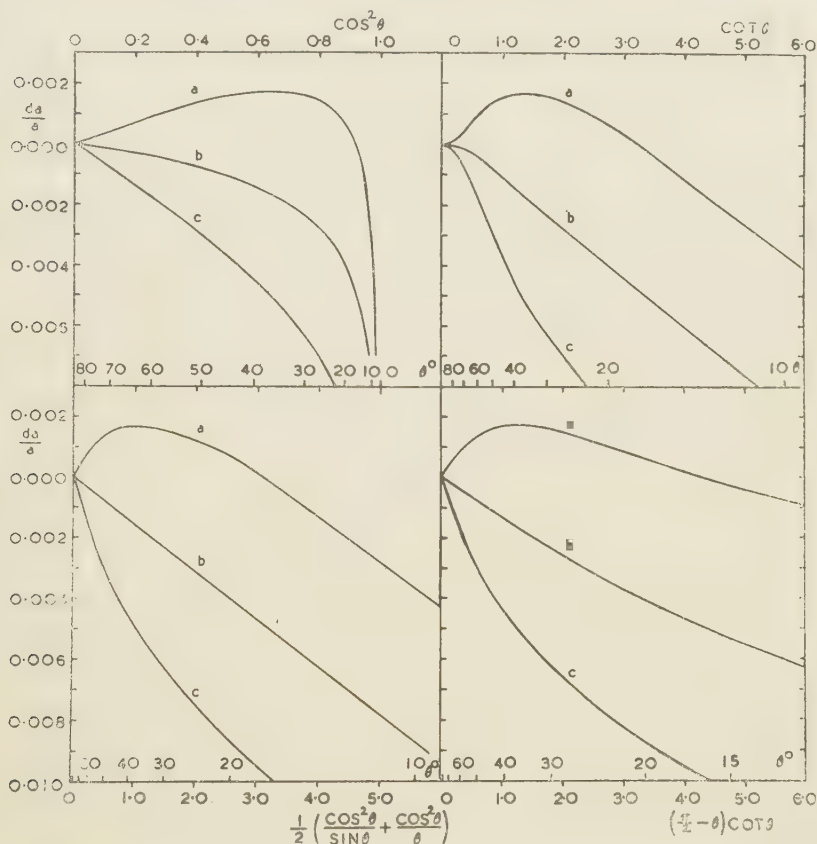


Figure 4. Typical extrapolation curves for exponential focus.

Camera radius  $R = 95.0$  mm.

Specimen-focus distance  $AX = 150.0$  mm.

Specimen radius  $r = 0.25$  mm.;  $\mu r = 2.0$ .

(a)  $p \cos \phi = 0.50$  mm.

(b) No eccentricity, or  $p \cos \phi = 0$  mm.

(c)  $p \cos \phi = -0.50$  mm.

When eccentricity is present, the error curve takes the form

$$\frac{da}{a} = -\frac{k}{2R} \left( \frac{\cos^2 \theta}{\sin \theta} + \frac{\cos^2 \theta}{\theta} \right) + 2p \cos \phi \cos^2 \theta. \quad \dots (12)$$

This departs quite appreciably from the curve of equation (11) if plotted against  $\frac{1}{2} \left( \frac{\cos^2 \theta}{\sin \theta} + \frac{\cos^2 \theta}{\theta} \right)$  as shown in figure 4 (drawn for  $p \cos \phi = \pm 0.5$  mm.). The

curvature is rather exaggerated by the crowding of the high-order reflexions into a range very close to the axis of ordinates.

If we increase the horizontal scale until it is comparable with that for the  $\cos^2\theta$  plot, we find that in the range 30 to 90° the curves are not very different from each other. The great advantage to be gained by plotting  $a$  against  $\frac{1}{2} \left( \frac{\cos^2\theta}{\sin\theta} + \frac{\cos^2\theta}{\theta} \right)$  is that in the absence of eccentricity the curve becomes a perfectly straight line, and the fullest use can be made of the lowest orders.

It should not be difficult to make cameras free from eccentricity. Should eccentricity be present in an existing camera, it could be allowed for in the first stages of the  $\theta$  calculations by correcting all values of  $S$  by the amount  $\Delta S_{ecc} = -2p \cos\phi \sin 2\theta$ . The magnitude  $2p \cos\phi$  is a constant of the camera. It could be obtained by direct measurement or by plotting extrapolation curves for a cubic crystal and finding by trial a value of  $2p \cos\phi$ , which leads to a straight-line plot of  $a$  against  $\frac{1}{2} \left( \frac{\cos^2\theta}{\sin\theta} + \frac{\cos^2\theta}{\theta} \right)$ .

### Point focus

This is an idealized case. The  $\Delta r$  curve illustrated by (a) in figure 2 can be matched over the range 60 to 90° by the expression

$$\Delta r = k \cos\theta. \quad \dots\dots (13)$$

Thus, in the absence of eccentricity,

$$\begin{aligned} \frac{da}{a} &= - \frac{k \cos\theta}{2R} \cdot \cot\theta \\ &= - \frac{k \cos^2\theta}{2R \sin\theta}, \quad \dots\dots (14) \end{aligned}$$

and a plot of parameter against  $\frac{\cos^2\theta}{\sin\theta}$  is perfectly linear over the range 60 to 90°.

Since  $\sin\theta$  changes very slowly, from 0.8660 to 1.0000 over this range, there is only a slight curvature in a  $\cos^2\theta$  plot. This is, of course, the reason why Bradley and Jay's extrapolation proves to be so good.

An attempt was made to fit an expression of the form  $\Delta r = k \left( \cos\theta + \frac{\sin 2\theta}{2\theta} \right)$  to the  $\Delta r$  curve for the point focus. The calculated points shown by triangles in figure 2 are rather high in the low orders and low in the high orders, with coincidences at 0°, 45° and 90°. The agreement is sufficiently close, even in this case, to justify an extrapolation of  $a$  against  $\frac{1}{2} \left( \frac{\cos^2\theta}{\sin\theta} + \frac{\cos^2\theta}{\theta} \right)$ .

### § 4. CONCLUSIONS

With careful camera construction there should be no eccentricity of the specimen. In that event perfectly linear extrapolation-curves can be drawn covering the range  $\theta = 0^\circ$  to  $\theta = 90^\circ$  for the real cases of uniform and exponential foci. Which type of plot should be used can easily be ascertained by taking a

powder photograph of a cubic crystal, plotting extrapolation curves of  $a$  against  $(\pi/2 - \theta) \cot \theta$  and  $\frac{1}{2} \left( \frac{\cos^2 \theta}{\sin \theta} + \frac{\cos^2 \theta}{\theta} \right)$  and finding which gives a straight-line plot over the whole measurable range.

These straight-line extrapolation plots require fewer reflexions to obtain the same accuracy in spacing as given by  $\cos^2 \theta$  curves, for the maximum use can be made of those low-order reflexions which lie in the region of  $10^\circ$ . Also, any "scatter" of the calculated parameters which personal errors introduce into film measurement can easily be allowed for by using the method of least squares to derive the most probable straight-line extrapolation curve.

In the past it has proved very difficult to make accurate parameter measurements on non-cubic crystals owing to the small number of reflexions with suitable indices. Instead, the complicated analytical method of M. U. Cohen (1935 and 1936) had to be employed. The straight-line plots described above should remove these difficulties.

It is felt that the new types of linear extrapolation-curve will enable lattice parameters to be measured with a much higher degree of accuracy than the one part in 50,000 which has hitherto been possible. It is quite probable that in the near future a greater precision in the determination of the x-ray wave-lengths will be required if full use is to be made of the increased accuracy in spacing determination. It will also be more necessary than ever to keep the temperature of the specimen constant while the powder photograph is being taken.

#### ACKNOWLEDGMENTS

The authors wish to thank the English Electric Company for their permission to publish this paper, and Dr. D. P. Riley, of the Cavendish Laboratory, Cambridge, for his very helpful discussions.

#### REFERENCES

- BRADLEY, A. J. and JAY, A. H., 1932. *Proc. Phys. Soc.* **44**, 563 ; 1933. *Ibid.* **45**, 507.  
 BUERGER, M. J., 1942. *X-ray Crystallography* (J. Wiley and Sons).  
 COHEN, M. U., 1935. *Rev. Sci. Instrum.* **6**, 68 ; 1936. *Z. Kristallogr. (A)*, **94**, 288.  
 COMPTON, A. H. and ALLISON, S. K., 1935. *X-rays in Theory and Experiment* (London : Macmillan and Co., Ltd., 2nd edition), pp. 279 and 672.  
 JETTE, E. R. and FOOTE, F., 1935. *J. Chem. Phys.* **3**, 10.  
 KETTMANN, G., 1929. *Z. Phys.* **53**, 198.  
 TAYLOR, A. and SINCLAIR, H., 1945. *Proc. Phys. Soc.* **57**, 108.  
 WEIGLE, J., 1934. *Helv. phys. Acta*, **7**, 46.  
 WILSON, A. J. C. and LIPSON, H., 1941. *Proc. Phys. Soc.* **53**, 245.

# RECENT IMPROVEMENTS IN A PRECISION BALANCE AND THE EFFICACY OF RHODIUM PLATING FOR STANDARD WEIGHTS

BY JOHN JOB MANLEY,

Bournemouth; formerly Fellow of Magdalen College, Oxford

*MS. received 7 November 1944*

**ABSTRACT.** The main theme of this paper is a description of the improvements introduced into our precision balance with the object of enhancing its already high sensitivity and thus ensure a corresponding increase in accuracy in weighing.

As a secondary objective we have investigated the claim made for highly polished rhodium-plated weights and have found that weights so protected are superior to all others we have critically examined.

## § 1. INTRODUCTORY

IN former papers\* dealing with high-grade balances we have shown how certain of their inherent defects may be allowed for and a truer value obtained for any mass that is being weighed. In this present paper is given an account of more recent refinements, the introduction of which have enabled us to attain a degree of accuracy for a long time elusive and but recently realized. It may be noted that since the positions of the riders are each read to  $1/34$  of a minor division of the beam, the smallest measurable difference in weight is ( $0.01/34$  mg.). We now describe in detail (1) the several refinements introduced, and (2) how these enabled us to apply exacting tests as to the advantage following the use of rhodium-plated weights.

## § 2. IMPROVEMENTS IN THE BALANCE

Our most recent improvements are:

- ( $\alpha$ ) the substitution of a new scale for that engraved upon the beam;
- ( $\beta$ ) the use of pladuram wires for carrying the riders;
- ( $\gamma$ ) the employment of platinum wire grids for ascertaining when the loaded pans possess a common temperature;
- ( $\delta$ ) a screened bridge wire; and, finally,
- ( $\epsilon$ ) a new cell for enclosing the pans.

We describe the several changes in the order just given.

( $\alpha$ ) *New scale for the beam.* For ensuring the highest order of accuracy in former researches it was necessary to calibrate the scale engraved upon the beam and apply corrections for various errors. To obviate this procedure, another

\* *Philos. Trans. A*, **210**, 387–415 (1910); *ibid.* **212**, 227–260 (1912); *Proc. Phys. Soc.* **39**, pt. 5, 444–448 (1927); *Proc. Roy. Soc. A*, **86**, 591 (1912); "Balance", in Thorpe's *Dict. of Applied Chem.*, new edition (1937).

scale free from measurable discrepancies was obtained as follows:—First a thin strip of aluminium having the appropriate width and length was prepared and three holes drilled in it; one of these was at the centre and one near each end; that at the centre just admitted the passage of a screw, whilst the other two were slightly elongated horizontally; this done, the required scale was engraved with the aid of a dividing engine adjustable to 0.005 mm. and a lightly applied tool; the strip was then given a final polish and the scale calibrated with a travelling microscope. The result showed that within the limits of our measurements (0.005 mm.) the divisions were strictly equivalent. The scale was now secured to the beam by the central screw and the end screws driven so nearly home that although the strip made contact with the beam throughout, it was yet free to expand and contract consequent upon variations in temperature. It will however be granted that the slight difference in the expansions of aluminium and the phosphor-bronze composing the beam is wholly negligible.

( $\beta$ ) *The carrier wires for the riders.* Hitherto the riders designated *A* and *B*, the respective values of which are 10 and 1 mg., have been carried by platinum wires having a diameter of 0.1 mm. For these we have now substituted others of pladuram wire 0.07 mm. in diameter. It was found that the breaking load for this wire just exceeded 1 kg.; its tenacity was therefore 263, a value twice as great as that assigned to steel. The two wires were threaded through their respective riders, given the required, but not excessive, degree of tautness, and then, by means of nuts, permanently secured to the beam.

( $\gamma$ ) *New pan arrestors.* Before dealing with our next innovation, we remark that for ensuring high precision in weighing, a close approach to equality in the temperature of any two masses under comparison must obtain. In general this demand is met by placing the balance in a room for which variations in temperature are both small and slow; but for precision of the highest order stringent measures are imperative; and these must be such that we pass from assumption to certainty. The procedure was as follows. To begin with, the arrestors in use until now were in their entirety discarded for others constructed as shown in figure 1. Here the head *h* consists of a shallow brass cell having a copper cover *c* accurately fitting a recess. Two short quartz tubes,  $t_1$ ,  $t_2$ , pass through apertures in the floor of the cell and are secured therein with Faraday cement. The head of the screw *s* is supported by the quartz tube  $q_1$ , to which it is cemented. Surrounding  $q_1$  is a second tube  $q_2$ , also of quartz, the lower end of which was opened by grinding so as to admit the stem of the inverted and glass-hard steel stud *g*, the curved surface of which was polished and which, when *in situ*, rests upon its operative cam. The concentric positions of  $q_1$ ,  $q_2$  and *g* were rendered permanent by a tightly fitting ring of asbestos at *a*, and by the application of cement round and about *m*, as indicated by the dotted lines. The arrestors were now ready for the reception of the prepared grids, each consisting of a spiral of platinum wire wound upon a mica former *p*. The diameter of the wire is 0.03 mm., and at 14° c. each grid has a resistance of 49.22  $\Omega$ . The grids were united to their respective and equal silver wire leads by means of short intermediary pieces of gold wire, the several junctions being effected by fusion. Each grid was now insulated by inserting it between two thin mica discs, then placed within its cell and enclosed by means of the copper cover *c*. Next the

arrestors were given their normal positions beneath the balance pans with their contained grids forming two arms of a Carey Foster bridge. The auxiliary coils of the bridge are silk-covered constantan wires; these are wound bifilarly upon a shellac-covered aluminium rod 1 cm. in diameter and protected with silk. This done, the supporting aluminium rod was mounted upon ebonite and fixed centrally behind the pillar of the balance. Initial measurements were now made with the aid of a Moll galvanometer, an instrument which was ultimately displaced by a "short-period" galvanometer supplied by the Cambridge Instrument Co. The sensitivity of the new instrument proved to be considerably greater than that of the Moll, and on passing a current of 0.002 A. into the bridge, differences in the balancing point corresponding to 0.00002  $\Omega$  were measurable with certainty. Now a difference of 1° C. in the temperature

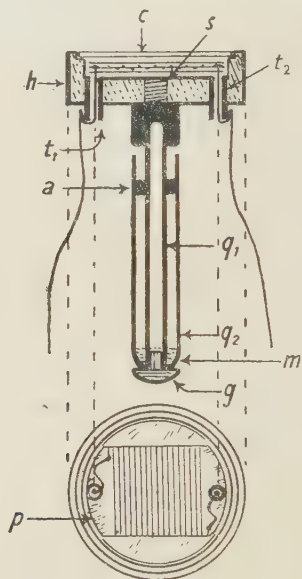


Figure 1.

in the two grids produces a difference in the resistances = 0.19  $\Omega$ ; hence variations of 1/10,000° C. can be detected.

( $\delta$ ) *The encased slide wire.* This was designed to ensure uniformity in the temperature of the bridge wire and its slider. During preliminary tests it was found that even when the pans of the balance were contained within an aluminium cell common to both (*vide infra*), they generally exhibited small differences in temperature. These were ultimately found to be due to differences in the temperature of the 1 m. bridge. The difficulty was overcome by the use of a platinum-iridium wire 13 cm. long and 1.5 mm. in diameter, mounted and protected as shown in figures 2 and 3.

In the first figure, this wire is seen to be an air-line bent in the form of an arc, and the slider a radial arm ending in a platinum contact; the contact is maintained in action by a weak terminal spring. The binding screws connected with the leads, which pass through quartz tubes, are mounted upon ebonite fixed

to the aluminium base, whilst the base itself is secured to a vertical aluminium plate screwed to the lower surface of the galvanometer shelf. The completed apparatus is shown in figure 3. Here the enclosing aluminium shield, having walls 2 mm. thick, is seen to carry a circular scale some 5 cm. long and placed parallel to the wire within. The arm *a* is insulated by mica and ebonite, and across its circular window is fixed an attenuated fiducial wire, just visible in the figure.

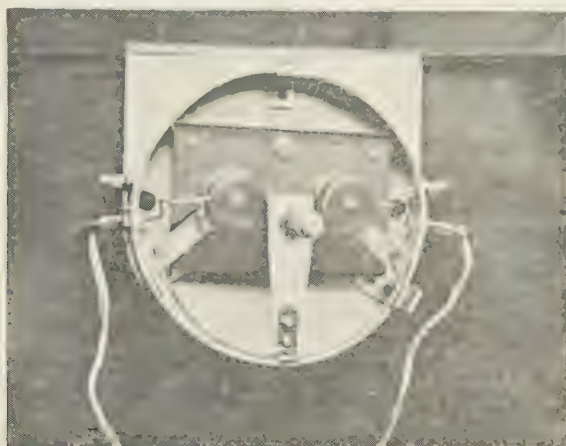


Figure 2.

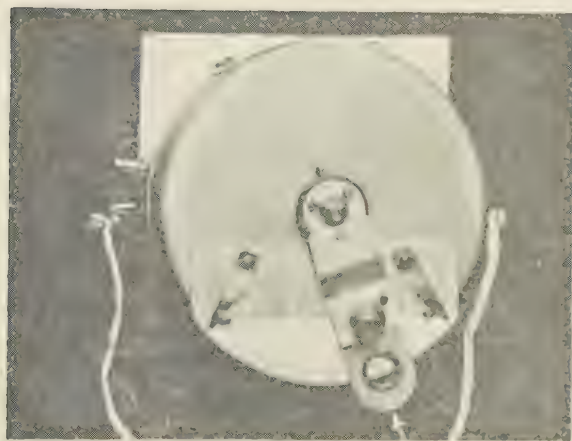


Figure 3.

( $\epsilon$ ) *The cell enclosing the pans.* The new aluminium cell, which encloses both pans, so that their temperatures are equal, is depicted in figure 4. Its upper edge *AB* makes continuous contact with the lower surface of the aluminium base-plate of the beam chamber. Within a slot cut in the fixed plate *P* is shown a pointer *t*, a side view of which is given in *c*. This supplementary pointer is a thin aluminium wire ending in a knife-edge; it is given rigidity by passing it through a thin-walled and closely fitting capillary tube of quartz and is normally attached horizontally to the normal pointer. Deflections are read by

means of a scale engraved as shown. Equilibrium of the loaded pans having been approximately established, the shutter *s*, with its pivot at *o*, is turned and the aperture closed; the relative values of the two masses are then precisely determined with the aid of a brightly illuminated scale and the vertical palladium mirror carried by the block of the central knife-edge. The pointer of light is 9 m. long and the sensitivity *S* of the balance equal to 461 mm. per 1 mg. The eye-piece of the telescope carries a micrometer with which deflections can be accurately read to 0.1 mm.; and if this be taken as the unit,  $S = 4610$ . Again referring to figure 4, it will be seen that access to the pans is provided by the use of sliding shutters. One of these, *x*, is open, and the other *y*, closed. Here it

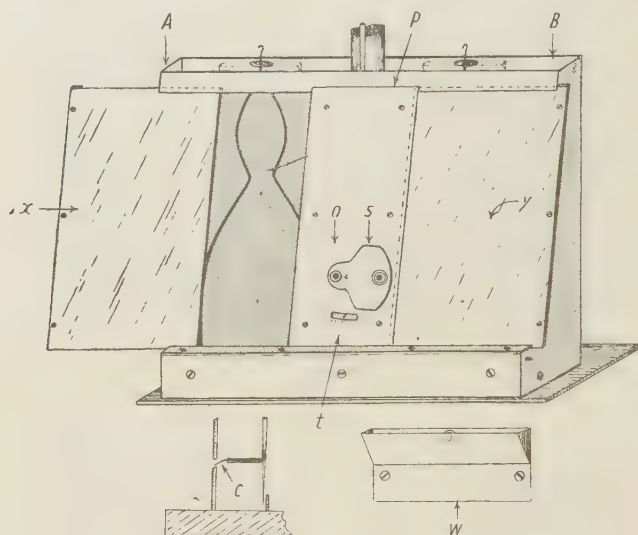


Figure 4.

may be added that all interior surfaces are coated with vegetable black attached with the aid of copal varnish and permanently fixed by heating.

Lastly, immediately behind each pan suspension is a small weir, into which from the posterior side, is delivered a slow stream of air purified by passing it successively through concentrated sulphuric acid, soda-lime and granulated calcium chloride.\* One of these, *w*, is shown in figure 4. We conclude our descriptions of the most recent alterations in our balance by stating that the panels of the case, the top, and also the base, are completely enclosed with polished sheets of aluminium, and as a further aid to the establishment and maintenance of uniformity in temperature, the whole, with the exception of the front sliding aluminium shutter, is surrounded with a wooden case having walls 2 cm. thick.

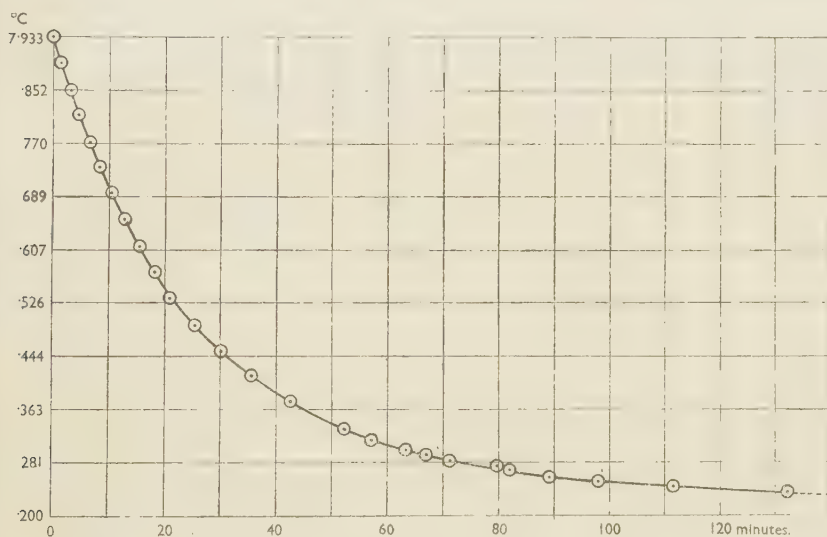
### § 3. TESTS OF THE EFFECTIVENESS OF THE NEW IMPROVEMENT

Experiments designed to test the efficacy of the several innovations were now carried out. We begin by describing one made to ascertain the time required

\* All new vulcanized rubber connections must be treated for the removal of volatile sulphur compounds. This is shown by the fact that by so doing 10 cm. of tubing having an internal diameter of 7 mm. yielded, when heated with a solution of pure sodium hydrate and hydrogen peroxide, 0.014 gm. of sulphur in the form of barium sulphate.

or a 100-gm. chromium-plated weight to cool after having been slightly warmed.

First, two similar 100-g. weights were placed in their respective pans and left overnight. On the following morning the ordinary air was displaced from the chamber (figure 4) enclosing the pans by streams of air purified as already described. Next, one of the two weights was held in the hand, and thus slightly warmed; it was then wiped with silk, replaced in its pan, the chamber closed and the streams of purified air maintained; this done, further procedure was as follows: Using a 1-m. Carey Foster bridge, in which the pan grids are the resistances under comparison, the slider was placed at a point corresponding to  $0^{\circ}7$  c. in excess of that of the second or unwarmed weight; then, when the chosen initial temperature had been nearly reached, the circuit was kept closed and the



March 14, 1944

Figure 5. Cooling curve for 100-gm. Cr-plated weight placed within chamber common to both pans. Data obtained after all final precautions had been completed. A second 100-gm. Cr-plated weight not handled was in the other pan.

shift of the galvanometer deflection followed, and as this crossed zero the chronometer was started; then the slider was moved forward to a first predetermined point and the time noted for a second zero reading.

Proceeding thus some 26 zero points were obtained. From the data now required, the cooling-curve, figure 5, was drawn. And here it may be noted (1) that the curve is almost perfectly smooth, and (2) that although, after a period of 130 minutes, equilibrium of temperature had not been established, effects following the want of it are insignificant and are treated as non-existent. In this experiment the reassumption of a temperature common to both weights required a period approaching a maximum. For other weights having more highly radiating surfaces the time for cooling would be less.

We now deal with changes in the sensitivity of the balance for various loads.\*

\* Here it may not be inappropriate to emphasize again the merits of a phosphor-bronze steelyard beam having its terminal knife-edges *within* instead of *beyond* the outer struts,

Hitherto, in so far as we could discover, the sensitivity of the balance had been one and the same for all loads, but now that this had been largely increased, it was deemed necessary to retest the beam. Accordingly this was done, use being made of loads ranging in value from 0 to 200 g. The results are represented in figure 6.

The changes, small in themselves, and varying within the limits of  $6 \times 10^{-4}$  and  $7 \times 10^{-5}$  mg. must nevertheless be taken into account when seeking to ensure the highest order of accuracy. We remark that the steep part of the curve indicates an initial and very slight relative readjustment of one or more of the knife-edges, the probability being that the central one only was affected. We conclude by drawing attention to some experiments made to test the relative merits of the two methods used for screening the pans.

In one method we attempted to establish a common and uniform temperature in and about the pans and their contents by protecting them not only with their individual brass cylinders, but also by enclosing the sides, the front sliding panel,

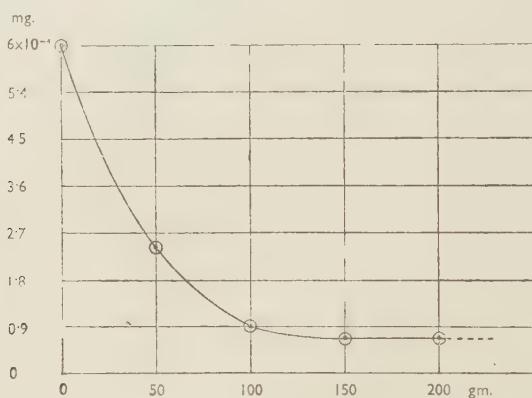


Figure 6. Sensitivity of balance.

and also the top of the case, with sheets of bright aluminium. In the other we relied upon a theoretical efficacy resulting from the use of a chamber (figure 4) common to both. For each group of experiments the pans were unloaded: this to ensure quick response.

The first series of experiments was carried out on a bright and sunny day, the second during an overcast sky and the third on a day when calm and rainy weather prevailed. The results are shown graphically in figure 7.

It will be seen that the several maximum variations in temperature of the two pans are respectively  $0^{\circ}.075$ ,  $0^{\circ}.030$  and  $0^{\circ}.012$  c. Now these variations in temperature would affect the apparent weight of a body having a volume of 100 c.c. to the extent of  $\pm 30 \times 10^{-6}$ ,  $12 \times 10^{-6}$  and  $4.8 \times 10^{-6}$  respectively, and all these come within the range of the balance and can be measured with certainty. We now pass to a brief consideration of our final series of experiments made with the pans enclosed within one and the same chamber (figure 4), and for which we used the circular bridge wire (figures 2 and 3).

Again, the pans being empty, several series of observations were carried out on succeeding *sunny* days. Within that time the temperature varied by some

c.; yet, notwithstanding this, the mean variations in the temperature of the 70 grids and, therefore, of the pans was  $\pm 0^{\circ}0004$  c. only. This is  $1/30$ th of the minimum difference noted during the corresponding experiments of the first series, and the effect is, as will be seen, wholly negligible. A graphical

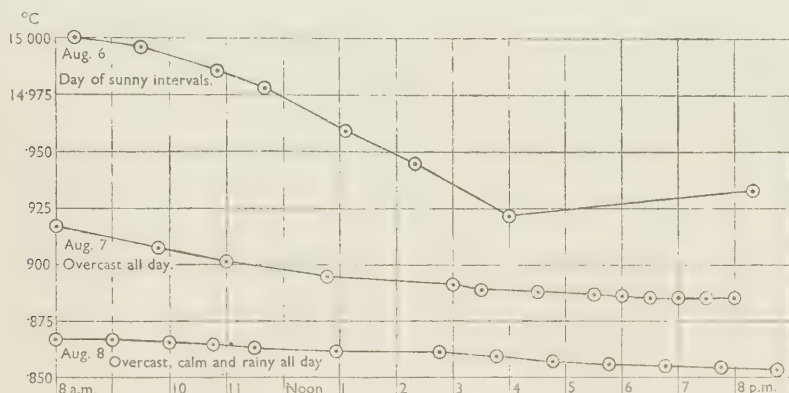


Figure 7.

presentation of the data results, if put forth on the scale used in figure 7, in a straight horizontal line. Having now achieved our first and main objective, we pass to the second and minor problem, namely, as to whether rhodium, used as a protective, surpasses chromium, hitherto found to excel all others.

#### § 4. THE EFFICACY OF RHODIUM-PLATING

For this investigation there were available two sets of rhodium-plated weights, the one by Oertling and the other by Bunge. Each set consisted of weights ranging in value from 1 to 500 gm., and both were stored as described in a former paper.\* Measurements were carried out with the heavier weights only, this, owing to their larger surfaces, offering a greater mass of the film to be determined. We were, however, limited to the use of weights of 200 gm., the maximum load for which the balance had been built. Our inquiry was, however, somewhat enlarged by the examination of three 100-gm. weights. One of these was coated with rhodium and another with chromium; the third consisted of the alloy known as nichrome. All these weights were, as usual, first thoroughly wiped with silk which had been successively cleansed with dilute ammonia and distilled water, then dried and finally washed with highly purified benzene and again dried. The wiped weights were then brushed with newly cleansed camel's hair and placed within their respective cells. A period of 18 months having been allowed for storage, the several weights were successively tested for any film that might have been acquired. As usual, two equal weights (say 200 and 200), were lifted from their cells, lightly brushed with camel's hair and placed the one in the L-pan and the other in the R-pan of the balance; then, observing all known precautions, a number of comparisons were made during the two or three ensuing days. The several series of determinations before plating having been completed, one of the two weights (say 200), was transferred

\* *Phil. Mag.* **19**, 243 (1935).

to the silk duster and gently rubbed with the same; this done, the weight was again brushed with camel's hair to remove all loose particles, then replaced in the pan whence it had been taken, and a second and final series of weighings carried out. Knowing the temperature coefficient of the balance for the given load, it was now possible to reduce all the observations for a common temperature, and this was accordingly done, with the results set forth in the following table:—

Weight	Maker	Coating	Period	Area of weight	Total film	Film per 1 cm. <sup>2</sup>
			months	cm. <sup>2</sup>	mg.	mg.
200	Oertling	Rhodium	18	53	·00212	·00004
200	"	"	18	53	±0	0
200	Bunge	"	18	46	±0	0
200	"	"	18	46	±0	0
*100	Oertling	"	69	34	·01292	·00038
†100	"	Chromium	19	27	·04773	·00177
‡100	"	Nichrome weight	26	30·3	·00424	·00014

\* The charcoal beneath the weight was not re-heated during storage.

† Stored in a cell of African blackwood in absence of charcoal.

‡ Stored over charcoal which was heated at intervals.

From the above tabulated results we note that of the four major weights tested, the first alone was adversely affected; but even so, the observed loss approximated to 1 in  $10 \times 10^7$  parts only.

Regarding the tests made with the three 100-gm. weights, we remark that these afforded an opportunity for ascertaining whether their values were affected under the several conditions imposed, and, if so, to what extent. In the first it will be seen that even when a weight is rhodium-plated it yet acquires a definite film unless the charcoal is periodically heated. In the present case the film was some three times greater than one that is normal.

The chromium-plated weight stored in African blackwood acquired a film some 90 times larger than that usually found. Here, then, we have an example illustrating the important rôle played by coconut charcoal.

In conclusion, we remark that the film found upon the nichrome 100-gm. weight, after it had been stored for 26 weeks in charcoal, was strictly normal and, therefore, calls for no further comment.

## REVIEWS OF BOOKS

*The Simple Calculation of Electrical Transients*, by G. W. CARTER. Pp. viii + 120. (Cambridge : University Press, 1944.) 8s. 6d. net.

The sub-title, *An Elementary Treatment of Transient Problems in Linear Electric Circuits* by Heaviside's Operational Methods, together with the restriction (stated in the introduction) to circuits with "lumped" parameters, sufficiently indicates the scope of the book. The impedance and admittance operators are rational algebraic fractions which can be decomposed into partial fractions of a few standard types, so that rules for interpretation can be concisely and completely given. But a large number of interesting and important problems do lie within this restricted field, and each advance of technique is illustrated by the solution of a problem of real practical significance. The freshness and practicality of the worked examples is one outstanding merit of the book.

There is no claim to "make things easy", but any interested student with a knowledge of mathematics up to that of an average engineering graduate should be able easily to master the contents of this book. Indeed, it would seem to the present writer to be the most successful *elementary* treatment he has so far met. Its value would, however, be very considerably enhanced by the provision, say at the end of each chapter, of a few exercises for the student to work for himself.

A useful series of appendices contains, besides a list of interpretations of the simpler operational forms, formulae in trigonometry, calculus, and theory of equations relevant to the subject—the last including Routh's criteria of stability. W. G. B.

*Five-figure Logarithm Tables*. Pp. 1-73, i-xx, 30-119. (Published for the Ministry of Supply by His Majesty's Stationery Office, 1944.) 7s. 6d. net.

This compilation is, as explained in the preface, a war-time measure, and consists of prints of existing five-decimal tables of logarithms of numbers and trigonometric functions.

The first portion (pp. 1-73) is a reprint, from the stereos, of Chappell's table of logarithms, which gives five-decimal mantissae of the logarithms of numbers from 10000 to 40000 and from 4000 to 10000. Modal differences per line are given, and as these never exceed ten (in units of the fifth decimal), interpolation is linear, and might well be mental, although proportional parts are provided in the second portion of the table.

The third portion is a photographic reprint of pp. 30-119 of Bremiker's table of five-decimal logarithms of sines, tangents, cotangents and cosines for the range  $0^{\circ}00$  ( $0^{\circ}01$ )  $45^{\circ}00$ —i.e., every hundredth of a degree from  $0^{\circ}$  to  $45^{\circ}$ . It is taken from the sixteenth, stereotyped, edition, dated 1925. First differences are given, and proportional parts for angles greater than  $3^{\circ}$ .

The "difficult" range ( $0^{\circ}$ – $5^{\circ}$  for sines and tangents, and  $85^{\circ}$ – $90^{\circ}$  for cosines and cotangents) is covered by von Rohr's addition, paged i-xx, to Bremiker, consisting of logarithms of sines and tangents for the range  $0^{\circ}000$  ( $0^{\circ}001$ )  $5^{\circ}000$ —i.e., every thousandth of a degree from  $0^{\circ}$  to  $5^{\circ}$ . Differences are not given, but proportional parts appropriate to angles of upwards of  $0^{\circ}5$  are.

Explanatory matter has been omitted, on the justifiable ground that potential users will be sufficiently experienced not to need it.

There is no point in criticizing the tabular material. It is by no means new, and the best available has been chosen.

The fact of greatest significance is the use of degrees and *decimals* of a degree in the trigonometrical tables. This practice has advantages, and seems to be rapidly superseding the use of minutes and seconds in many quarters. The need by the optical industry for a "fine-grained" table with such a subdivision of the degree seems to have been the primary incentive to the production of this volume. It is surprising that, if the need were great, the production has been delayed until after five years of war. Now that these tables are available, others also may find them useful.

It is a very great pity, however, that Bremiker's table of  $S$  and  $T$ , for converting  $\log A^\circ$  into  $\log \sin A^\circ$ , or  $\log \tan A^\circ$ , p. 170 of the original, and referred to in the P.P. column on p. 30, was not also reproduced. Linear interpolation ceases to be adequate in von Rohr's table below about  $0^\circ.2$ ; this table does not completely solve the interpolation problem, but the  $S$  and  $T$  tables do. If this one-page table were reproduced separately, say on thin card, it would enhance the usefulness of the book. A separate card would, indeed, be more convenient in use than a page bound up with the volume. W. G. B.

*What is Life?*, by ERWIN SCHRÖDINGER. Pp. viii + 91. (Cambridge: University Press, 1944.) 6s. net.

The middle section of this little book gives a clear and, to a physicist, convincing account of genetical principles and of the Delbrück model of a gene. According to this model, a gene is a very large single molecule, and a mutation, spontaneous or induced by x-ray dosage, is a quantum transition of the molecule to a new isomeric form. From his discussion of the Delbrück model, the author draws the general conclusion "that living matter, while not eluding the 'laws of physics' as established up to date, is likely to involve 'other laws of physics' hitherto unknown, which, however, once they have been revealed, will form just as integral a part of this science as the former". The final chapters are concerned with clarifying this conclusion, which, we are told, provided the only motive for writing the book. While these chapters and the opening chapter enlarge, in an interesting way, on the statistical element in physical laws and on the "statistical tendency of matter to go over into disorder" as contrasted with the organism's astonishing gift of concentrating a 'stream of order' on itself, they leave the main conclusion still rather obscure. The inference from the Delbrück model is presumably that, when the principles of quantum theory are included among the laws of physics, the behaviour of living organisms becomes explicable. What place then remains for "other laws of physics", unless the title of "laws of physics" is conferred on the regularities of biological behaviour which are explained?

The reconciliation of Determinism and Free Will is considered in a five-page Epilogue, in which the Upanishads, double personality, Schopenhauer, plurality of souls, Kant and the tree in the quad, all have their reference—a fairly rich philosophical bolus.

In the difficult field between physics and biology a clear-cut argument is not to be required, and although the reader, like the reviewer, may find the author's main point (quoted above) somewhat too subtle and not unconnected with an ambiguous use of the term "physical law", he can hardly fail to find the book, as a whole, illuminating and stimulating. W. S. S.

---

## CORRIGENDUM

In *Proc. Phys. Soc.* 57, part 1, the first line of p. 19 should follow the first line of p. 18 and precede the line appearing as the second of p. 18.

---

## RECENT REPORTS AND CATALOGUES

*Co-operative Electrical Research.* Pp. 62. 1944. THE BRITISH ELECTRICAL AND ALLIED INDUSTRIES RESEARCH ASSOCIATION, 15 Savoy Street, London W.C.2.

*Report on the Needs of Research in Fundamental Science after the War.* Pp. 61. Printed for private circulation, January 1945. THE ROYAL SOCIETY, Burlington House, Piccadilly, London W.1.



## Selenium Photo Cells

are available for immediate delivery to those satisfied with only the best.

Every cell is guaranteed.

**EVANS  
ELECTROSELENIUM  
LIMITED**

BISHOP'S STORTFORD  
HERTFORDSHIRE

## BINDING CASES for the PROCEEDINGS

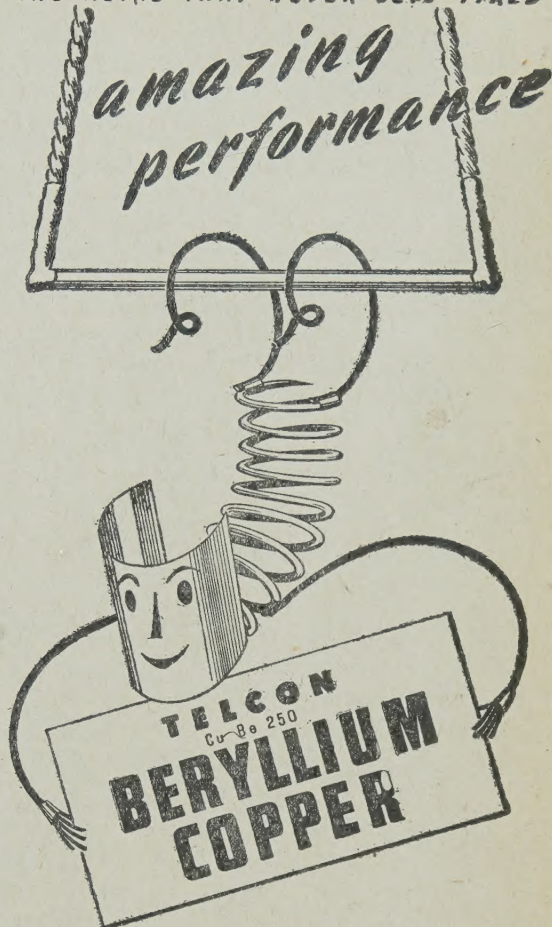
Binding Cases for volume 56 (1944) and previous volumes may be obtained for 6d., inclusive of postage. For 7s. 9d. the parts of a volume will be bound in the publisher's binding cases and returned.

THE PHYSICAL SOCIETY  
Lowther Gardens, Exhibition Road,  
London S.W.7

## WANTED

SENIOR RESEARCH OFFICER for new seas organisation investigating the field of industrial diamond. Preferably Ph.D. with industrial research experience, capable of investigating the Chemical, Physical and other properties of industrial diamonds. A knowledge of Metallurgy or Powder Metallurgy would be an asset. Submit applications, complete with details of training and experience, with references, to: PRO, c/o PHYSICAL SOCIETY, 1 LOWTHER GARDENS, EXHIBITION ROAD, LONDON S.W.7.

"THE METAL THAT NEVER GETS TIRED"



Here is an outstanding performer and no mistake. Springs really do 'spring to it' when made from Telcon Beryllium-Copper Alloy (Cu Be 250). Known as *the metal that never gets tired*, it has exceptionally high tensile strength and conductivity; Brinell hardness up to 400; and offers greater resistance to fatigue than any other metal of the non-ferrous group. Available as strip, rod and wire. Leaflet and full details on request.



# TELCON METALS

Manufactured by:

**THE TELEGRAPH CONSTRUCTION & MAINTENANCE CO. LTD.**

Head Office: 22 OLD BROAD ST., LONDON, E.C.2. Tel: LONDON Wall 3141

Sole Distributors:

**BERYLLIUM & COPPER ALLOYS LTD.** 39 Victoria St. London, SW1

Tel.: ABBey 6259

# SCIENTIFIC BOOKS

Messrs H. K. LEWIS can supply from stock or to order any book on the Physical and Chemical Sciences.

**German Technical Books.** A twelve-page list together with an eight-page supplement giving details of reproductions of German technical publications issued under the authority of the Alien Property Custodian in Washington has just been prepared; a copy will be sent on application.

**SECOND-HAND SCIENTIFIC BOOKS.** An extensive stock of books in all branches of Pure and Applied Science may be seen in this department. Large and small collections bought. Back volumes of Scientific Journals.

Old and rare Scientific Books. Mention interests when writing.

140 GOWER STREET.

## SCIENTIFIC LENDING LIBRARY

Annual subscription from One Guinea. Details of terms and prospectus free on request.

**THE LIBRARY CATALOGUE** revised to December 1943, containing a classified index of authors and subjects: to subscribers 12s. 6d. net., to non-subscribers 25s. net., postage 8d.

Quarterly List of Additions, free on application

Telephone: EUSton 4282

Telegrams: "Publicavit,  
Westcent, London"

**H. K. LEWIS & Co. Ltd.**

136 GOWER STREET, LONDON, W.C.1

*Crown 4to. Published Monthly. Price 10s.*

## The Philosophical Magazine and Journal of Science

Conducted by Sir LAWRENCE BRAGG, O.B.E., M.A., D.Sc., F.R.S., Sir GEORGE THOMSON, M.A., D.Sc., F.R.S., and ALLAN FERGUSON, M.A., D.Sc.

### Contents for December, 1944

Energy Distribution in the Spectrum of a Frequency Modulated Wave—Part I.: A. S. Gladwin, B.Sc., A.R.T.C., A.M.I.E.—Diffusion in Spherical Shells, and a New Method of Measuring the Thermal Diffusivity Constant: R. M. Barrer, D.Sc., Ph.D., F.R.I.C.—The tabulation of some Bessel Functions  $K_\nu(x)$  and  $K'_\nu(x)$  of Fractional Order: H. F. R. Carsten, Dr.-Ing., F.Inst.P., and Miss N. W. McKerrow, B.Sc.—The Field between Equal Semi-infinite Rectangular Electrodes or Magnetic Pole-pieces: N. Davy, University College, Nottingham.—Alternating Loads on Sleeve Bearings: J. Dick, B.Sc., Ph.D.—An Application of the Method of Finite Difference Equations to a Problem of Bending Moments: N. J. Durant.—Transient Response in Frequency Modulation: Letters on, and replies by the author, D. A. Bell, M.A., B.Sc., A.M.I.E.E.

Annual Subscription £5 2s. 6d. post free.

TAYLOR & FRANCIS, LTD., RED LION COURT, FLEET STREET, LONDON, E.C.4